Heavy Flavor Physics - II

Presented at HCPSS24

Joel Butler, Fermilab, CMS

August 1, 2024

Outline

- Case studies: These decays are promising ones for observing New Physics (NP) and there has been recent activity on them
  - $B_{s,d} \rightarrow \mu^+\mu^-$
  - $b \rightarrow s\, \mu^+\mu^-$
  - CP Violation in B_s
  - What's up with Lepton Flavor Universality?
- A few comments on areas not covered (if time)

An overview of recent experimental results

Case Study 1: Rare decay

$B_{s,d} \rightarrow \mu^+\mu^-$

$B_{s,d} \to \mu^+\mu^-$ in the Standard Model

- In the Standard Model, $B_{s,d} \to \mu^+\mu^-$ decays are <u>**highly suppressed**</u>:
  - Flavor Changing Neutral Current (FCNC) processes in SM are forbidden at tree level but can proceed through Z-pengiun, and box diagrams
  - Helicity suppressed: $[m_\mu/m_B]^2$
    - Makes $B_{s,d} \to e^+e^-$ inaccessible
  - CKM suppressed by $|V_{tq}|^2$:
    - $B^o \to \mu^+\mu^-$ further Cabibbo suppressed by $|V_{td}/V_{ts}|^2$, relative to B_s, which gives about a factor of 20 lower branching fraction.
      - Slightly compensated in rate at LHC since B^o has 2X the cross section of B_s.
- Resulting **tiny branching fractions**, but <u>rather *robust SM theory predictions are available*</u>

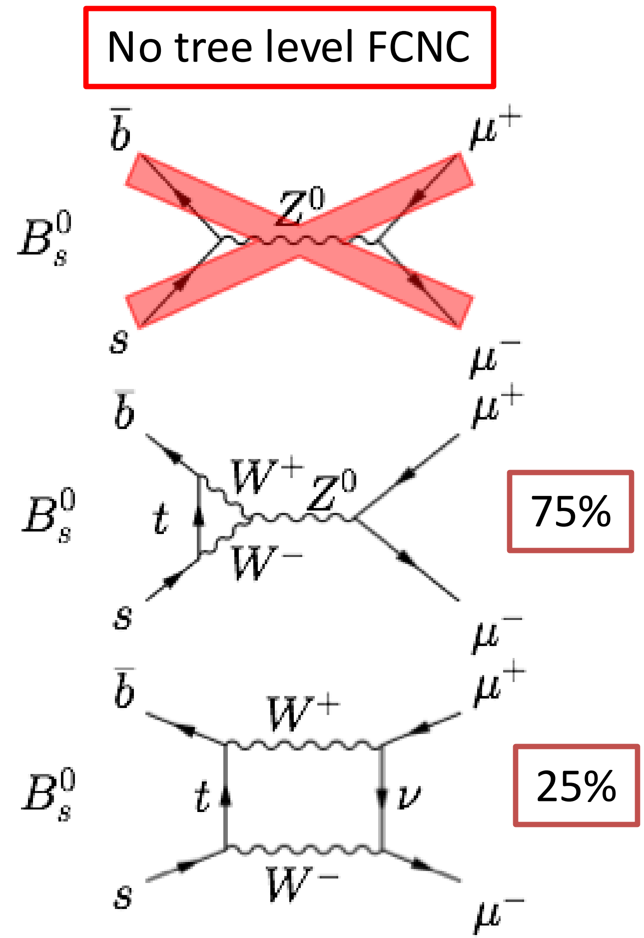

$B_{s,d} \rightarrow \mu^+\mu^-$: the potential for New Physics

- Loop diagram + Suppressed SM + **Theoretically clean**
  ➔ ***An excellent place to look for new physics***.
- Sensitive to extended Higgs sectors
  ⇒ Constrains NP parameter spaces.
- A few NP examples:
  - **2HDM**: $B \propto \tan^4\beta$, and $m(H^+)$
  - **CMSSM/mSUGRA**: $B \propto \tan^6\beta$
  - **Leptoquarks**
- **In some BSM models, the same physics that could influence $b \rightarrow sll$ or LFU could affect $B_{s,d} \rightarrow \mu^+\mu^-$ but in other cases they would not be related.**

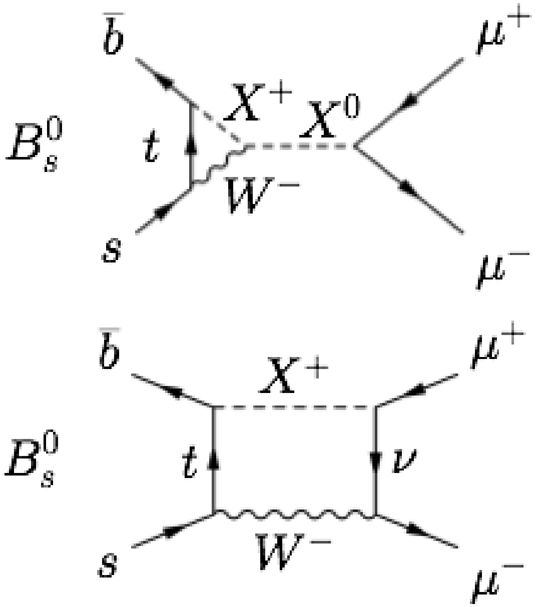

Any difference in branching fraction from SM could provide a strong indication of new physics.

B_s and B_d are different

- In addition to being suppressed by being higher order , these decays are helicity suppressed by a factor $(2m_\mu/M_{B(s,d)})^2$.
- The decay diagrams for B_s have a V_{ts} and and those of B_d have V_{td}, so B_d is additionally Cabibbo suppressed.
  - For B_s, this leads to stronger coupling between CP even and CP odd, bigger Δm (faster oscillation) .
- The lifetimes are determined by tree-level charged current processes, which are ~ the same for B_d and B_s so
  - Ratio of mixing frequency over decay rate are quite different:
    - $x_s = \Delta m_s/\Gamma$ ~19, $x_d = \Delta m_s/\Gamma$ ~0.7!!
  - Also, the two states, CP(even) and CP(odd) have slightly different lifetime for B_s but they are almost identical for Bd:
    - $y_s = \Delta\Gamma_s/\Gamma$ ~0.1, $x_d = \Delta\Gamma/\Gamma$ =0.0

Information on B_s is now exclusively from hadron colliders (Tevatron, LHC). Some results came from LEP. FCC-ee, running on the Z-pole, will make a large number of B_s mesons.

Standard Model Prediction simplified

Decay constant

Proxy for full amplitude

$$\overline{B}_{q\ell} = \frac{|N|^2 M_{B_q}^3 f_{B_q}^2}{8\pi \Gamma_H^q} \beta_{q\ell} r_{q\ell}^2 |C_A(\mu_b)|^2 + \mathcal{O}(\alpha_{em})$$

$$N = V_{tb}^{\star} V_{tq} G_F^2 M_W^2 / \pi^2 \quad r_{q\ell} = 2m_\ell / M_{B_q} \quad \beta_{q\ell} = \sqrt{1 - r_{q\ell}^2}$$

Flavor mixing in the SM produces two mass eigenstates, denoted as $B^o_{s,d\,L}$ and $B^o_{s,d\,H}$, where (L,H → light, heavy), which are CP-even and CP-odd, respectively. A dimuon can be shown to be CP odd, so the parent of the decay is also CP odd. The widths (lifetimes) of these states are $\Gamma_L (\tau_L)$ and $\Gamma_H (\tau_H)$, respectively. These two widths (lifetimes) are nearly identical for B_d but somewhat different for B_s

The SM predictions for the branching fractions are:

$$\mathcal{B}(B^o_s \rightarrow \mu^+\mu^-) = (3.66 \pm 0.14) \times 10^{-9}$$
$$\mathcal{B}(B^o \rightarrow \mu^+\mu^-) = (1.03 \pm 0.05) \times 10^{-10}$$

These predictions include next-to-leading order corrections of EW origin and next-to-next-to-leading order QCD corrections. <u>The largest contribution to the theoretical uncertainty is from the determination of the CKM matrix element values, in particular $|V_{cb}|$!</u>

Measurement of the $B_s \rightarrow \mu^+\mu^-$ decay properties and search for the $B_d \rightarrow \mu^+\mu^-$ from CMS

Phys. Lett. B 842 (2023) 137955

- **The $B_{s,d} \rightarrow \mu^+\mu^-$ signal**
  - two **isolated, opposite signed** muons forming a good displaced vertex; dimuon momentum aligned with flight direction from primary and secondary vertex; dimuon mass consistent with $M(B_{s,d})$ (in the unblinding process)
- **Background sources**
  - two semileptonic B decays
  - one semileptonic B + a misidentified hadron
  - rare background from single B meson decays: e.g. $B \rightarrow K\pi/KK$ (*peaking*), $B_s \rightarrow K^-\mu^+\nu$, $\Lambda_b \rightarrow p\mu\nu$ (*not peaking*), where hadrons either appear to be muons through decays or "punch-through"

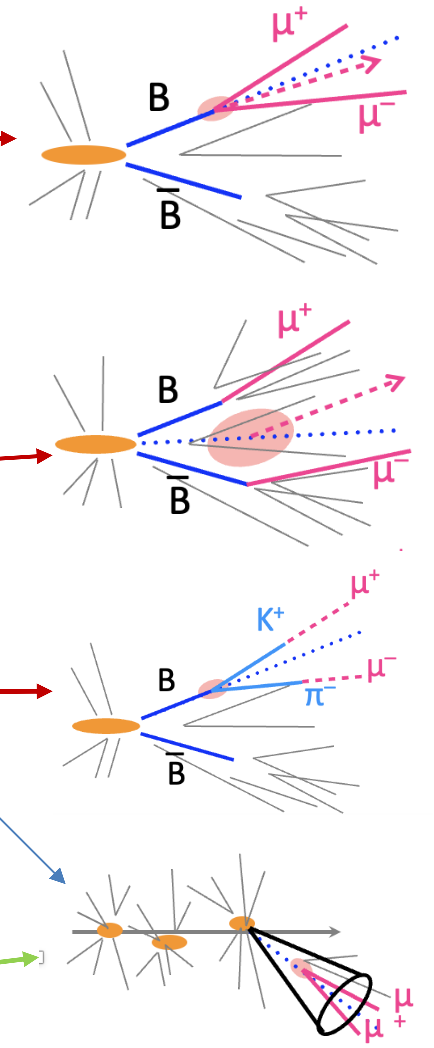

Powerful background suppression reached by muon quality, well-reconstructed secondary vertex, muon and B isolation, pointing angle, and M(μμ) resolution.

Most Recent Result – CMS

- Based on 140 fb^{-1} from 2016, 2017, 2018, [*Phys. Lett. B* 842 (2023) 137955]

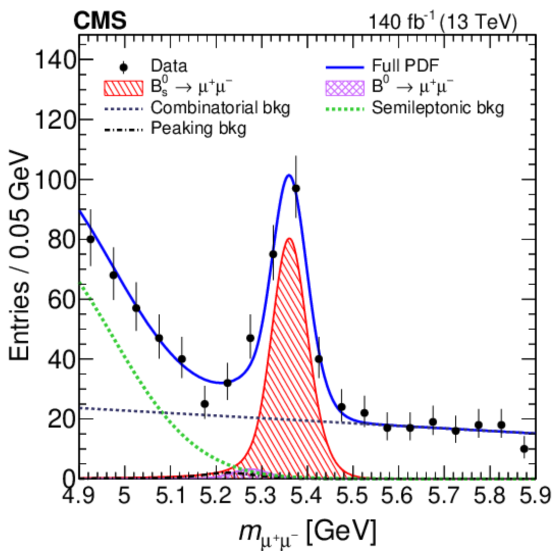

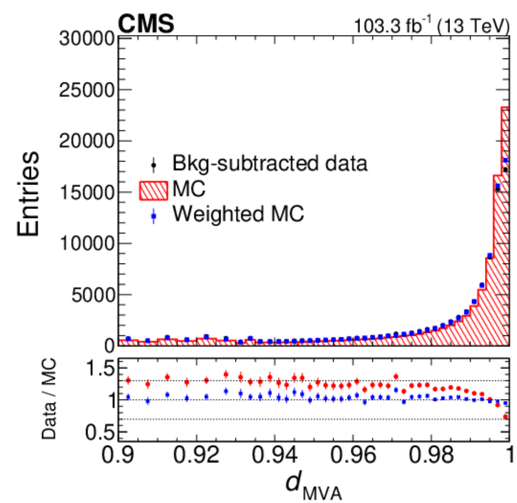

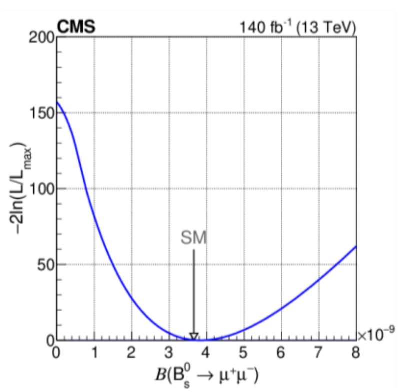

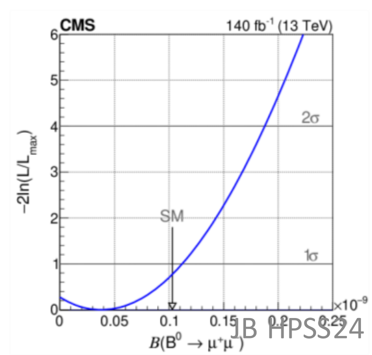

- Blinded analysis
- Same muon MVA, with minor change in cut on MVA output
- New Analysis MVA using XGBoost library
  - Optimized using signal Monte Carlo and background from data sidebands
    - K-folding used to avoid including possible correlations
- Unbinned ML fit to dimuon mass distribution, which includes model for signal, combinatoric background, and peaking background blinded region.
- Normalization using $B^+ \rightarrow J/\psi K^+$.
  - Also used to get efficiencies, resolutions, etc
- Improvements in analysis sensitivity
  - Relaxed preselection (let MVA do it work)
  - Developed new discriminating observables
  - Added much more background data to the training model
  - Used a more advanced machine learning algorithm

Normalization using $B^+ \rightarrow \psi(\mu^+\mu^-)K^+$

$$\mathcal{B}(B_s^0 \to \mu^+\mu^-) = \mathcal{B}(B^+ \to J/\psi K^+)\frac{N_{B_s^0\to\mu^+\mu^-}}{N_{B^+\to J/\psi K^+}}\frac{\varepsilon_{B^+\to J/\psi K^+}}{\varepsilon_{B_s^0\to\mu^+\mu^-}}\frac{f_u}{f_s}$$

$$\mathcal{B}(B_d^0 \to \mu^+\mu^-) = \mathcal{B}(B^+ \to J/\psi K^+)\frac{N_{B_d^0\to\mu^+\mu^-}}{N_{B^+\to J/\psi K^+}}\frac{\varepsilon_{B^+\to J/\psi K^+}}{\varepsilon_{B_d^0\to\mu^+\mu^-}}\frac{f_u}{f_d}$$

N_x number of candidates of decay X from fit
ε_X is the full selection efficiency from MC
f_u, f_d, f_s are the production fractions for B^+, B^o, and B_s mesons, respectively

The production fractions were thought of as constants, independent of P_T and η, with $f_u = f_d$ via isospin.
The external inputs to the calculation of the branching ratios were

But LHCb establishes that there is a P_T and center of mass energy dependence, but no η dependence **Phys. Rev. D 104, 032005.** We use the P_T distribution observed in our CMS measurement to compute an effective f_s/f_d ratio.

The external inputs then are:

- $\mathcal{B}(B^+ \to J/\psi K^+) = (1.020 \pm 0.019) \times 10^{-3}$,
- $\mathcal{B}(J/\psi \to \mu^+\mu^-) = (5.961 \pm 0.033) \times 10^{-2}$, and
- $f_s/f_u = 0.231 \pm 0.008$.

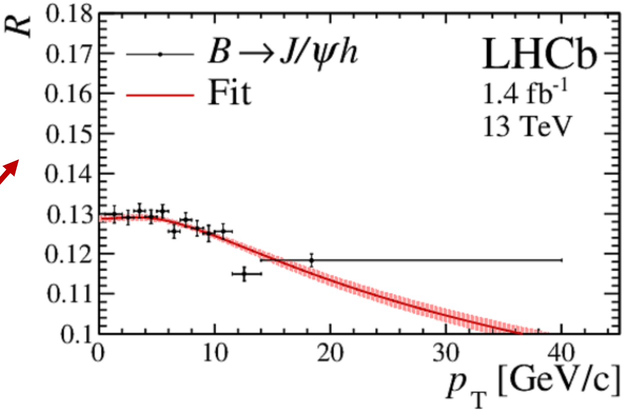

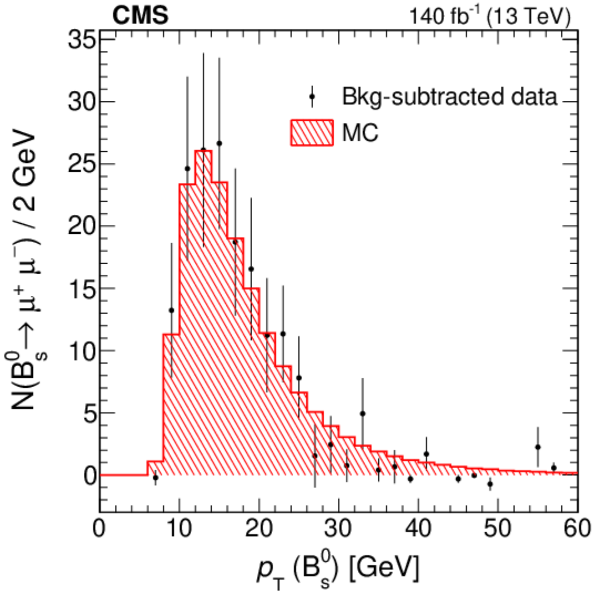

Lifetime of B_{sH} from CMS

A dimuon from a spin 0^- state is CP odd, so the parent of the decay is CP odd. The widths (lifetimes) of these states are called $\Gamma_L\,(\tau_L)$ **and** $\Gamma_H\,(\tau_H)$, respectively. These two widths (lifetimes) are nearly identical for B_d but quite different for B_s

$$\bar{t}_{\mu^+\mu^-} = \frac{L_{xy}\, m^{\mathrm{PDG}}_{B_s^0}}{p_T^{B_s^0}}$$

$$\tau_{B_s^0\to\mu^+\mu^-} \equiv \frac{\int_0^\infty t\,\langle\Gamma\left(B_s^0\to\mu^+\mu^-\right)\rangle\,dt}{\int_0^\infty \langle\Gamma\left(B_s^0\to\mu^+\mu^-\right)\rangle\,dt} = \frac{\tau_{B_s^0}}{1-y_s^2}\left[\frac{1+2\mathcal{A}_{\Delta\Gamma}y_s+y_s^2}{1+\mathcal{A}_{\Delta\Gamma}y_s}\right],$$

$$y_s \equiv \frac{\Delta\Gamma_s}{2\Gamma_s}, \qquad \mathcal{A}_{\Delta\Gamma} \equiv \frac{R_H^{\mu^+\mu^-}-R_L^{\mu^+\mu^-}}{R_H^{\mu^+\mu^-}+R_L^{\mu^+\mu^-}},$$

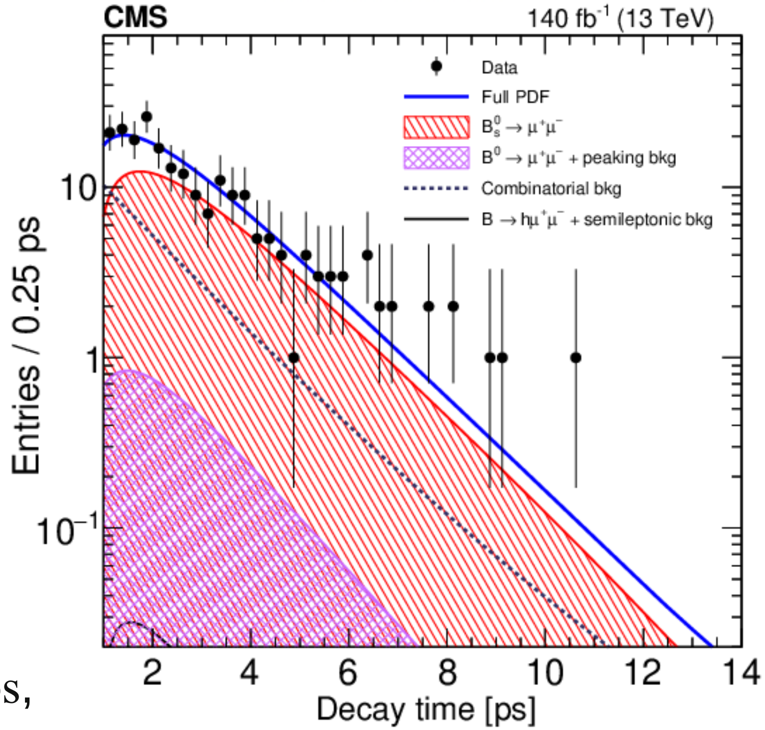

$A_{\Delta\Gamma}$ can vary from +1 to -1. **$A_{\Delta\Gamma} = 1$ in the SM**
And is an observable for NP

From flavor-specific hadronic decays
$\tau\,(B_{sH}) = 1.609 \pm 0.010$ ps, $\tau\,(B_{sl}) = 1.413 \pm 0.006$ ps,

This measurement: $\bar{\tau} = 1.83\,^{+0.23}_{-0.20}\,(\mathrm{stat})\,^{+0.04}_{-0.04}\,(\mathrm{syst})\,\mathrm{ps}.$

More statistics needed before any conclusion relative to NP can be made

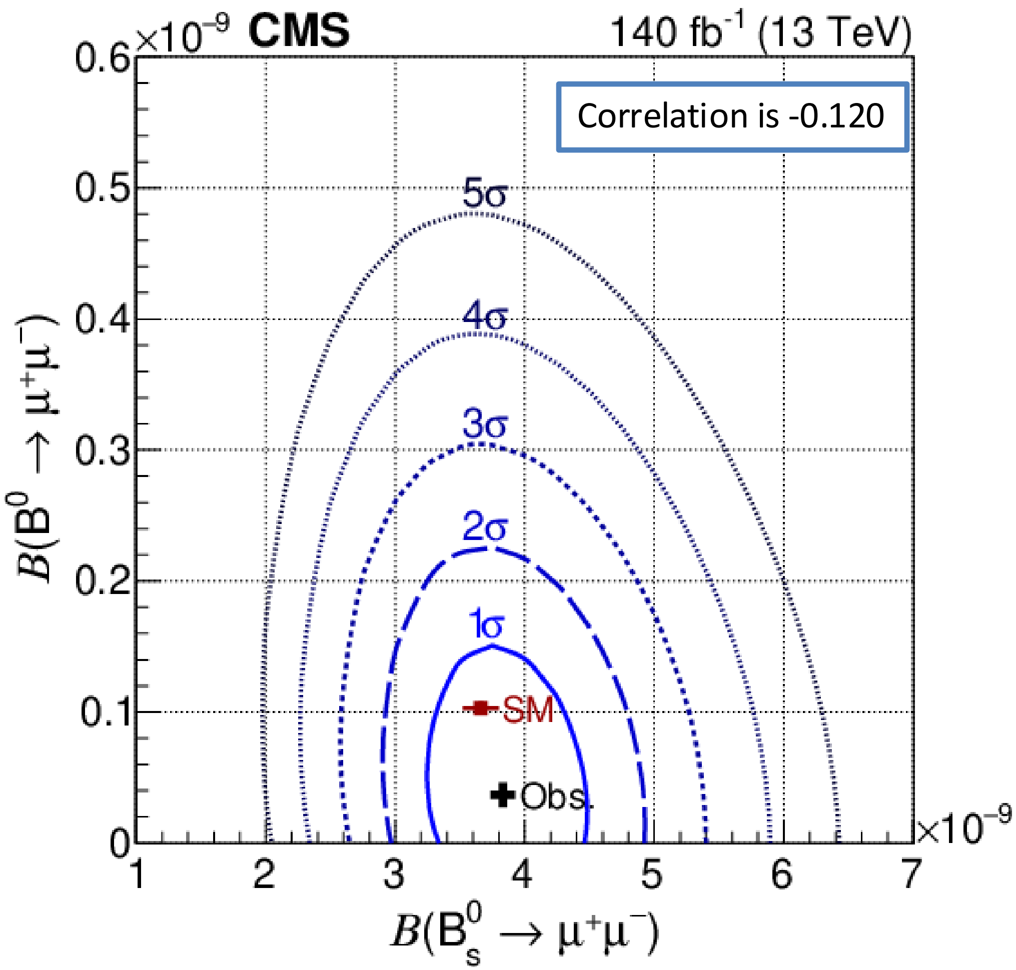

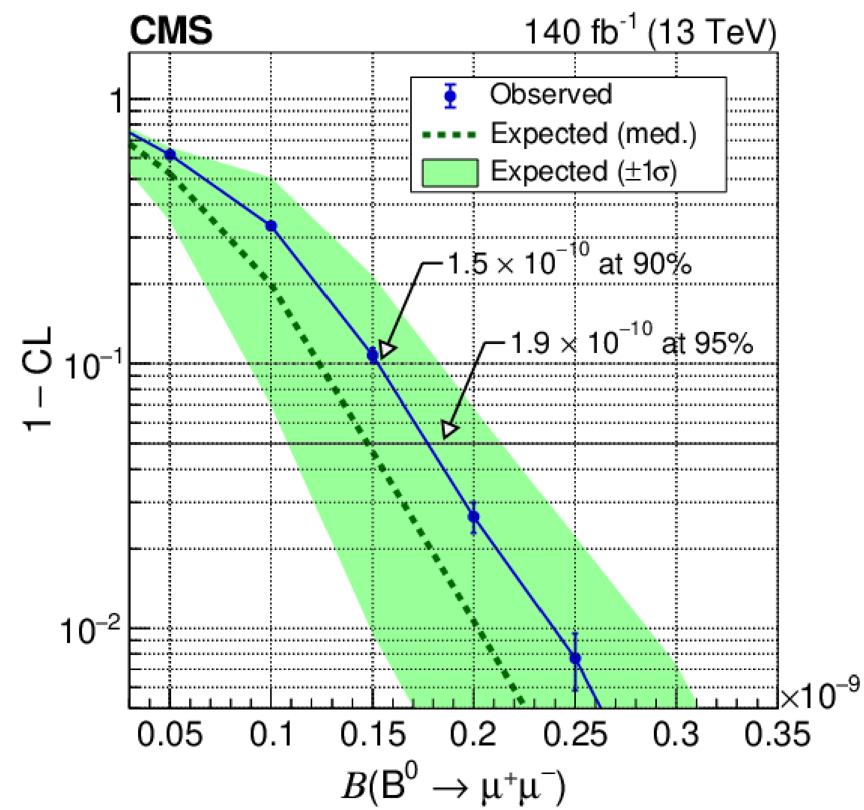

Upper limits on $B^o \to \mu^+\mu^-$ branching fraction using the CL_s method.

$$\mathcal{B}(B_s^0 \to \mu^+\mu^-) = \left[3.83^{+0.38}_{-0.36}\,(\text{stat})\,^{+0.19}_{-0.16}\,(\text{syst})\,^{+0.14}_{-0.13}\,(f_s/f_u)\right] \times 10^{-9},$$
$$\mathcal{B}(B^0 \to \mu^+\mu^-) = \left[0.37^{+0.75}_{-0.67}\,(\text{stat})\,^{+0.08}_{-0.09}\,(\text{syst})\right] \times 10^{-10}.$$

$$\mathcal{B}(B^0 \to \mu^+\mu^-) < 1.5 \times 10^{-10} \text{ at 90\% CL},$$
$$\mathcal{B}(B^0 \to \mu^+\mu^-) < 1.9 \times 10^{-10} \text{ at 95\% CL},$$

The result can be rescaled if the averaged value of fs/fd should change and the systematic uncertainty is separated out so it can be recomputed

Summary of World Data

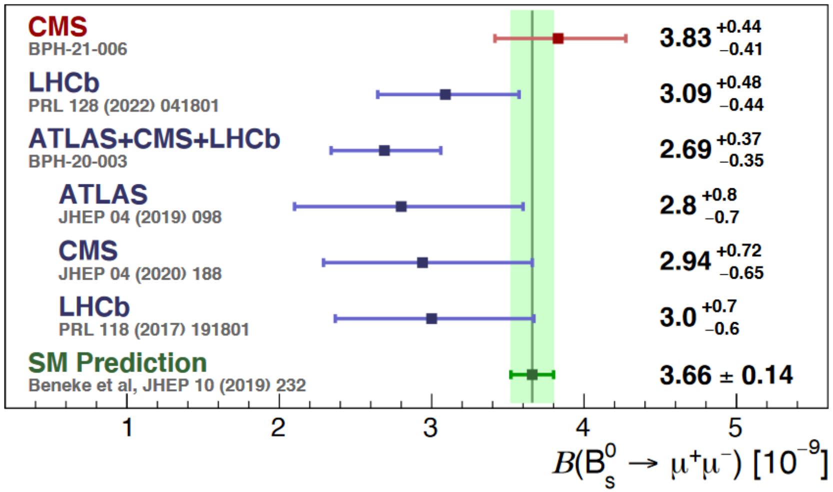

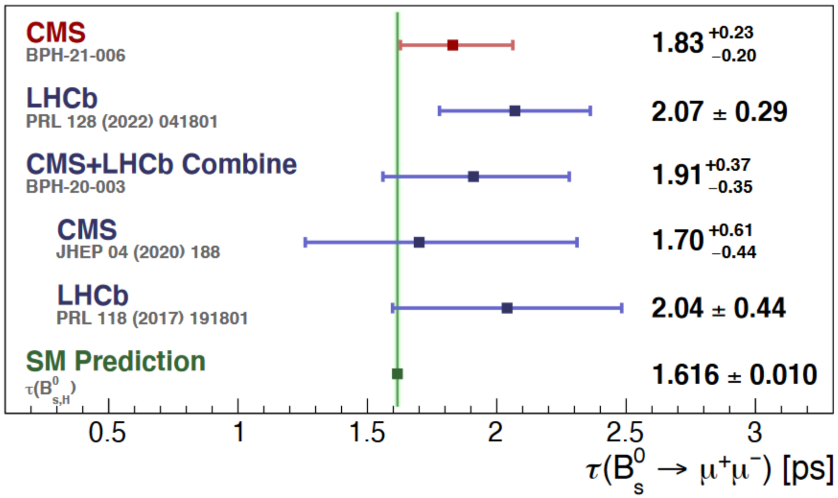

- The CMS result uses 140 fb^{-1} from 2016, 2017, and 2018
- Compared with previous CMS measurement. the relative uncertainty is reduced from 23% to 11%
- CMS is about 1.2 standard deviations higher than LHCb
- There is some tension with previously combined result, ATLAS+CMS+LHCb in plot

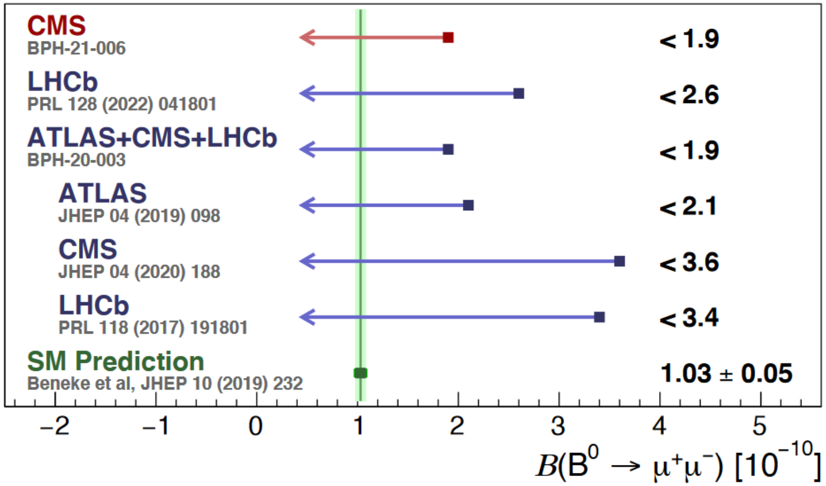

Lifetime $B_{s\ Effective}$ from ATLAS

Data from 2015 and 2016

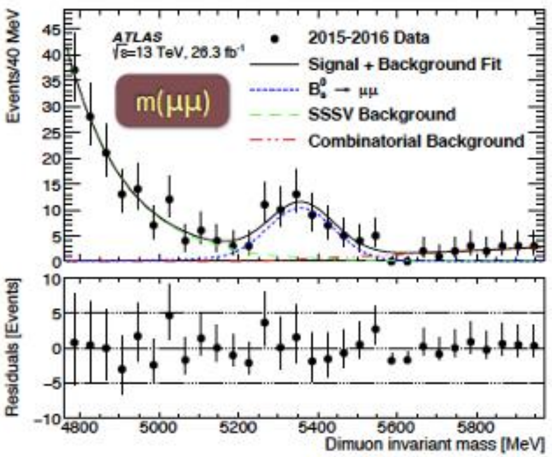

- ATLAS performed a measurement of $B_s \to \mu\mu$ effective lifetime with 26.3 fb^{-1} data at 13 TeV.
- 58±13 background-subtracted (*sPlot method*) signal candidates included in the fit.
- Uncertainties are extracted with **Neyman construction**; major systematics: data-MC discrepancies.

$B_s \to \mu^+\mu^-$ Effective Lifetime
$\tau = 0.99^{+0.42}_{-0.07}\,(\text{stat}) \pm 0.17\,(\text{syst})\ [\text{ps}]$

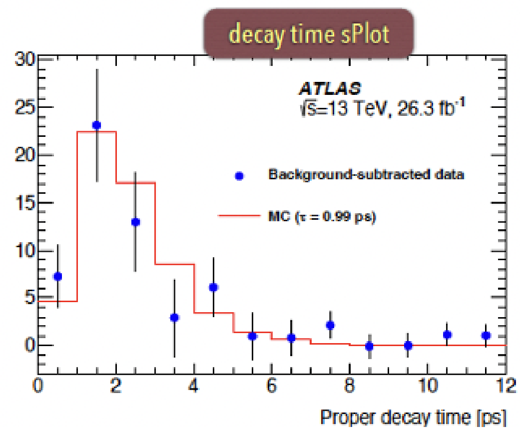

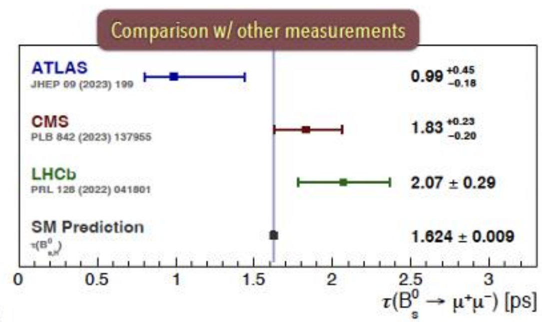

Ref. ATLAS
JHEP 09 (2023) 199

LHCb Search for $B_s \rightarrow \mu^+\mu^-\gamma$

LHCb SEARCH FOR $B_s \rightarrow \mu^+\mu^-\gamma$

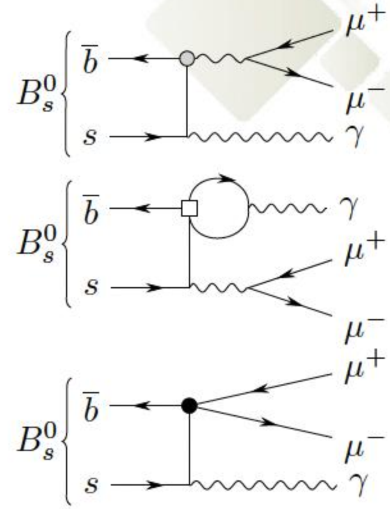

- A powerful probe for investigating any deviations from the SM, with sensitivity to a wider set of operators.
  - The chiral suppression in $B_s \rightarrow \mu\mu$ is relaxed with the additional photon, compensating the addition of the QED vertex.
- First studied as the partial reconstructed background for the $B_s \rightarrow \mu\mu$ analysis and the first upper limit for high q^2 region was reported (ref. LHCb PRL 128 (2022) 041801).
- A dedicated analysis in **three q^2 regions of interests:**

q^2 bin	I	II	III
q^2 [GeV²]	$[4m^2_\mu, 2.89]$	$[2.89, 8.29]$	$[15.37, m^2_{Bs}]$
$m(\mu\mu)$ [GeV]	$[2m_\mu, 1.70]$	$[1.70, 2.88]$	$[3.92, m_{Bs}]$
$10^{10} \times \mathcal{B}(B_s \rightarrow \mu^+\mu^-\gamma)$	82 ± 15	2.54 ± 0.34	9.1 ± 1.1

Ref. LHCb arXiv:2404.03375, submitted to JHEP

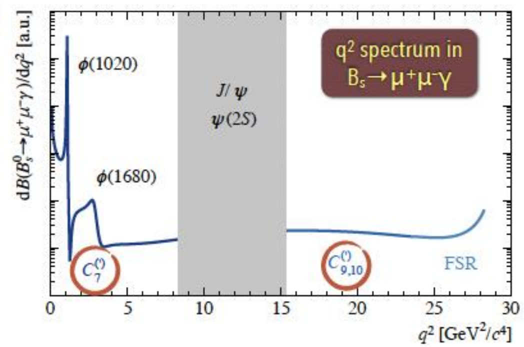

5

Case Study 2: angular dependence of the rare decays $b \rightarrow s\, \mu^+\mu^-$

Why use $b \rightarrow s\, \mu^+\mu^-$ to search for new physics

- To observe physics beyond the SM, i.e., New Physics (NP), need processes highly suppressed in SM
  - ➢ Here N_{SM} is part of the "background", **so we want it to be small!**
- Transitions $b \rightarrow s\, \ell^+\ell^-$ are forbidden at tree level in SM. They can only proceed via higher-order electroweak (loop, box) diagrams, which are small.
  - **These transitions constitute powerful probes for NP since new particles can appear in the loop**
- Observables that can reveal new physics are
  - Branching fractions, including differential BFs vs dimuon mass
  - Angular observables -- to locate a corner of phase space where NP stands out.
  - Ratio of branching fractions between decays with different flavors of leptons, i.e., for tests Lepton Universality (LU) **(discussed in a latter case study)**
- Must have a reliable theory prediction with only small uncertainties in hadronic corrections for the $b \rightarrow s$ transition.
- Must be able to trigger and reconstruct the state with high efficiency and low backgrounds

Semi-leptonic

Flavour changing neutral current

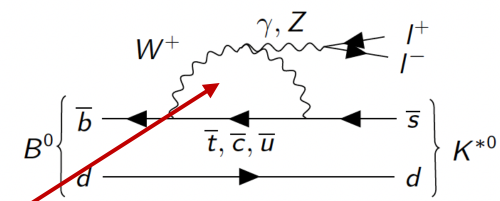

- rare penguin decays
- branching fraction $< 10^{-6}$
  - ▶ suppressed in SM
  - ▶ mediated via loops

Related to $B_s \rightarrow \mu^+\mu^-$ Leptonic decay. Similar but no spectator quark

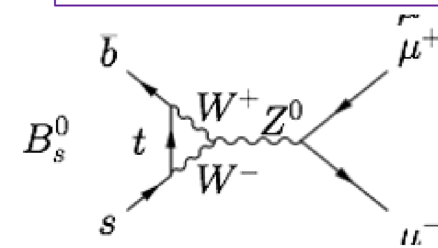

$B^o \rightarrow K^{*o}(890)(\rightarrow K^+\pi^-)\mu^+\mu^-$

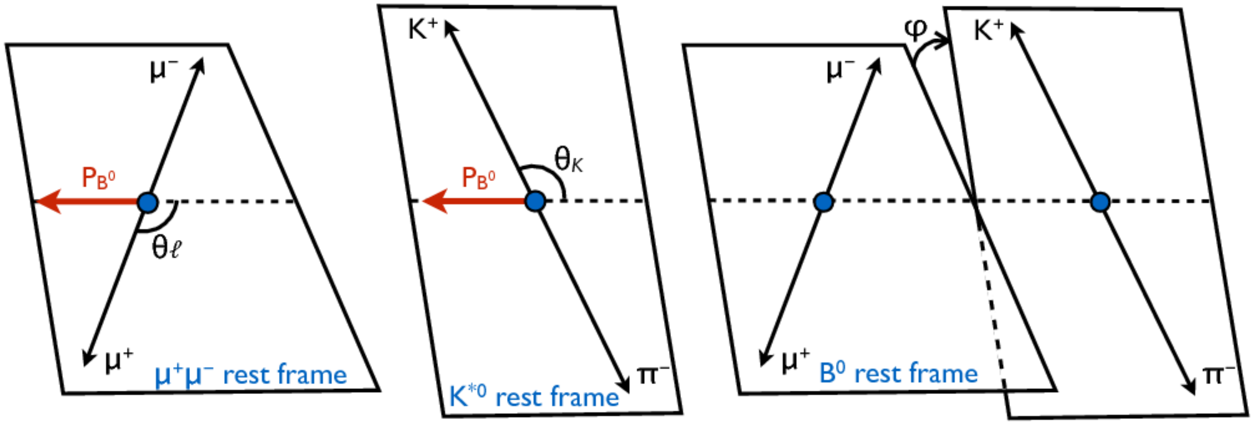

q^2 is the invariant mass squared of the dimuon

- The $K^+\pi^-$ from the K*(890) are in a P-wave. An S-wave contribution to the $K^+\pi^-$ mass region acts as a contamination to the K*(890) angular observables and must be accounted for in the fits.

P-wave

$$\frac{1}{d(\Gamma+\bar{\Gamma})/dq^2}\frac{d^4(\Gamma+\bar{\Gamma})}{dq^2\,d\vec{\Omega}}\bigg|_P = \frac{9}{32\pi}\Big[\frac{3}{4}(1-F_L)\sin^2\theta_K + F_L\cos^2\theta_K + \frac{1}{4}(1-F_L)\sin^2\theta_K\cos 2\theta_l - F_L\cos^2\theta_K\cos 2\theta_l + S_3\sin^2\theta_K\sin^2\theta_l\cos 2\phi + S_4\sin 2\theta_K\sin 2\theta_l\cos\phi + S_5\sin 2\theta_K\sin\theta_l\cos\phi + \frac{4}{3}A_{FB}\sin^2\theta_K\cos\theta_l + S_7\sin 2\theta_K\sin\theta_l\sin\phi + S_8\sin 2\theta_K\sin 2\theta_l\sin\phi + S_9\sin^2\theta_K\sin^2\theta_l\sin 2\phi\Big],$$

P-wave + S-wave

$$\frac{1}{d(\Gamma+\bar{\Gamma})/dq^2}\frac{d^4(\Gamma+\bar{\Gamma})}{dq^2\,d\vec{\Omega}}\bigg|_{S+P} = (1-F_S)\frac{1}{d(\Gamma+\bar{\Gamma})/dq^2}\frac{d^4(\Gamma+\bar{\Gamma})}{dq^2\,d\vec{\Omega}}\bigg|_P + \frac{3}{16\pi}F_S\sin^2\theta_l + \frac{9}{32\pi}(S_{11}+S_{13}\cos 2\theta_l)\cos\theta_K + \frac{9}{32\pi}(S_{14}\sin 2\theta_l + S_{15}\sin\theta_l)\sin\theta_K\cos\phi + \frac{9}{32\pi}(S_{16}\sin\theta_l + S_{17}\sin 2\theta_l)\sin\theta_K\sin\phi,$$

F_L is the longitudinal polarization F_L=S_1; the forward-backward asymmetry A_{FB} = 3/4S_6

Special Considerations

- q^2 interval (dimuon mass^2) restrictions: the dimuon can be resonant, i.e., J/ψ or ψ'.
  - These q^2 intervals must be excluded from the $s \rightarrow b\ell\ell$ amplitude analysis or handled specially.
    - **The resonant final states enter the analysis process, as control, calibration, channels.**
  - The q^2 intervals are based on the q^2 resolution of each experiment, which determines bin width and migration
- There are still theoretical uncertainties in some of the coefficients from QCD
  - "Optimized" observables for which the leading $B^0 \rightarrow K^{*0}$ form-factor uncertainties cancel, can be built from F_L, A_{FB}, and S_3
  - Examples of such optimized observables include the P'_i series of observables .,

Resonant dimuons

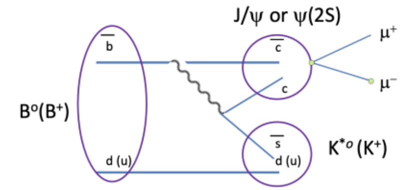

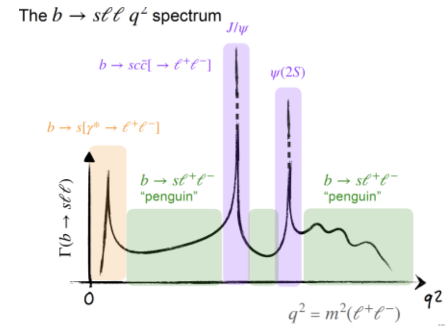

The optimized observables commonly used are:

$$P_1 = \frac{2S_3}{1-F_L},$$

$$P_2 = \frac{2}{3}\frac{A_{FB}}{1-F_L},$$

$$P_3 = \frac{-S_9}{1-F_L} \text{ and}$$

$$P'_{4,5,6,8} = \frac{S_{4,5,7,8}}{\sqrt{F_L(1-F_L)}}.$$

$B^0 \rightarrow K^{*0}(890)(\rightarrow K^+\pi^-)\mu^+\mu^-$ from LHCb

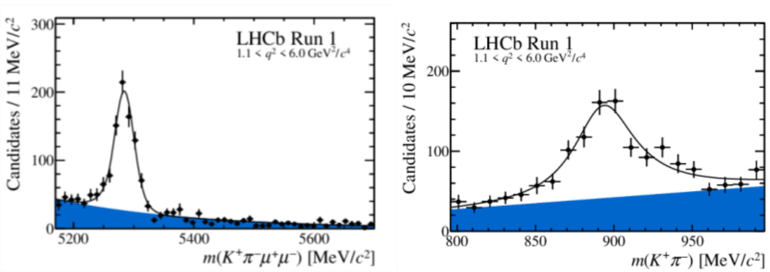

PRL **125**, 011802 (2020)

4.7 fb^{-1}

cos θ_ℓ

cos θ_k

ϕ

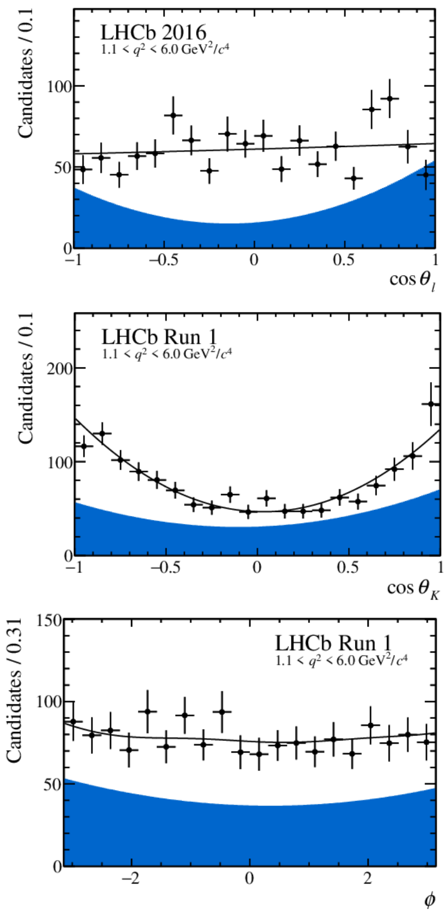

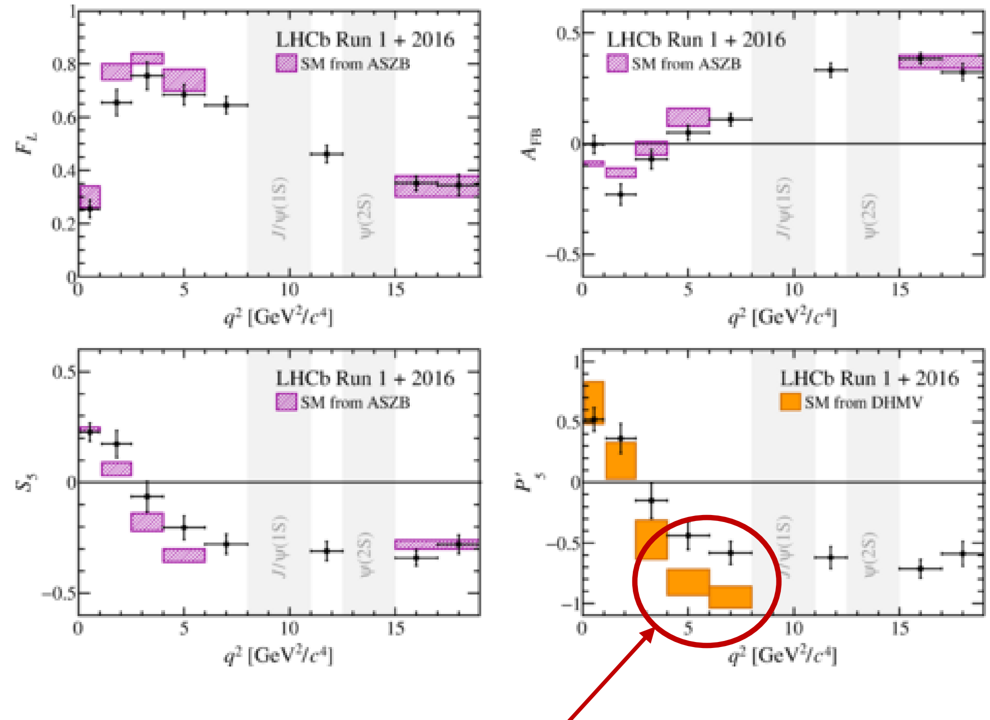

- This shows the small tension in P_5' that has caused excitement. Note the excluded regions in q^2.

$B^o \rightarrow K^{*o}(890)(\rightarrow K^+\pi^-)\mu^+\mu^-$ from CMS and ATLAS

Similar distributions from CMS and ATLAS.

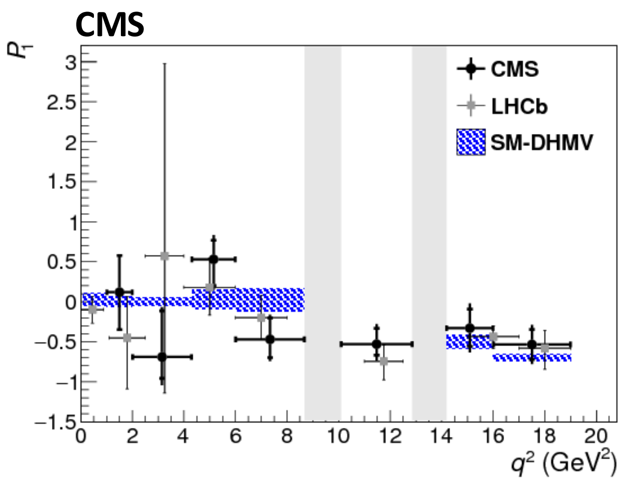

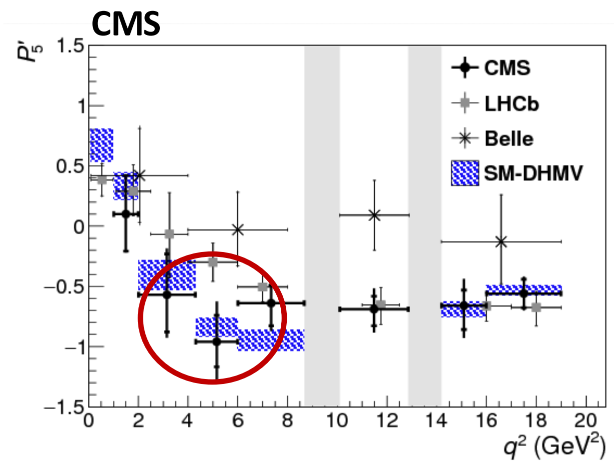

[Physics Letters B](#), [Vol. 781](#), 10 June 2018, Pages 517-541

CMS result at 8 TeV

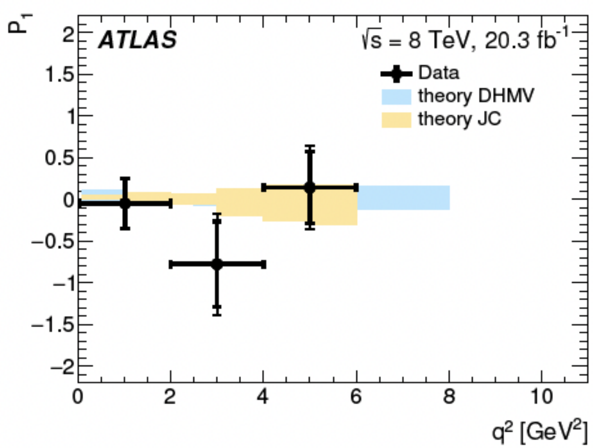

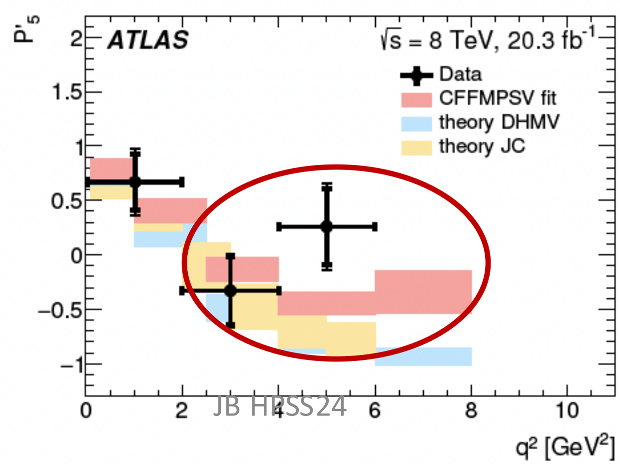

[*JHEP* 10 (2018) 047](#)

CMS Analysis of 140 fb^{-1} at 13 TeV

[CMS PAS BPH-21-002]

- Mass and angular distributions for $4.3<q^2<6$ GeV^2

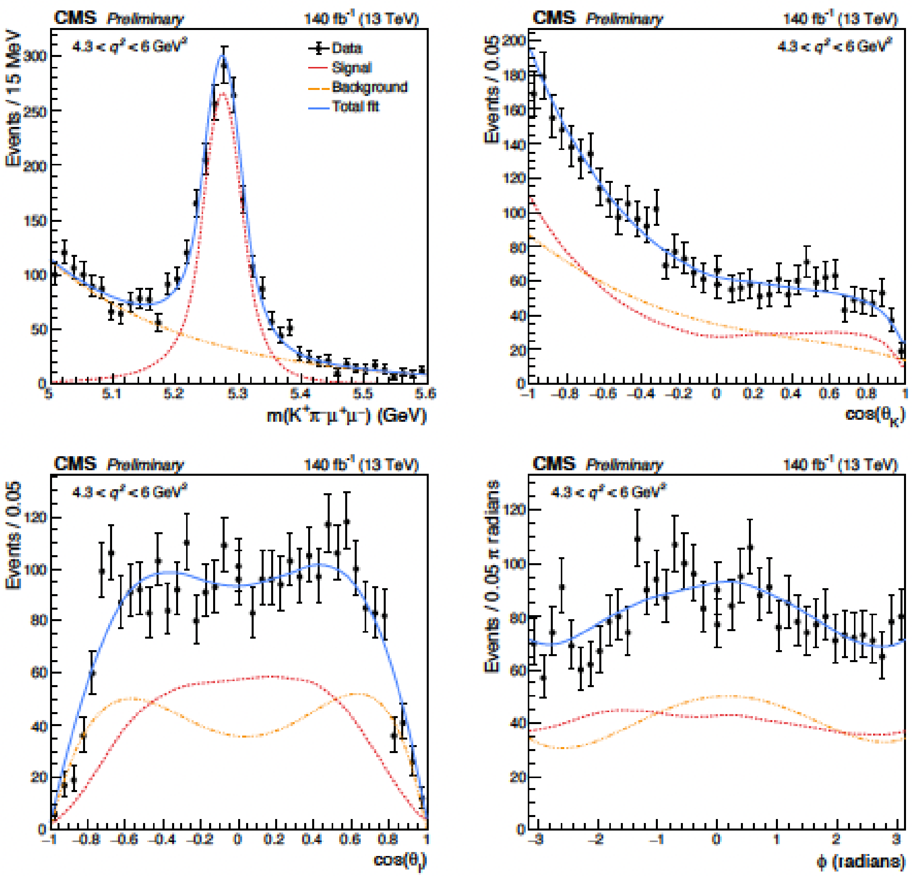

s

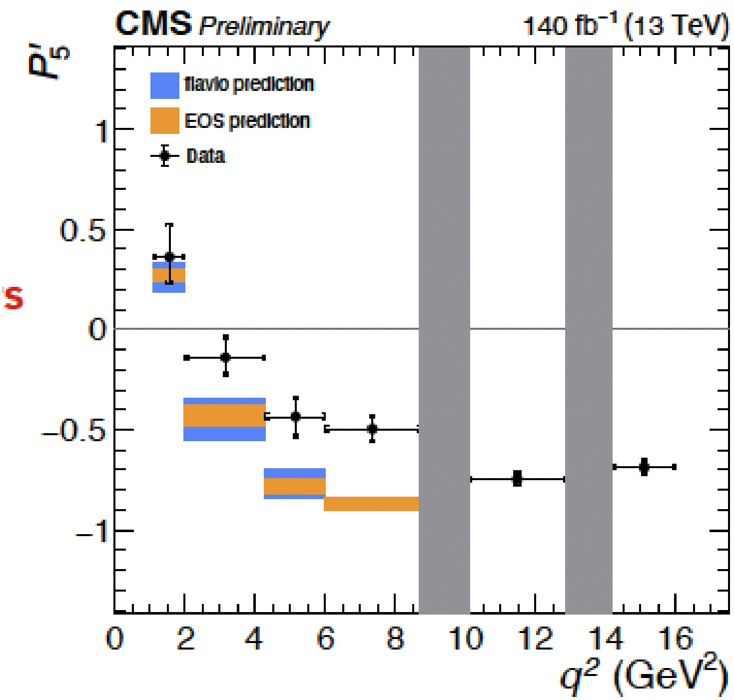

CMS Analysis of 140 fb^{-1} at 13 TeV

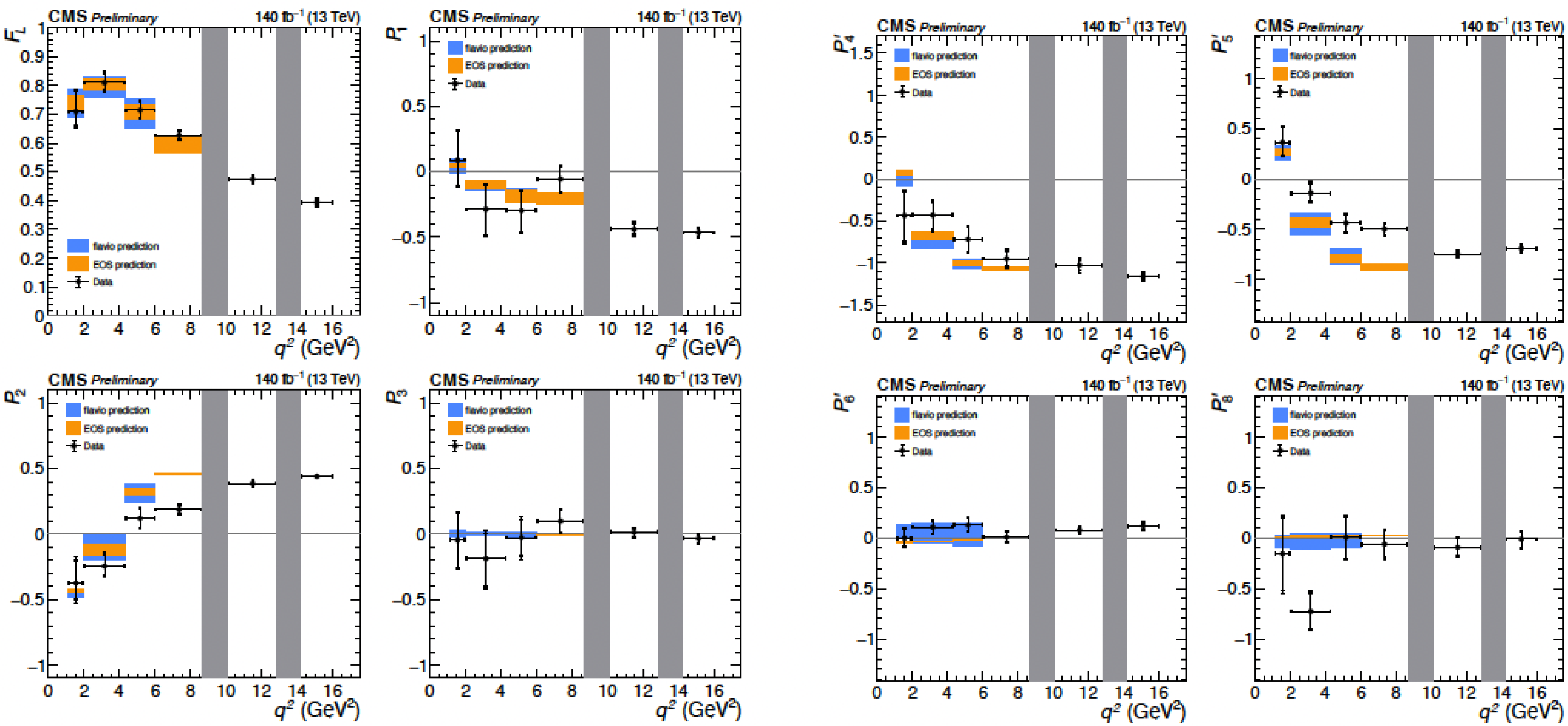

Measured CP averaged angular observables. CMS data at 13 TeV indicates some tension with SM prediction for P5'.

Comparison with previous results

New!! $B^0 \to K^{*0}\mu^+\mu^-$ with 140 fb^{-1} from CMS

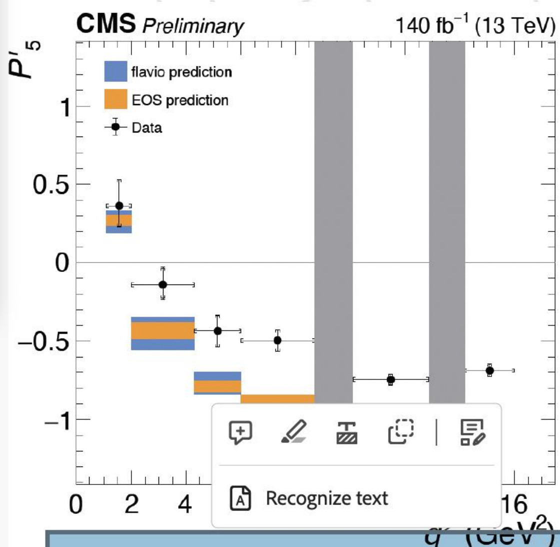

Table 1: Preliminary results, CMS Run 2

	$1.1 < q^2 < 2$ GeV^2	$2 < q^2 < 4.3$ GeV^2	$4.3 < q^2 < 6$ GeV^2
F_L	$0.709^{+0.073}_{-0.054} \pm 0.021$	$0.810^{+0.036}_{-0.030} \pm 0.016$	$0.714^{+0.032}_{-0.030} \pm 0.012$
P_1	$0.089^{+0.234}_{-0.204} \pm 0.040$	$-0.285^{+0.187}_{-0.208} \pm 0.051$	$-0.297^{+0.153}_{-0.168} \pm 0.038$
P_2	$-0.374^{+0.173}_{-0.125} \pm 0.095$	$-0.244^{+0.094}_{-0.077} \pm 0.039$	$0.121^{+0.080}_{-0.076} \pm 0.030$
P_3	$-0.045^{+0.209}_{-0.216} \pm 0.044$	$-0.187^{+0.196}_{-0.218} \pm 0.089$	$-0.027^{+0.143}_{-0.143} \pm 0.081$
P'_4	$-0.436^{+0.289}_{-0.323} \pm 0.111$	$-0.431^{+0.160}_{-0.185} \pm 0.075$	$-0.717^{+0.154}_{-0.158} \pm 0.074$
P'_5	$0.363^{+0.165}_{-0.132} \pm 0.028$	$-0.139^{+0.103}_{-0.087} \pm 0.039$	$-0.435^{+0.096}_{-0.101} \pm 0.027$
P'_6	$0.000^{+0.094}_{-0.097} \pm 0.021$	$0.108^{+0.075}_{-0.071} \pm 0.018$	$0.129^{+0.074}_{-0.071} \pm 0.011$
P'_8	$-0.157^{+0.368}_{-0.369} \pm 0.113$	$-0.727^{+0.193}_{-0.184} \pm 0.056$	$0.007^{+0.215}_{-0.216} \pm 0.036$
	$6 < q^2 < 8.68$ GeV^2	$10.09 < q^2 < 12.86$ GeV^2	$14.18 < q^2 < 16$ GeV^2
F_L	$0.627^{+0.016}_{-0.016} \pm 0.011$	$0.474^{+0.011}_{-0.013} \pm 0.009$	$0.394^{+0.012}_{-0.012} \pm 0.009$
P_1	$-0.056^{+0.101}_{-0.102} \pm 0.046$	$-0.439^{+0.051}_{-0.047} \pm 0.030$	$-0.465^{+0.037}_{-0.037} \pm 0.025$
P_2	$0.188^{+0.039}_{-0.040} \pm 0.014$	$0.386^{+0.021}_{-0.019} \pm 0.018$	$0.440^{+0.008}_{-0.010} \pm 0.008$
P_3	$0.099^{+0.092}_{-0.090} \pm 0.014$	$0.013^{+0.041}_{-0.043} \pm 0.007$	$-0.034^{+0.037}_{-0.038} \pm 0.010$
P'_4	$-0.949^{+0.102}_{-0.101} \pm 0.058$	$-1.025^{+0.064}_{-0.066} \pm 0.059$	$-1.159^{+0.042}_{-0.038} \pm 0.041$
P'_5	$-0.495^{+0.067}_{-0.067} \pm 0.023$	$-0.746^{+0.033}_{-0.032} \pm 0.014$	$-0.688^{+0.038}_{-0.036} \pm 0.021$
P'_6	$0.010^{+0.052}_{-0.052} \pm 0.016$	$0.080^{+0.037}_{-0.041} \pm 0.011$	$0.121^{+0.040}_{-0.039} \pm 0.011$
P'_8	$-0.061^{+0.143}_{-0.143} \pm 0.042$	$-0.093^{+0.104}_{-0.094} \pm 0.029$	$-0.011^{+0.086}_{-0.089} \pm 0.022$

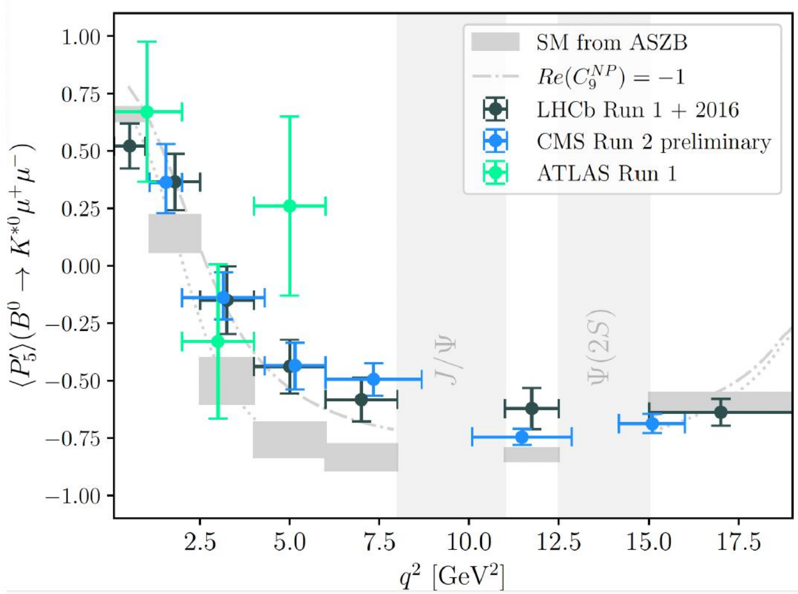

47

Proposed standard q^2 intervals

- Since it is important to be able to compare, and ultimately to combine, experimental results, it would help in combining if all experiments used the same q^2 intervals
- This is a proposal

Bin	q^2 range [GeV^2]
1	1.1 - 4.0
2	4.0 - 6.0
3	6.0 - 8.0
4 (J/ψ)	8.0 - 11.0
5	11.0 - 12.5
6 ($\psi(2S)$)	12.5 - 15.0
7	15.0 - 17.0
8	17.0 - 23.0

Why have a theory framework?

- A theory framework can help us get an integrated view of results across various states under study and across experiments
  - There have been times that we have found (in some case by purposeful research, others by good intuition, and sometimes by stumbling around) a discovery based on one big, impressive signal
    - We can't always count on that
    - Even then, there have sometimes been early indications from other than the "smoking gun" state that may have helped the research converge, e.g. for J/psi.
  - We may see small tensions w.r.t. the SM appear at about the same level in several states.
    - If we could connect the dots, the statistical significance of an ensemble of measurements might be quite large even though no one channel rises to the level of discovery
      - This has happened for example is piecing together some of the Higgs couplings
    - Of course, issues like selection bias and look elsewhere effect would come into play
    - However, if used more to guide additional data taking and analysis work rather than claiming a discovery, this could be very productive, maybe even critical.

Theory Framework

- SM and NP contributions to rare decays can be described by the effective Hamiltonian framework, which provides a model-independent description based on the Wilson coefficients of dimension 6 operators:

$$\mathcal{H}_{\rm eff} = -\frac{4G_F}{\sqrt{2}} V_{tb} V_{ts}^* \frac{\alpha}{4\pi} \sum_i \left[(C_i^{\rm SM} + \Delta C_i) O_i + \Delta C_i' O_i' \right],$$

- The most important operators for these decays are

$$\begin{aligned} O_7 &= \frac{1}{e}(\bar{s}\sigma_{\mu\nu}P_R b)F^{\mu\nu}, \\ O_9 &= (\bar{s}\gamma_\mu P_L b)(\bar{\ell}\gamma^\mu \ell), \\ O_{10} &= (\bar{s}\gamma_\mu P_L b)(\bar{\ell}\gamma^\mu\gamma_5 \ell), \\ O_S &= m_b(\bar{s}P_R b)(\bar{\ell}\ell), \\ O_P &= m_b(\bar{s}P_R b)(\bar{\ell}\gamma_5 \ell), \end{aligned} \qquad \begin{aligned} O_7' &= \frac{1}{e}(\bar{s}\gamma_\mu P_L b)F^{\mu\nu}, \\ O_9' &= (\bar{s}\gamma_\mu P_R b)(\bar{\ell}\gamma^\mu \ell), \\ O_{10}' &= (\bar{s}\gamma_\mu P_R b)(\bar{\ell}\gamma^\mu\gamma_5 \ell), \\ O_S' &= m_b(\bar{s}P_L b)(\bar{\ell}\ell), \\ O_P' &= m_b(\bar{s}P_L b)(\bar{\ell}\gamma_5 \ell). \end{aligned}$$

- The operators $O_{9,10}$ are SM operators. ΔC_i are deviations to the SM coefficients.
- The primed operators $O'_{9,10}$ are NP operators. $\Delta C_i'$ are deviations to the caused by the NP operators
- The strategy is to compare the values observed in the data for these coefficients with the SM predictions.

Searching for new physics

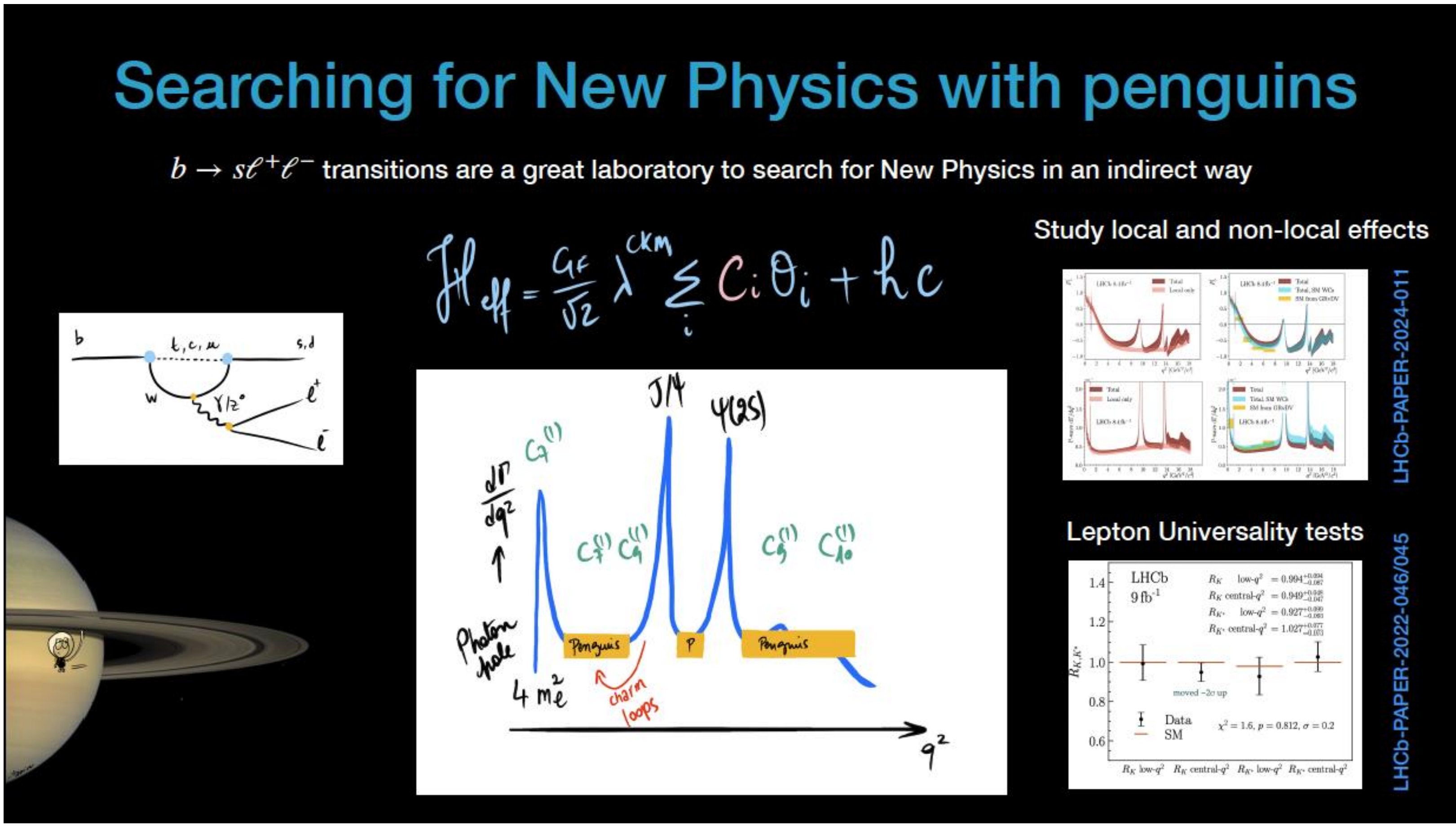

B→K*e^+e^- from LHCb

Angular analysis of $B \to K^* e^+ e^-$

4D unbinned weighted fit to the mass and angular distributions

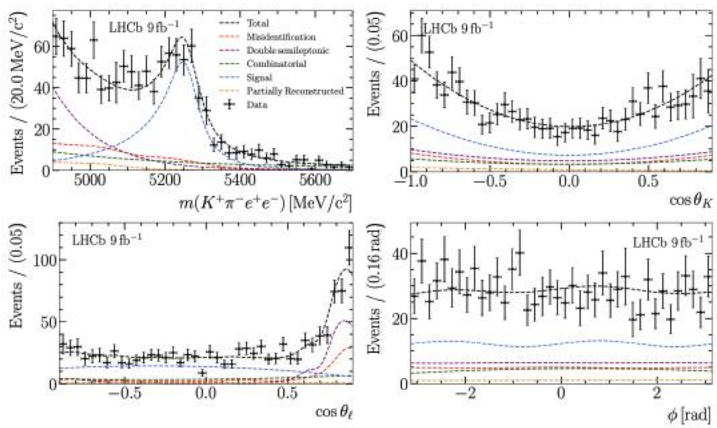

Allows the extraction of the angular observable in the central q^2 region

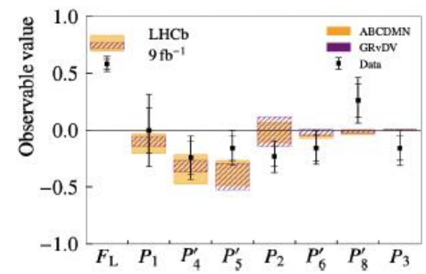

$Q_i = P_i^{(\mu)} - P_i^{(e)}$

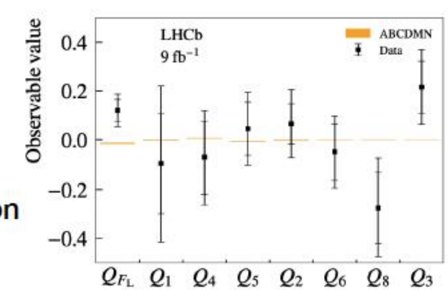

LHCb-PAPER-2024-022 in preparation

Most precise determination of angular observables and no sign of lepton flavour violating effects are observed

Prospects for $b \rightarrow s\, \mu^+\mu^-$ decays

- A large amount of work is being done on these channels and much progress has been made in last few years
  - New decay channels have been opened up, especially by LHCb, but some are accessible to ATLAS and CMS, such as $B_d \rightarrow \phi\, \mu^+\mu^-$
- LHCb has reported also on
  - $\Lambda_b \rightarrow \Lambda, \Lambda$ (1520) (pK) $\mu^+\mu^-$ fromLHCb arXiv:2302.08262
  - $B_s \rightarrow \phi(k^+k^-)\mu^+\mu^-$ from LHCb
    Phys. Rev. Lett. 127 (2021) 151801 , *JHEP* 2111 (2021) 043
- Whether or not any current hints survive, this path of searching for NP will remain promising and should be pursued
  - We have not even done all the analysis with data from Run 1 and 2, with only a few measurements using the full luminosity available and some are not started
  - We will have 2-3x more data by the end of Run 3 and 20x more by the end of the HL-LHC, bringing new decays and observables to the fore
  - It will be challenging to maintain the data quality because of radiation damage and aging of the detector which must continue to handle high rate and pileup
- Theoretical predictions need to be improved
- If some indications arise from a study based on a theory framework, it can be pursued with ever expanding amounts of data!!!!

Case Study 3: CP Violation in $B_s \rightarrow J/\psi\phi$

Motivations

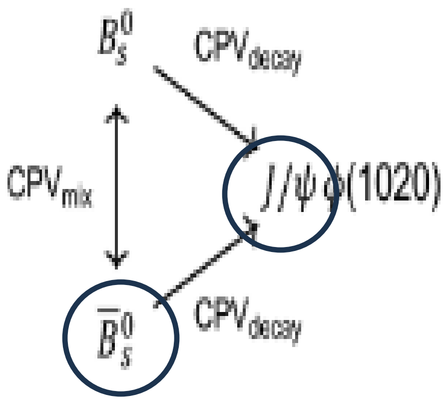

(This is the sketch I do not like)

$$\Gamma\left(B^0_{s\,(\rightsquigarrow \bar{B}^0_s)} \to f\right)(t) \overset{?}{\neq} \Gamma\left(\bar{B}^0_{s\,(\rightsquigarrow B^0_s)} \to f\right)(t)$$

- **B_s meson decays allow us to study the time-dependent CP violation generated by the interference between direct decays and flavor mixing**
  - CPV in the interference is possible even if there is no CPV in decay alone and mixing Alone
- **The weak phase ϕ_s is the main CPV observable**
  - β_s determined by CKM global fits to be $\boldsymbol{\phi_s \approx -2\beta_s}$

$$\phi_s^{SM} \simeq -37 \pm 1 \text{ mrad} \qquad \Delta\Gamma_s^{SM} = 0.091 \pm 0.013 \text{ ps}^{-1}$$

s

- New physics can change the value of ϕ_s up to ~100% via new particles contributing to the flavor oscillations [RMP88(2016)045002]

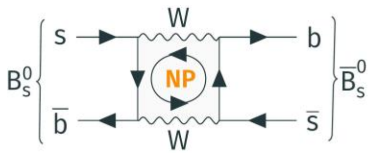

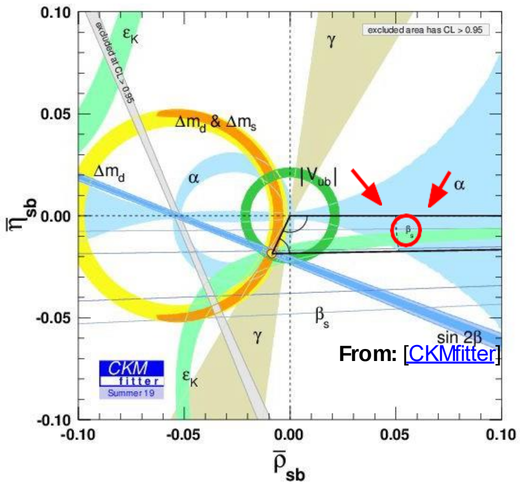

From: [CKMfitter]

We therefore study $B_s \to J/\psi\ \phi(1020) \to \mu^+\mu^- K^+K^-$

- Neglecting contributions from higher-order diagrams ($\Delta\varphi^{loop} \approx 3\pm10$ mrad)

A long history: flagship CPV analysis at LHC

- ϕ_s has been **first measured** by the **Tevatron** experiments D0 and CDF
- At LHC ϕ_s has been measured several times by ATLAS, LHCb, and CMS
  - LHCb has measured ϕ_s in several other channels, such as $B_s \to J/\psi\, \pi^+\pi^-$, $B_s \to J/\psi(e^+e^-)\, K^+K^-$, $B_s \to \psi\, K^+K^-$, $B_s \to D_s^+ D_s^-$, …
- Preliminary world-average (before this work): $\phi^{J/\psi KK} = -50 \pm 17$ mrad [JevticLiCERNSeminar(2023)]

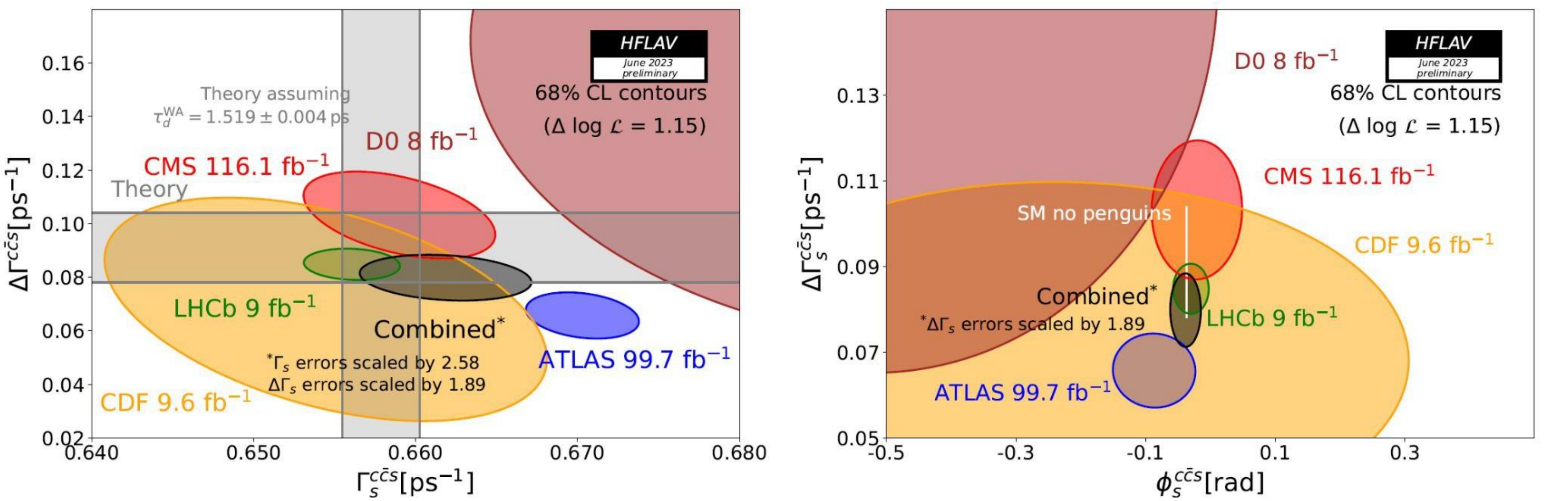

From: [Jevtic and Li, CERN seminar (2023)]

A time-, flavor- and angular-dependent measurement

final-state CP eigenvalue → CP violation → flavor oscillations

$$a_{CP}(t) = \frac{-\eta_{fs}\sin(\phi_s)\sin(\Delta m_s t)}{\cosh(\frac{1}{2}\Delta\Gamma_s t) - \eta_{fs}\cos(\phi_s)\sinh(\frac{1}{2}\Delta\Gamma_s t)}$$

Core ingredients

- **Time-dependent angular analysis** to separate the CP eigenstates
- "transversity basis" is used because it separates the various angular momenta between the J/ψ and ϕ
- **Time-dependent flavor analysis** to resolve the rapid B mixing oscillations (T ~ 350 fs)

$$\text{sensistivity} \propto \sqrt{\frac{\epsilon_{tag}\mathcal{D}^2_{tag}N_{sig}}{2}}\sqrt{\frac{N_{sig}}{N_{sig}+N_{bkg}}}\,e^{-\frac{\sigma_t^2\Delta m_s^2}{2}}$$

Transversity basis

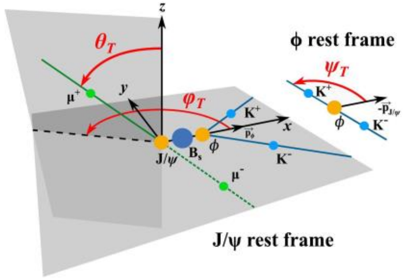

Decay rate for a CP-even final state

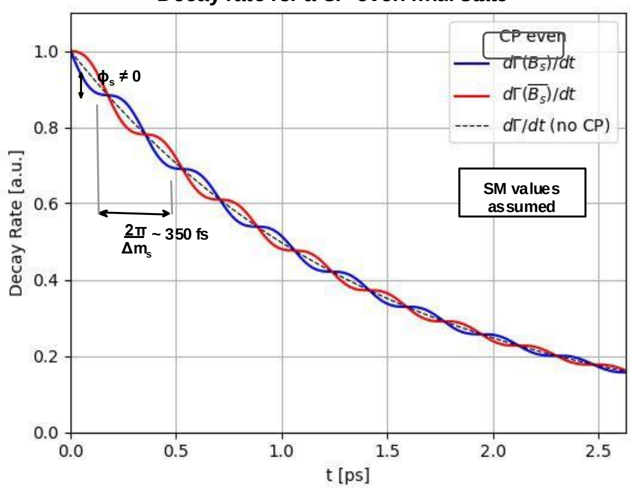

Decay rate model

Flavor tag decision (flips c_i and d_i signs)

Mistag probability

Decay time

$$\frac{d^4\Gamma(B_s)}{d\Theta dt} \propto \sum_{i=1}^{10} \mathcal{O}_i(t,\alpha)\, g_i(\Theta)$$

$$\mathcal{O}_i(t,\alpha) = N_i e^{-\Gamma_s t}\left[a_i \cosh\left(\frac{\Delta\Gamma_s t}{2}\right) + b_i \sinh\left(\frac{\Delta\Gamma_s t}{2}\right) + c_i\xi(1-2\omega)\cos(\Delta m_s t) + d_i\xi(1-2\omega)\sin(\Delta m_s t)\right]$$

Angular variables

Most sensitive terms for SM ϕ_s

i	$g_i(\theta_T,\psi_T,\varphi_T)$	N_i	a_i	b_i	c_i	d_i
1	$2\cos^2\psi_T(1-\sin^2\theta_T\cos^2\varphi_T)$	$\|A_0(0)\|^2$	1	D	C	$-S$
2	$\sin^2\psi_T(1-\sin^2\theta_T\sin^2\varphi_T)$	$\|A_\parallel(0)\|^2$	1	D	C	$-S$
3	$\sin^2\psi_T\sin^2\theta_T$	$\|A_\perp(0)\|^2$	1	$-D$	C	S
4	$-\sin^2\psi_T\sin 2\theta_T\sin\varphi_T$	$\|A_\parallel(0)\|\|A_\perp(0)\|$	$C\sin(\delta_\perp-\delta_\parallel)$	$S\cos(\delta_\perp-\delta_\parallel)$	$\sin(\delta_\perp-\delta_\parallel)$	$D\cos(\delta_\perp-\delta_\parallel)$
5	$\frac{1}{\sqrt{2}}\sin 2\psi_T\sin^2\theta_T\sin 2\varphi_T$	$\|A_0(0)\|\|A_\parallel(0)\|$	$\cos(\delta_\parallel-\delta_0)$	$D\cos(\delta_\parallel-\delta_0)$	$C\cos(\delta_\parallel-\delta_0)$	$-S\cos(\delta_\parallel-\delta_0)$
6	$\frac{1}{\sqrt{2}}\sin 2\psi_T\sin 2\theta_T\cos\varphi_T$	$\|A_0(0)\|\|A_\perp(0)\|$	$C\sin(\delta_\perp-\delta_0)$	$S\cos(\delta_\perp-\delta_0)$	$\sin(\delta_\perp-\delta_0)$	$D\cos(\delta_\perp-\delta_0)$
7	$\frac{2}{3}(1-\sin^2\theta_T\cos^2\varphi_T)$	$\|A_S(0)\|^2$	1	$-D$	C	S
8	$\frac{1}{3}\sqrt{6}\sin\psi_T\sin^2\theta_T\sin 2\varphi_T$	$k_{SP}\|A_S(0)\|\|A_\parallel(0)\|$	$C\cos(\delta_\parallel-\delta_S)$	$S\sin(\delta_\parallel-\delta_S)$	$\cos(\delta_\parallel-\delta_S)$	$D\sin(\delta_\parallel-\delta_S)$
9	$\frac{1}{3}\sqrt{6}\sin\psi_T\sin 2\theta_T\cos\varphi_T$	$k_{SP}\|A_S(0)\|\|A_\perp(0)\|$	$\sin(\delta_\perp-\delta_S)$	$-D\sin(\delta_\perp-\delta_S)$	$C\sin(\delta_\perp-\delta_S)$	$S\sin(\delta_\perp-\delta_S)$
10	$\frac{4}{3}\sqrt{3}\cos\psi_T(1-\sin^2\theta_T\cos^2\varphi_T)$	$k_{SP}\|A_S(0)\|\|A_0(0)\|$	$C\cos(\delta_0-\delta_S)$	$S\sin(\delta_0-\delta_S)$	$\cos(\delta_0-\delta_S)$	$D\sin(\delta_0-\delta_S)$

$$C = \frac{1-|\lambda|^2}{1+|\lambda|^2} \qquad S = -\frac{2|\lambda|\sin\phi_s}{1+|\lambda|^2} \qquad D = -\frac{2|\lambda|\cos\phi_s}{1+|\lambda|^2}$$

Sensitive to direct CPV

Sensitive to $\phi_s \sim 0$

Sensitive to $\phi_s \sim \pi/2$

Conventions

- $|A_\parallel|^2 = |A_0|^2 - |A_\perp|^2$
- $\delta_0 = 0$
- $\delta_{S\perp} = \delta_S - \delta_\perp$
- $\Delta\Gamma_s > 0$

Physics parameters

- ϕ_s, $|\lambda|$
- $\Delta\Gamma_s$, Γ_s, Δm_s
- $|A_0|^2$, $|A_\perp|^2$, $|A_S|^2$
- $\delta_\parallel$, $\delta_\perp$, $\delta_{S\perp}$

S-P wave effective coupling
$k_{SP} \approx 0.54$

- Introduced since $m(K^+K^-)$ is not fitted
- Evaluated from the S- and P-wave lineshape interference

Proper Time Dependent Angular Distribution!

- The B_s has two components because of the mass splitting.
- The heavy one is CP even and has a shorter lifetime.
- They each have their own angular distribution but the overall distribution changes with the proper time as the ratio of heavy to light changes

$$\frac{d^2\Gamma}{d\cos\theta\, dt} = \tfrac{3}{8}p(t)(1+\cos^2\theta) + \tfrac{3}{4}m(t)\sin^2\theta$$
$$= \tfrac{3}{8}[p(t)+2m(t)] + \tfrac{3}{8}[p(t)-2m(t)]\cos^2\theta\,,$$

As the balance shifts with time towards the longer-lived state, this term becomes more prominent

Where:

$$p(t) = p(0)e^{-\Gamma_L t} \quad (\text{CP even})\,,$$
$$m(t) = m(0)e^{-\Gamma_H t} \quad (\text{CP odd})\,,$$

So that the probability of having a CP-even (CP –odd) state at proper time t is”

p(t)/(p(t) + m(t))

The normalization of the angular distributions are: $\frac{d\Gamma}{dt} = \int_{-1}^{1} d(\cos\theta)\frac{d^2\Gamma}{d\cos\theta\, dt} = p(t) + m(t)\,.$

Trigger strategy

PLB816(2021)136188 (superseded)

Muon-tagging **trigger**

- $J/\psi \rightarrow \mu^+\mu^-$ candidate plus an additional muon (for tagging)
- **≈50 000** signal candidates
- Used for time resolution modeling
- Tagging algorithms deployed: OS-muon
    - P_{tag} ~ **10%** (muon at trigger level enhance tagging efficiency)

Standard **trigger**

- Displaced $J/\psi \rightarrow \mu^+\mu^-$ candidate + $\phi(1020) \rightarrow K^+K^-$
- **≈450 000** signal candidates
- Tagging algorithms deployed: OS-muon, OS-electron, OS-jet, Same Side
    - P_{tag} ~ **5%**

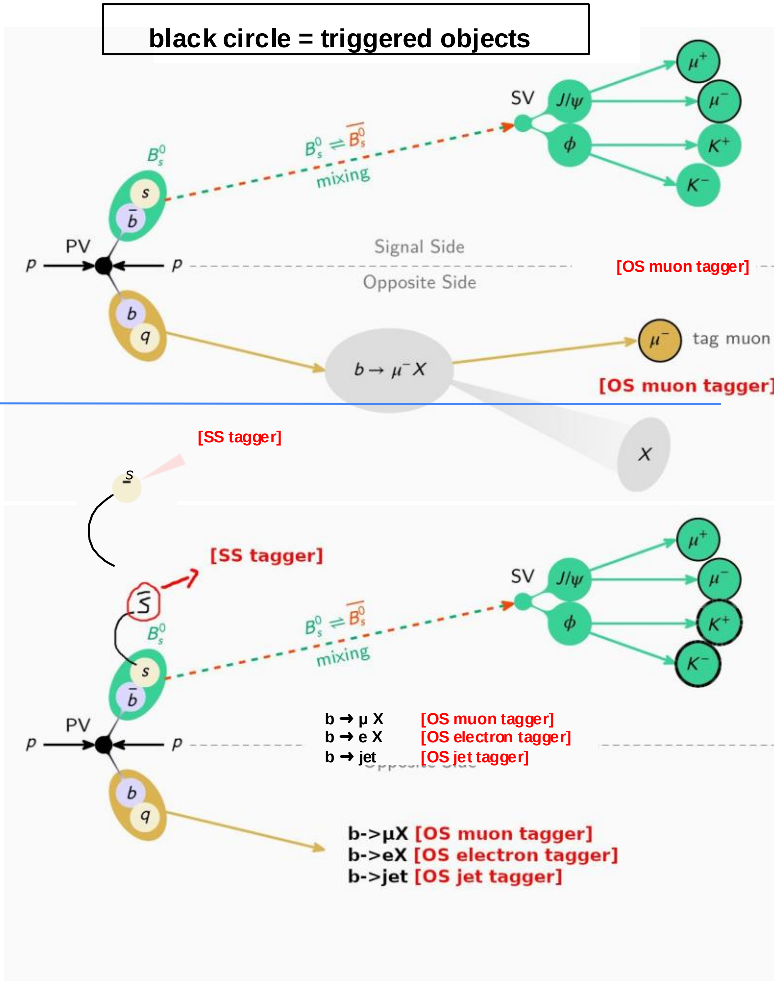

Dataset and selection

- **Dataset**: L_{int} = 96 fb^{-1} collected in 2017-2018
  - Did not use 2016 data because it very different data set (old inner tracker detector with worse time resolution and different trigger menu)
- **Signal candidates: 491 270 ± 950!**
- Notable selection requirements:

Variable	Requirement
ct (*muon-tagging* HLT)	> 60 μm
ct (*standard* HLT)	> 100 μm
ct/σ_{ct} (*standard* HLT)	> 3
$\lvert m(K^+K^-) - m_{\phi(1020)}\rvert$	< 10 MeV
$\lvert m(\mu^+\mu^-) - m_{J/\psi}\rvert$	< 150 MeV

- To avoid **overlaps**, events that pass both trigger category selections are placed only in the *muon-tagging* one
  - This depletes the *standard* trigger category of OS muons
- The PV of choice is the closest in 3D to the line that passes through the SV and parallel to the B_s momentum

Invariant mass and proper decay length distributions for the *standard* trigger (2018)

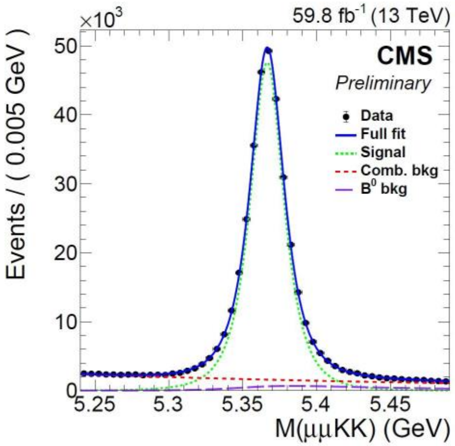

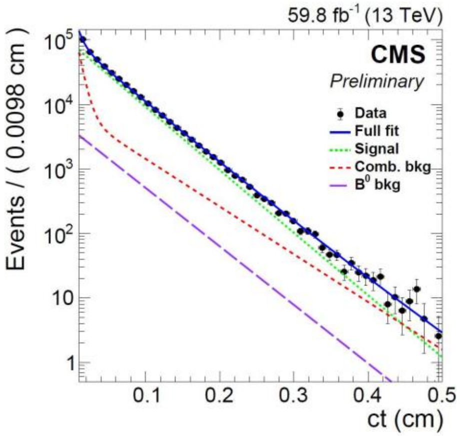

Decay time and its resolution

- The time dependence of the decay rate is parametrized with the **proper decay length** ct, measured in the transverse plane as

$$ct = c \cdot \frac{m_{Bs}^{w.a.} \cdot L_{xy}}{p_T} \quad \text{with} \quad L_{xy} \equiv ||\bar{r}_{xy}(SV) - \bar{r}_{xy}(PV)||$$

- Its **uncertainty** is obtained by fully propagating the uncertainties in L_{xy} and p_T
  - The uncertainty on L_{xy} dominates for most of the ct spectrum, with $\sigma(p_T)$ taking over at high values (ct ≳ 3 mm)
- **The ct uncertainty is calibrated in a prompt data sample** of $B_s \rightarrow J/\psi\ \phi$, obtained by removing the displacement requirement in the *muon-tagging* data sets
  - Modeled with two gaussians to obtain the effective dilution and resolution

$$\delta_{\text{eff}} = \sqrt{\frac{-2\ln\mathcal{D}}{\Delta m_s^2}} \quad \text{with} \quad \mathcal{D} = \sum_{i=1}^{2} f_i \exp\left(-\frac{\sigma_i \Delta m_s^2}{2}\right)$$

- **Excellent agreement** found, with corrections ~5%

Proper decay length uncertainty distribution for the *standard* trigger (2018)

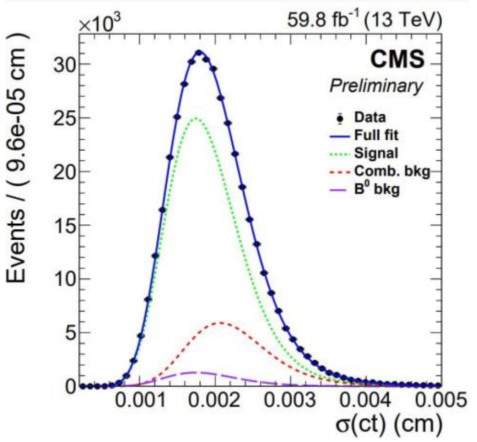

Time resolution calibration for 2018 data

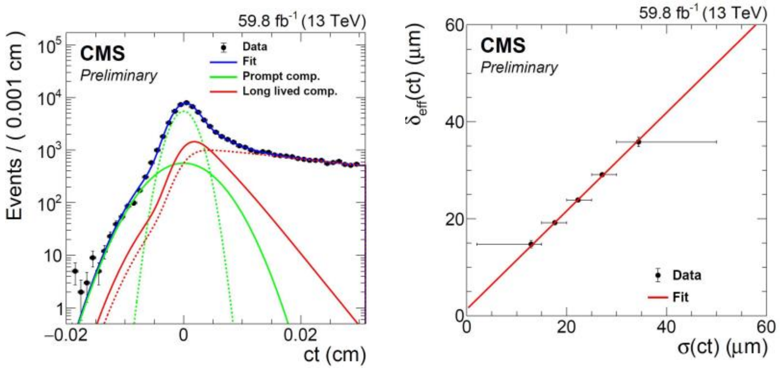

Flavor tagging overview

- A **cutting-edge flavor tagging framework** has been engineered to extract the best possible results from data
- **Four DNN-based algorithms are used**, divided into two main categories
  - **Same side (SS):** exploits the B_s fragmentation
    1. **SS tagger**: leverages charge asymmetries in the B_s fragmentation
  - **Opposite side (OS)**: exploits decay products of the other B hadron in the event
    2. **OS muon**: leverages $b \rightarrow \mu^- X$ decays
    3. **OS electron**: leverages $b \rightarrow e^- X$ decays
    4. **OS jet**: capitalizes on charge asymmetries in the OS *b*-jet
- Only the OS-muon tagger is applied in the *muon-tagging* trigger category
  - The OS-electron, OS-jet and SS are applied only to the *standard* trigger category

Schematic representation of a generic event

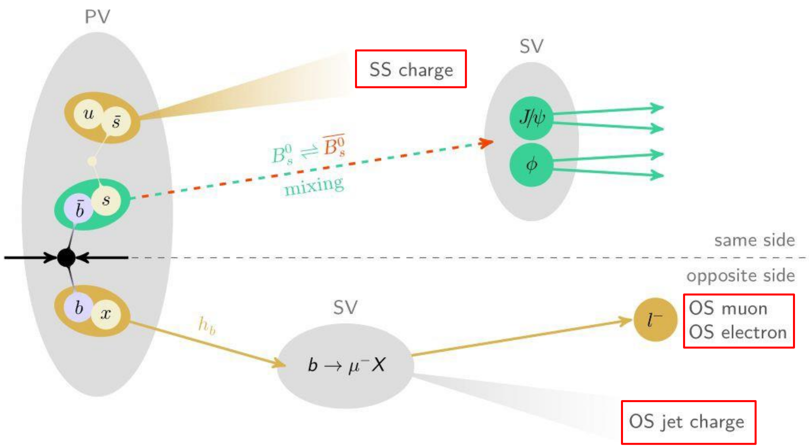

Useful definitions

$$\xi_{tag} = \begin{cases} +1 & \text{for } B_s \\ -1 & \text{for } \overline{B}_s \\ 0 & \text{if no tagging decision is made} \end{cases}$$

$$\epsilon_{tag} = \frac{N_{tag}}{N_{tot}}, \quad \omega_{tag} = \frac{N_{mistag}}{N_{tag}}, \quad \mathcal{D}_{tag} = 1 - 2\omega_{tag}, \quad P_{tag} = \epsilon_{tag}\mathcal{D}^2_{tag}$$

Flavor, neural networks, and probabilities

- The **tagging inference logic** differs between algorithms
  - **Lepton taggers** (OS muon, OS electron)
    - Lepton charge ➜ ξ_{tag}; DNN score ➜ ω_{tag} *(DNN trained for correct-tag vs mistag)*

$$\text{OS } \ell^- \to \text{OS } b \xrightarrow{\text{tag}} \text{signal } B_s$$
$$\text{OS } \ell^+ \to \text{OS } \overline{b} \xrightarrow{\text{tag}} \text{signal } \overline{B}_s$$

$$\omega_{tag} = 1 - s_{DNN}$$

DNN score

  - **Charge-based taggers** (OS jet, SS)
    - DNN score ➜ Prob(B_s) ➜ ξ_{tag}, ω_{tag} *(DNN trained for B_s vs $\overline{B}_s$)*

$$s_{DNN} > 0.5 + \epsilon \xrightarrow{tag} \text{signal } B_s \quad \text{with} \quad \omega_{tag} = 1 - s_{DNN}$$
$$s_{DNN} < 0.5 - \epsilon \xrightarrow{tag} \text{signal } \overline{B}_s \quad \text{with} \quad \omega_{tag} = s_{DNN}$$

    - ϵ is used to remove events with ω_{tag} ~ 50%
- **The algorithms are optimized and trained in simulated events and calibrated in data with self-tagging B^+ ➜ J/ψ K^+ decays**
  - **The calibration is performed by comparing ω_{tag} predicted by the DNN and the one measured in data**

OS-lepton tagging

- **OS-lepton tagging techniques search for b → ℓ^-X decays of the other B hadron in the event**
- The **charge** of the lepton is used as tagging feature and **a fully connected DNN is used to estimate the mistag probability**
- **Lepton selection**
  - Loose kinematic cuts
  - Separated from the signal B meson
  - MVA discriminator against fakes
  - OS-electrons are searched only if no OS-muon is found in the event (explicit orthogonality)
- **Mistag estimation**
  - Fully connected DNN with ReLU activation and dropout
  - Inputs: lepton kinematics and surrounding activity
- **Trained on simulated B_s → J/ψ ϕ(1020) events and calibrated in B^+ → J/ψ K^+ data**

OS-Muon calibration
(*muon-tagging* trigger 2018)

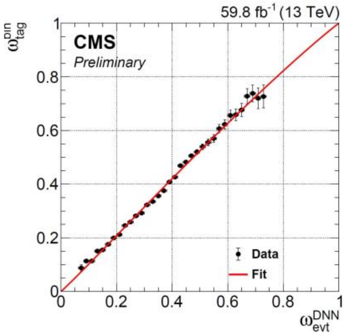

OS-Electron calibration (2018)

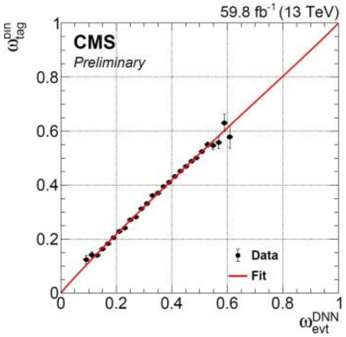

OS-jet tagging

- **The OS-jet algorithm exploits charge asymmetries in the jet structure and is based on a DNN called *DeepJetCharge***
  - Inputs: features from signal B meson, OS jet and its constituents
    - NB: The only flavor asymmetry is in the charges
  - Based on the *DeepSets* architecture [ref]
- **Jet selection**
  - No OS-lepton candidate
  - At least 2 tracks with $|IP_z| < 1$ cm
  - Separated from the signal B meson
  - jet b-tagging discriminator
- Additional nearby tracks are used due to the poor jet clustering performance in the kinematic region of interest ($p_T \lesssim 20$ GeV)
- Trained on simulated $B_s \rightarrow J/\psi\, \phi$ events and calibrated in $B^+ \rightarrow J/\psi\, K^+$ data
- **The trained network produces the probability of signal B meson containing a b quark (i.e. being a B_s)**
- The score is finally used to compute both ξ_{tag} and ω_{tag}

$$s_{DNN} > 0.52 \xrightarrow{\text{tag}} \text{signal } B_s \quad \text{with} \quad \omega_{tag} = 1 - s_{DNN}$$
$$s_{DNN} < 0.48 \xrightarrow{\text{tag}} \text{signal } \overline{B}_s \quad \text{with} \quad \omega_{tag} = s_{DNN}$$

$\omega_{tag} > 0.48 \rightarrow$ untagged

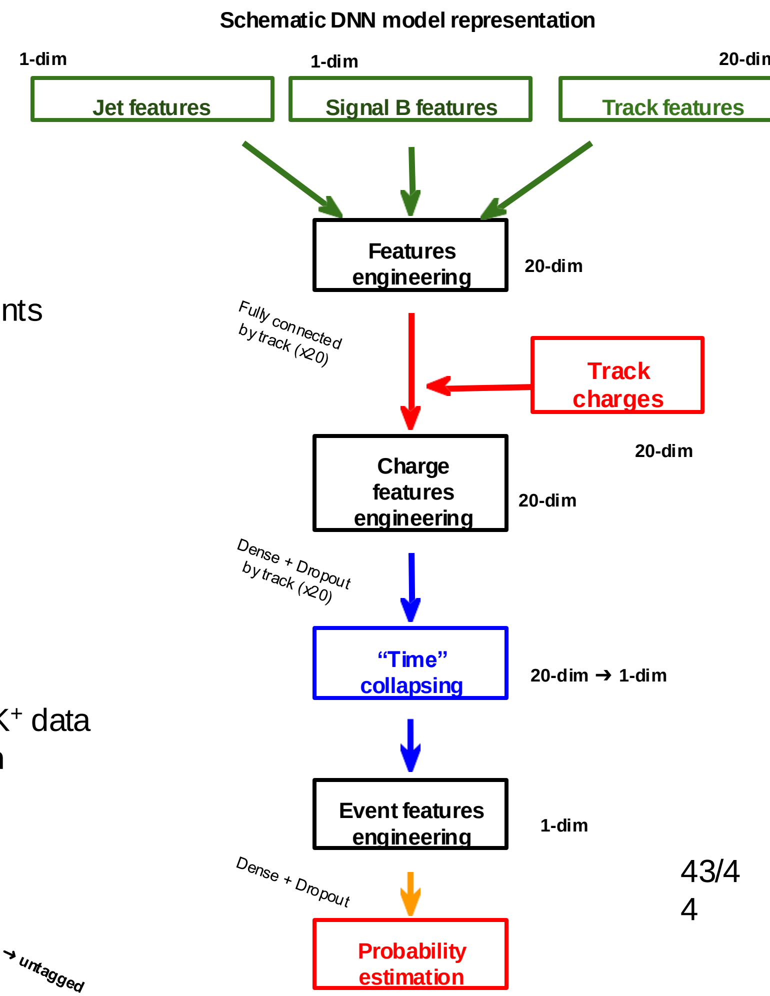

SS tagger

- **The SS tagger consists of a DNN (*DeepSSTagger*), derived from *DeepJetCharge*, able to probe the fragmentation products of a B meson and exploit tracks with high flavor correlation**
- *DeepSSTagger* uses the kinematic information from up to 20 tracks (ordered by $|IP_z|$) around the reconstructed B meson
- **Track selection**
  - $\Delta R(\text{trk}, B) < 0.8$, $|IP_z(PV)| < 0.4$ cm, $|IP_{xy}(PV)|/\sigma_{dxy} < 1$
  - Overlap with signal and OS is carefully avoided with geometrical cuts and vetos
- **Trained on an equal-weight mixture** of $B_s \rightarrow J/\psi\,\phi$ and $B^+ \rightarrow J/\psi\,K^+$ to make the model invariant for $B_s \leftrightarrow B^+$ for calibration purposes
  - Calibration directly in B_s was found to be not feasible in CMS
    - Tested: $B_s \rightarrow D_s^- \pi^+$ (not enough stat.) and $B_s^{**} \rightarrow B^{+(*)}K^-$ (too much uncer. from B^{0**} bkg)
  - The trained network produces the probability of signal B meson containing a negatively charged quark alongside the b quark (i.e., being a B_s or B^-)
- **Calibration**
  - The SS is calibrated $B^+ \rightarrow J/\psi\,K^+$ data, with residual differences ~10% corrected with simulations
  - Events with $\omega_{tag} > 0.46$ are removed before the calibration and assumed untagged

Same-side tagger calibration (B^+ data 2018)

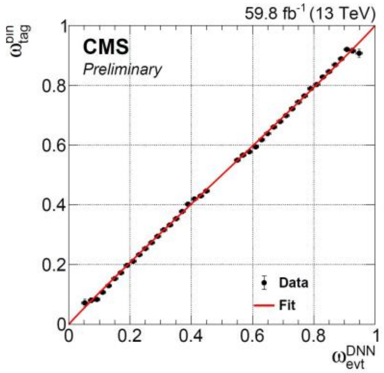

Comparison between Same-side tagger B^+ and B_s calibrations (2018)

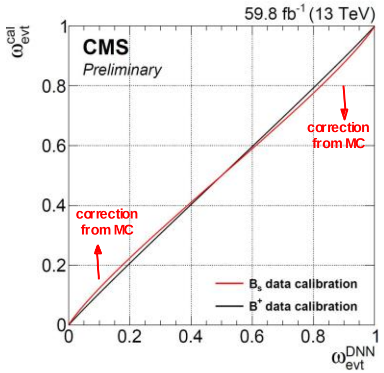

Flavor tagging performance

- The SS and any one of the OS algorithms overlap in about 20% of the events
  - In these cases, the information is combined to improve the tagging inference
- **The combined flavor tagging framework achieves a tagging power of P_{tag} = 5.6%** when applied to the B_s data sample
  - Among the highest ever recorded at LHC
  - x3~4 improvement with respect to prev. CMS results
- **This is the first CMS implementation of the OS jet and same-side tagging techniques**
  - SS accounts for half of the performance
- Largest ever effective statistics $N_{B_s} \cdot P_{tag}$ (490k · 5.6% ≈ 27.5k) for a single ϕ_s measurement
- The flavor tagging framework is validated in the $B^0 \to J/\psi K^{*0}$ data control channel with flavor mixing measurements, both integrated and time-dependent

ω_{tag} distribution in the *muon-tagging* trigger category (left) and the *standard* one (right) for 2018 data

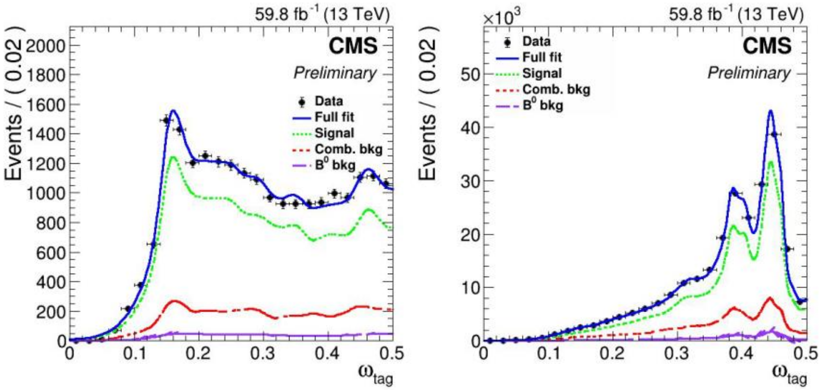

Flavor tagging performance (mutually exclusive categories)

Category	ε_{tag} [%]	$\mathcal{D}^2_{eff}$	P_{tag} [%]
Only OS muon	6.07 ± 0.05	0.212	1.29 ± 0.07
Only OS electron	2.72 ± 0.02	0.079	0.214 ± 0.004
Only OS jet	5.16 ± 0.03	0.045	0.235 ± 0.003
Only SS	33.12 ± 0.07	0.080	2.64 ± 0.01
SS + OS muon	0.62 ± 0.01	0.202	0.125 ± 0.003
SS + OS electron	2.77 ± 0.02	0.150	0.416 ± 0.005
SS + OS jet	5.40 ± 0.03	0.124	0.671 ± 0.006
Total	55.9 ± 0.1	0.100	5.59 ± 0.02

Much higher than in previous CMS analysis

Tagging validation with B^0 events

- **The flavor tagging framework is validated in the $B^0 \rightarrow J/\psi\, K^{*0}$ control channel** (~2M events)
- The time-dependent **mixing asymmetry** is measured to extract the flavor mixing oscillation frequency Δm_d with a precision of *~1%* (comparable with BaBar and Belle)
  - Excellent agreement with world-averages is observed
    - ➜ **No bias in mixing frequency measurements**
- Study performed also in each tagging category (see backup)
- The **time-integrated mixing** is also measured for each tagger and their dependency on the expected tagging dilution is compared
  - The dependency between the measured A_{mix} and the estimated D_{tag} is found to be well described by a linear relationship, indicating that all four techniques behave in the same predictable way

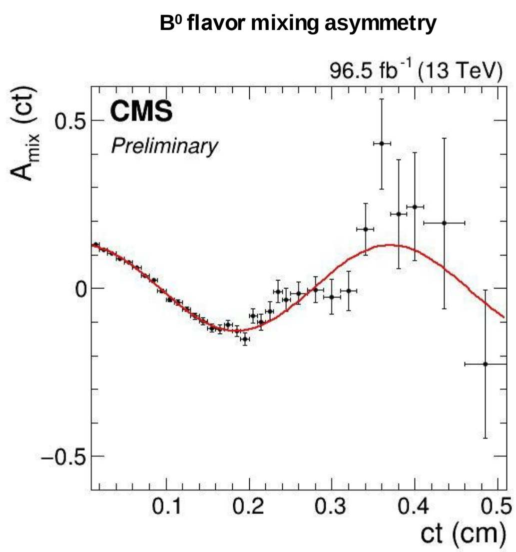

$$A_{mix}(ct) = \frac{N_{unmix}(ct) - N_{mix}(ct)}{N_{unmix}(ct) + N_{mix}(ct)}$$

Fit model

- The physics parameters are extracted with **unbinned multidimensional extended maximum-likelihood (UML) fit** performed simultaneously on **12 data sets** (2 trig. cat. x 2 years x 3 ξ_{tag} values)
  - *Physics parameters*: ϕ_s, $|\lambda|$, $\Delta\Gamma_s$, Γ_s, Δm_s, $|A_0|^2$, $|A_\perp|^2$, $|A_S|^2$, $\delta_\parallel$, $\delta_\perp$, $\delta_{S\perp}$
  - *Observables*: m_{Bs}, ct, σ_{ct}, $\cos\theta_T$, $\cos\psi_T$, ϕ_T, ω_{tag}
- **Fit model**

$$P = f_{sig} P_{sig} + f_{bkg} P_{bkg} + f_{bkg\,B^0} P_{bkg\,B^0}$$

Angular eff; $B_s \to J/\psi\,\phi$ decay rate; Observables pdfs

SIGNAL $$P_{sig} = \varepsilon(\Theta)\,[\tilde{f}(\Theta, ct \mid \alpha, \xi_{tag}, \omega_{tag}) \otimes G(ct, \sigma_{ct})]\, P_{sig}(m_{B_s})\, P_{sig}(\sigma_{ct})\, P_{sig}(\omega_{tag})$$

COMBINATORIAL BKG $$P_{bkg} = [P_{bkg}(ct) \otimes G(ct, \sigma_{ct})]\, P_{bkg}(\Theta)\, P_{bkg}(m_{B_s})\, P_{bkg}(\sigma_{ct})\, P_{bkg}(\omega_{tag})$$

$B^0 \to J/\psi K^{0*}$ BKG $$P_{bkg\,B^0} = [P_{bkg\,B^0}(ct) \otimes G(ct, \sigma_{ct})]\, P_{bkg\,B^0}(\Theta)\, P_{bkg\,B^0}(m_{B_s})\, P_{bkg\,B^0}(\sigma_{ct})\, P_{bkg\,B^0}(\omega_{tag})$$

Bkg time pdf; Time resolution convolution

- The time efficiency is implemented as a *re-weighting* of the data events to drastically improve fit time
- The statistical uncertainties and fit bias are estimated with **1300 *bootstrap* distributions**
- The yield for the **$B^0 \to J/\psi K^{*0}$ is estimated directly in data** with a 2D fit to the B_s invariant mass and its B^0 reflection
- The background from **$\Lambda_b \to J/\psi K^- p^+$ is found to be negligible** and is treated as a systematic uncertainty

Systematic uncertainty overview

	ϕ_s [mrad]	$\Delta\Gamma_s$ [ps^{-1}]	Γ_s [ps^{-1}]	Δm_s [$\hbar$ps^{-1}]	$\lvert\lambda\rvert$	$\lvert A_0\rvert^2$	$\lvert A_\perp\rvert^2$	$\lvert A_S\rvert^2$	$\delta_\parallel$ [rad]	$\delta_\perp$ [rad]	$\delta_{S\perp}$ [rad]
Statistical uncertainty	23	0.0043	0.0015	0.035	0.014	0.0016	0.0021	0.0033	0.074	0.089	0.15
Model bias	4	0.0011	0.0002	0.004	0.006	0.0012	0.0022	0.0006	0.015	0.017	0.03
Flavor tagging	4	$<10^{-4}$	0.0005	0.007	0.002	$<10^{-4}$	$<10^{-4}$	0.0006	0.012	0.016	0.03
Angular efficiency	4	0.0002	$<10^{-4}$	0.015	0.011	0.0042	0.0019	0.0001	0.017	0.044	0.02
Time efficiency	<1	0.0014	0.0026	$<10^{-3}$	$<10^{-3}$	0.0004	0.0005	$<10^{-4}$	0.001	0.002	$<10^{-2}$
Time resolution	<1	$<10^{-4}$	$<10^{-4}$	$<10^{-3}$	$<10^{-3}$	$<10^{-4}$	$<10^{-4}$	$<10^{-4}$	$<10^{-3}$	0.001	$<10^{-3}$
Model assumptions	—	0.0005	0.0006	—	—	—	—	—	—	—	—
B^0 background	<1	0.0002	0.0003	$<10^{-3}$	$<10^{-3}$	$<10^{-4}$	$<10^{-4}$	$<10^{-4}$	$<10^{-3}$	$<10^{-3}$	$<10^{-2}$
Λ_b^0 background	—	—	0.0004	—	—	0.0004	0.0003	—	—	—	—
S-*P* wave interference	<1	$<10^{-4}$	$<10^{-4}$	$<10^{-3}$	$<10^{-3}$	$<10^{-4}$	$<10^{-4}$	$<10^{-4}$	$<10^{-3}$	$<10^{-3}$	$<10^{-2}$
$P(\sigma_{ct})$ uncertainty	<1	0.0002	0.0003	$<10^{-3}$	$<10^{-3}$	0.0001	0.0001	$<10^{-4}$	$<10^{-3}$	$<10^{-3}$	$<10^{-2}$
Total systematic uncertainty	7	0.0019	0.0028	0.017	0.012	0.0044	0.0030	0.0009	0.025	0.050	0.05

- **Model bias, flavor tagging, and angular efficiency are found to be the leading systematic sources for ϕ_s**
- **The measurement is still heavily statistically limited for ϕ_s**

Cross check: fit with individual tagging techniques

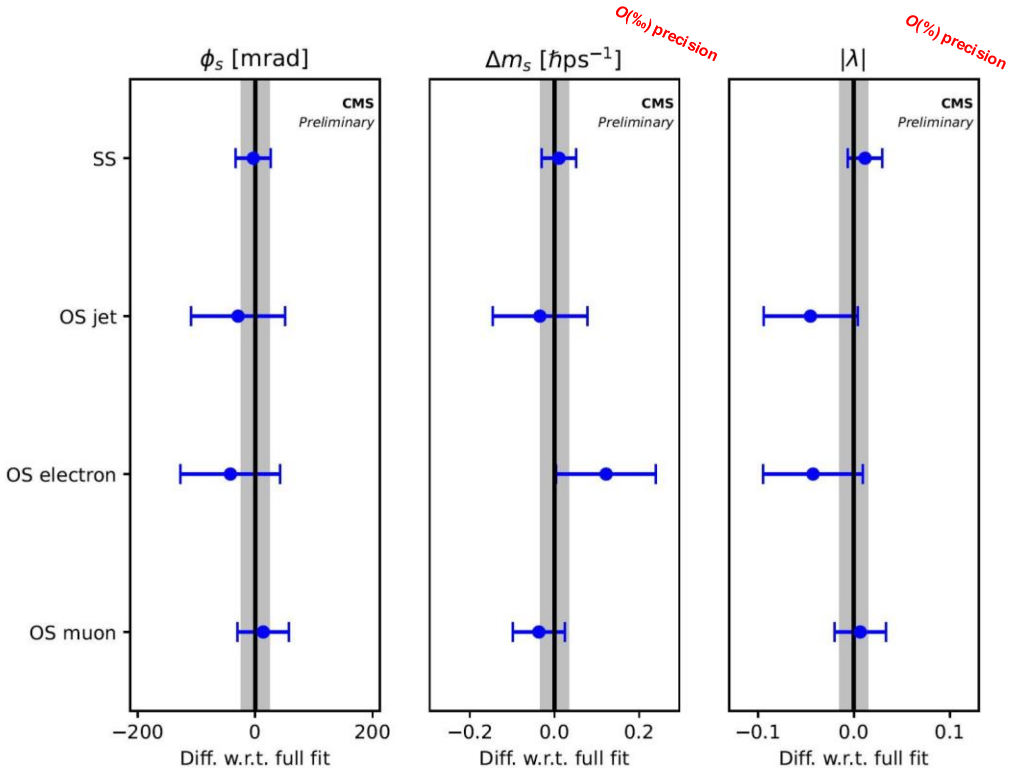

- **To check the consistency and stability of the tagging framework, the fit to data is repeated with only one tagging algorithm deployed at a time**
  - The grey area represents the result and statistical uncertainty of the full fit
  - Only flavor-sensitive parameters are presented
- **Excellent agreement between the various tagging techniques**

Results

Fit results

Parameter	Fit value	Stat. uncer.	Syst. uncer.
ϕ_s [mrad]	-73	$\pm\,23$	$\pm\,7$
$\Delta\Gamma_s$ [ps^{-1}]	0.0761	$\pm\,0.0043$	$\pm\,0.0019$
Γ_s [ps^{-1}]	0.6613	$\pm\,0.0015$	$\pm\,0.0028$
Δm_s [$\hbar$ps^{-1}]	17.757	$\pm\,0.035$	$\pm\,0.017$
$\|\lambda\|$	1.011	$\pm\,0.014$	$\pm\,0.012$
$\|A_0\|^2$	0.5300	$\pm\,0.0016$	$\pm\,0.0044$
$\|A_\perp\|^2$	0.2409	$\pm\,0.0021$	$\pm\,0.0030$
$\|A_S\|^2$	0.0067	$\pm\,0.0033$	$\pm\,0.0009$
$\delta_\parallel$	3.145	$\pm\,0.074$	$\pm\,0.025$
$\delta_\perp$	2.931	$\pm\,0.089$	$\pm\,0.050$
$\delta_{S\perp}$	0.48	$\pm\,0.15$	$\pm\,0.05$

Comparison with other LHC experiments

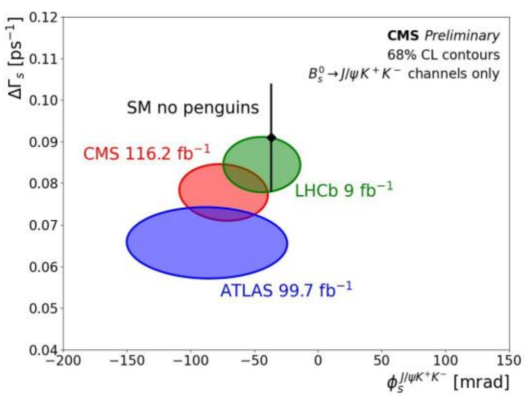

- **ϕ_s and $\Delta\Gamma_s$ are found in agreement with the SM**

  $\phi_s^{SM} \simeq -37 \pm 1$ mrad $\quad \Delta\Gamma_s^{SM} = 0.091 \pm 0.013$ ps^{-1}

- **Γ_s and Δm_s are consistent with the latest world averages**

  $\Gamma_s^{WA} = 0.6573 \pm 0.0023$ ps^{-1} $\quad \Delta m_s^{WA} = 17.765 \pm 0.006\ \hbar$ps^{-1}

- **$|\lambda|$ is consistent with no direct CPV ($|\lambda| = 1$)**

- This measurement utilizes the **largest ever** effective statistics

  N · P for a single ϕ measurement
  - The precision on ϕ_s is comparable with the world's most precise single measurement by LHCb (ϕ_s = -39 ± 22 (stat) ± 6 (syst) mrad) [PRL132(2024)051802]
  - This is the most precise single measurement of $\Delta\Gamma_s$ to date in this channel

1, 2, 3 standard deviations contours

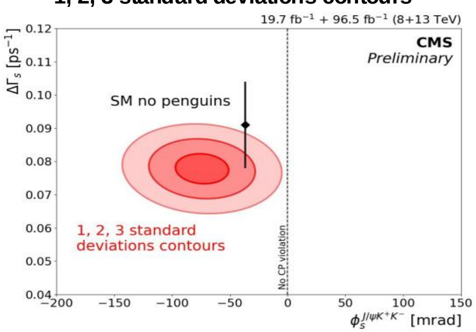

This is the first evidence of CPV in $B_s \to J/\psi\, K^+K^-$ decays

Recent associated result

$B_s \rightarrow J/\Psi\ K_s^0$

- Motivation: B_s mesons are produced in flavor eigenstates, but propagate as mass ones, which, if no **CPV** in the mixing, coincide with CP eigenstates

$$B_s^H \rightarrow \text{CP odd} \qquad B_s^L \rightarrow \text{CP even}$$

- These can have different lifetimes (as for the B_s), allowing the probe of the **mass eigenstate rate asymmetry $A_{\Delta\Gamma}$, directly related to the CPV observable λ**

$$A_{\Delta\Gamma} = \frac{R_H - R_L}{R_H + R_L} = \frac{-2\mathcal{R}(\lambda)}{1 + |\lambda|^2}$$

  - R_H and R_L are related to the untagged decay rate as

$$\Gamma(B_s \rightarrow f) + \Gamma(\overline{B}_s \rightarrow f) = R_H e^{-\Gamma_H t} + R_L e^{-\Gamma_L t}$$

- **CMS has measured of B_s effective lifetime τ in the CP-odd final state $J/\psi\ K_S$ performed with the Run 2 data set**
- This process is related to $B^0 \rightarrow J/\psi K_S$ via U-spin flavor symmetry
  - $A_{\Delta\Gamma}$ can be used to determine penguin contributions to the measurement of sin(2β)
  - The CKM angle γ can also be probed in $B_S \rightarrow J/\psi K_S$

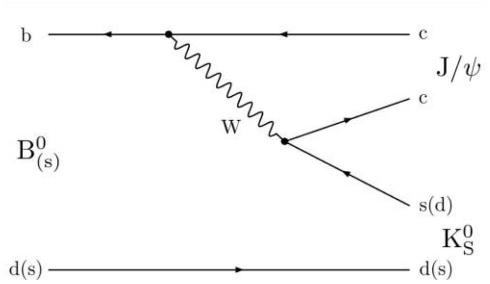

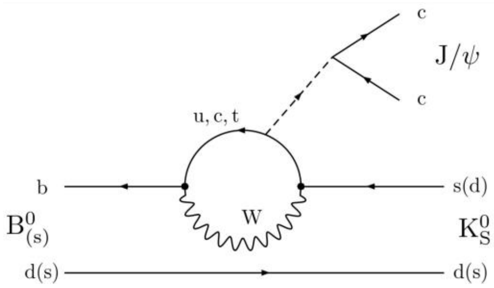

The effective lifetime

- **The effective lifetime is defined as the expected value of the untagged de**

Average lifetime

$$\tau(J/\psi K_S) \equiv \frac{\int_0^\infty t(\Gamma_{B_s\to J/\psi K_S} + \Gamma_{\overline{B}_s\to J/\psi K_S})dt}{\int_0^\infty (\Gamma_{B_s\to J/\psi K_S} + \Gamma_{\overline{B}_s\to J/\psi K_S})dt} = \frac{\tau_{B_s}}{1-y_s^2}\left(\frac{1+2A_{/}}{1+/}\right.$$

Normalized decay width difference
$y_s = \tau_{Bs}\Delta\Gamma/2$

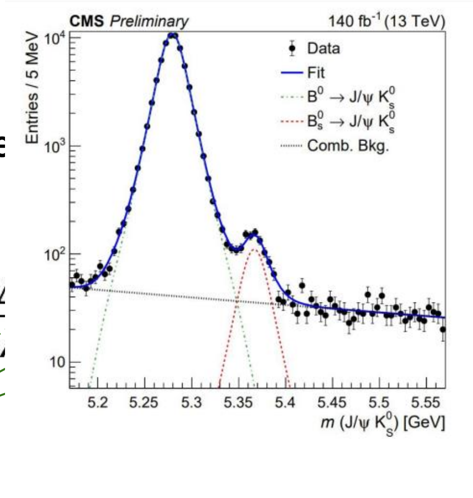

- **Using the latest measurements and assuming the SM** ($A_{\Delta\Gamma}$ = 0.94 ± 0.07, τ_{Bs} = 1.520 ± 0.(

$$\tau(J/\psi K_S)\big|_{SM} = 1.62 \pm 0.02 \text{ ps}$$

  - Available measurement from LHCb: $\tau(J/\psi K_S)$ = 1.75 ± 0.14 ps [Nucl.Phys.B(201

- In this analysis the decay time is measured in the transverse plane as

$$t = \frac{L_{xy}\cdot M_{B_s}}{p_T}$$

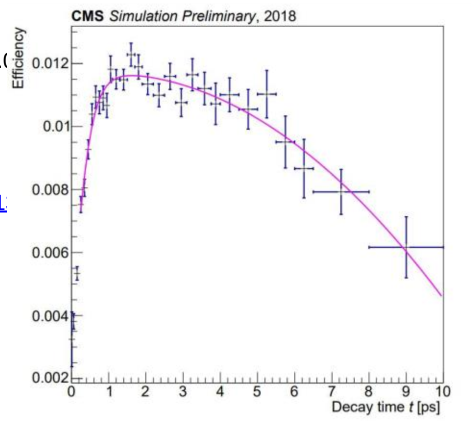

Fit and results

- **The effective lifetime is measured with a 2D UML fit to the invariant mass and proper decay time**
  - The decay time uncertainty is used as a conditional parameter
  - Both the effective lifetimes of the signal B_s and control channel B^0 are fitted
  - The control channel is used to validate most of the measurement components
- **Results** (using 727 ± 35 B_s signal candidates)

$$\tau(J/\psi\, K_S)^{eff} = 1.59 \pm 0.07\,(\text{stat}) \pm 0.03\,(\text{syst})\ \text{ps}$$

  - The control channel's effective lifetime is found to be in good agreement with the world-average value
- The measured $B_s \rightarrow J/\psi\, K_S$ effective lifetime is in agreement with the SM prediction and compatible with the previous LHCb results at 2.1σ
- **This is the most precise measurement of this quantity to date**

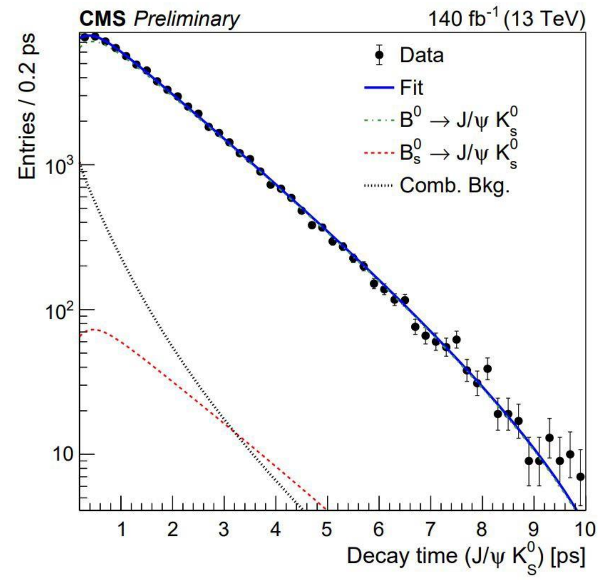

Source	Values (ps)
Deviation in control channel lifetime	0.002
Limited MC statistics	0.006
Efficiency modeling	0.002
Signal and background mass model	0.022
Background decay time model	0.014
Mass shape variation	0.007
Different fit strategy	0.006
Total	0.028

Case Study 4: Studies of Lepton Flavor Universality

CMS LFUV Studies

Rep. Prog. Phys. **87** (2024) 077802

SM

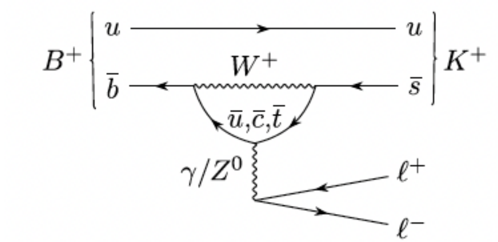

BSM

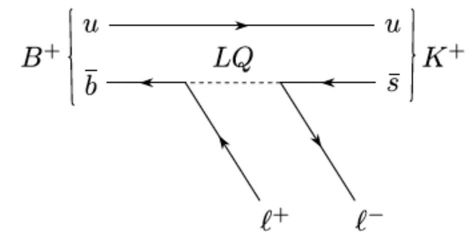

- Test of LFU in $B^\pm \rightarrow K\,\mu^+\mu^-$ and $B^\pm \rightarrow K\,e^+e^-$ at 13 TeV using data taken in 2018
- Use of “B Parking” strategy
  - Collection of ~10^{10} unbiased b hadron decays by triggering on one b hadron of the produced pair using a specific decay mode, the “tag” side’, while the other b hadron decay (the probe side) is unbiased by the trigger. Also takes advantage unused output trigger and DAQ bandwidth as the luminosity decreases during the store to record, but not immediately reconstruct, the events but instead to “park them” until a long LHC shutdown. This way, the B-parked stream does not compete for resources with the main CMS discovery program
  - Tag-side states require at least a muon and a displaced vertex
- The luminosity collected this way was 41.6 fb^{-1} compared to the 59.8 fb^{-1} taken with the main trigger and DAQ arrangement

Measured quantities

$$R(\mathrm{K})\,(q^2)\,[q^2_{\min},q^2_{\max}] = \frac{\left[\dfrac{\mathcal{B}(\mathrm{B}^+\to\mathrm{K}^+\mu^+\mu^-)\,[q^2_{\min},q^2_{\max}]}{\mathcal{B}(\mathrm{B}^+\to\mathrm{J}/\psi(\mu^+\mu^-)\mathrm{K}^+)}\right]}{\left[\dfrac{\mathcal{B}(\mathrm{B}^+\to\mathrm{K}^+e^+e^-)\,[q^2_{\min},q^2_{\max}]}{\mathcal{B}(\mathrm{B}^+\to\mathrm{J}/\psi(e^+e^-)\mathrm{K}^+)}\right]}.$$

$$R(\mathrm{K})_{\mathrm{theory}}\,[q^2_{\min},q^2_{\max}] = \frac{\mathcal{B}(\mathrm{B}^+\to\mathrm{K}^+\mu^+\mu^-)\,[q^2_{\min},q^2_{\max}]}{\mathcal{B}(\mathrm{B}^+\to\mathrm{K}^+e^+e^-)\,[q^2_{\min},q^2_{\max}]}$$

$$R(\mathrm{K}) = 0.78^{+0.46}_{-0.23}\,(\mathrm{stat})^{+0.09}_{-0.05}\,(\mathrm{syst}) = 0.78^{+0.47}_{-0.23},$$

which is within one standard deviation from the SM predic
of approximately unity. The summary of the available R
measurements is shown in figure A6.

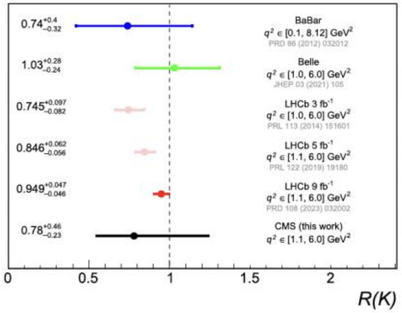

Figure A6. Summary of $R(\mathrm{K})$ measurements from BaBar [12], Belle [15], and LHCb [9, 19, 20] experiments, as well as the present CMS measurement. The pink data points of the first three LHCb measurements were superseded by the latest one, shown as the red point.

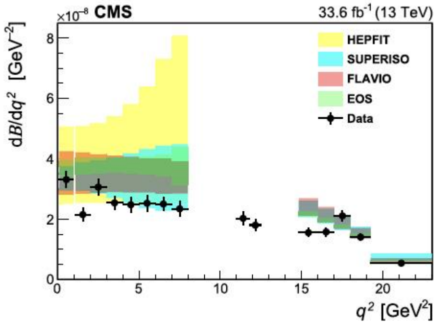

Figure 5. Comparison of the measured differential $\mathrm{B}^+\to\mathrm{K}^+\mu^+\mu^-$ branching fraction with the theoretical predictions obtained using HEPFIT, SUPERISO, FLAVIO, and EOS packages. The HEPFIT predictions are available only for $q^2 < 8\,\mathrm{GeV}^2$.

Table 10. The $\mathrm{B}^+\to\mathrm{K}^+\mu^+\mu^-$ branching fraction, $d(\mathcal{B}(\mathrm{B}^+\to\mathrm{K}^+\mu^+\mu^-)/q^2$ integrated over the specified q^2 range for the individual q^2 bins.. The uncertainties in the yields are statistical uncertainties from the fit, while the branching fraction uncertainties include both the statistical and systematic compone

q^2 range (GeV^2)	Signal yield	Branching fraction (10^{-8})
0.1–0.98	260 ± 20	2.91 ± 0.24
1.1–2.0	197 ± 19	1.93 ± 0.20
2.0–3.0	306 ± 23	3.06 ± 0.25
3.0–4.0	260 ± 21	2.54 ± 0.23
4.0–5.0	251 ± 23	2.47 ± 0.24
5.0–6.0	264 ± 27	2.53 ± 0.27
6.0–7.0	267 ± 21	2.50 ± 0.23
7.0–8.0	256 ± 23	2.34 ± 0.25
11.0–11.8	207 ± 19	1.62 ± 0.18
11.8–12.5	172 ± 16	1.26 ± 0.14
14.82–16.0	272 ± 20	1.83 ± 0.17
16.0–17.0	246 ± 17	1.57 ± 0.15
17.0–18.0	317 ± 19	2.11 ± 0.16
18.0–19.24	242 ± 19	1.74 ± 0.15
19.24–22.9	158 ± 19	2.02 ± 0.30

$B^{\pm} \rightarrow K\, \mu^{+}\mu^{-}$ and $B^{\pm} \rightarrow K\, e^{+}e^{-}$ at 13 TeV

Table 5. Signal yields in the muon channel in the low-q^2 bin and resonant CRs.

Channel	q^2 range [GeV^2]	Yield
$B^+ \to K^+\mu^+\mu^-$	1.1–6.0	1267 ± 55
$B^+ \to J/\psi(\mu^+\mu^-)K^+$	8.41–10.24	$728\,000 \pm 1000$
$B^+ \to \psi(2S)(\mu^+\mu^-)K^+$	12.60–14.44	$68\,300 \pm 500$

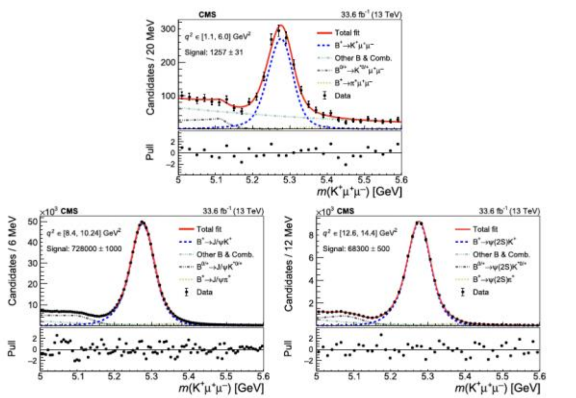

Figure 3. Results of an unbinned likelihood fit to the $K^+\mu^+\mu^-$ invariant mass distributions in the low-q^2 bin (upper), and in the $B^+ \to J/\psi(\mu^+\mu^-)K^+$ (lower left) and $B^+ \to \psi(2S)(\mu^+\mu^-)K^+$ (lower right) CRs. The error bars show the statistical uncertainty in data. The lower panels show the distribution of the pull, which is defined as the Poisson probability to observe the number of event counts in data, given the fit function, expressed in terms of the Gaussian significance.

Table 5. Signal yields in the muon channel in the low-q^2 bin and resonant CRs.

Channel	q^2 range [GeV^2]	Yield
$B^+ \to K^+\mu^+\mu^-$	1.1–6.0	1267 ± 55
$B^+ \to J/\psi(\mu^+\mu^-)K^+$	8.41–10.24	$728\,000 \pm 1000$
$B^+ \to \psi(2S)(\mu^+\mu^-)K^+$	12.60–14.44	$68\,300 \pm 500$

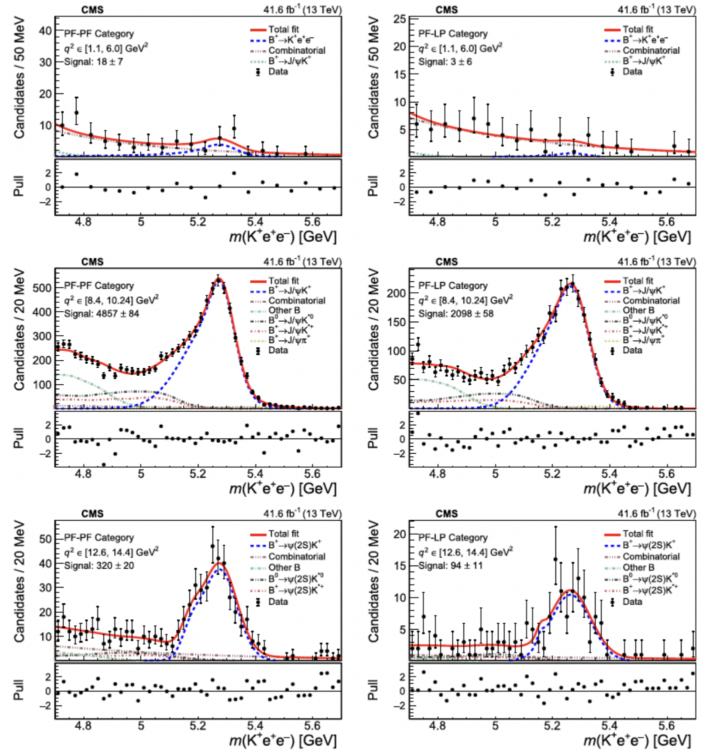

Figure 4. The $K^+e^+e^-$ invariant mass spectrum with the results of the fit shown with the red line in the low-q^2 region (upper row), $B^+ \to J/\psi(e^+e^-)K^+$ CR (middle row), and $B^+ \to \psi(2S)(e^+e^-)K^+$ CR (lower row) for the PF-PF (left column) and PF-LP (right column) categories. The shoulder below the nominal B^+ meson mass for the $\psi(2S)$ CR is due to the narrow q^2 range in this bin compared to the size of the radiative tail. Notations are as in figure 3.

Challenge is to get enough K e^+e^-

Table 5. Signal yields in the muon channel in the low-q^2 bin and resonant CRs.

Channel	q^2 range [GeV^2]	Yield
$B^+ \to K^+\mu^+\mu^-$	1.1–6.0	1267 ± 55
$B^+ \to J/\psi(\mu^+\mu^-)K^+$	8.41–10.24	728 000 ± 1000
$B^+ \to \psi(2S)(\mu^+\mu^-)K^+$	12.60–14.44	68 300 ± 500

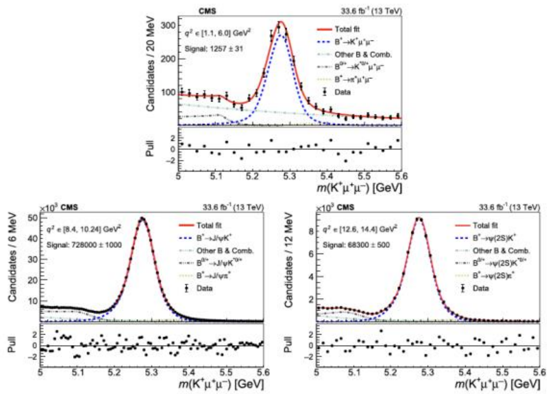

Figure 3. Results of an unbinned likelihood fit to the $K^+\mu^+\mu^-$ invariant mass distributions in the low-q^2 bin (upper), and in the $B^+ \to J/\psi(\mu^+\mu^-)K^+$ (lower left) and $B^+ \to \psi(2S)(\mu^+\mu^-)K^+$ (lower right) CRs. The error bars show the statistical uncertainty in data. The lower panels show the distribution of the pull, which is defined as the Poisson probability to observe the number of event counts in data, given the fit function, expressed in terms of the Gaussian significance.

Table 5. Signal yields in the muon channel in the low-q^2 bin and resonant CRs.

Channel	q^2 range [GeV^2]	Yield
$B^+ \to K^+\mu^+\mu^-$	1.1–6.0	1267 ± 55
$B^+ \to J/\psi(\mu^+\mu^-)K^+$	8.41–10.24	728 000 ± 1000
$B^+ \to \psi(2S)(\mu^+\mu^-)K^+$	12.60–14.44	68 300 ± 500

Table 7. Signal yields in the electron channel in the low-q^2 bin and resonant CRs.

Channel	q^2 range [GeV^2]	PF-PF yield	PF-LP yield
$B^+ \to K^+e^+e^-$	1.1–6.0	17.9 ± 7.2	3.0 ± 5.9
$B^+ \to J/\psi(e^+e^-)K^+$	8.41–10.24	4857 ± 84	2098 ± 58
$B^+ \to \psi(2S)(e^+e^-)K^+$	12.60–14.44	320 ± 20	94 ± 11

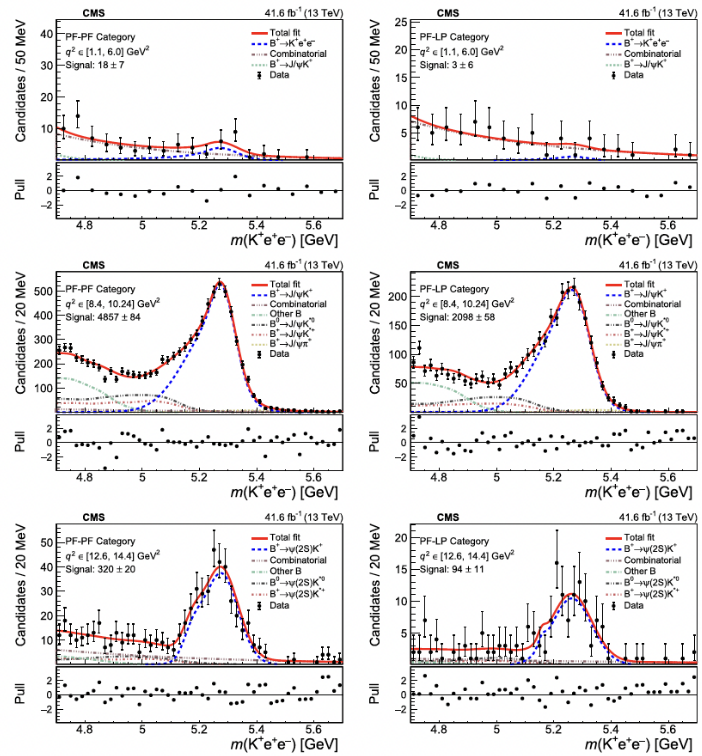

Figure 4. The $K^+e^+e^-$ invariant mass spectrum with the results of the fit shown with the red line in the low-q^2 region (upper row), $B^+ \to J/\psi(e^+e^-)K^+$ CR (middle row), and $B^+ \to \psi(2S)(e^+e^-)K^+$ CR (lower row) for the PF-PF (left column) and PF-LP (right column) categories. The shoulder below the nominal B^+ meson mass for the $\psi(2S)$ CR is due to the narrow q^2 range in this bin compared to the size of the radiative tail. Notations are as in figure 3.

LHCb LFUV Updated Results

Physical Review D **108**, 032002 (2023)

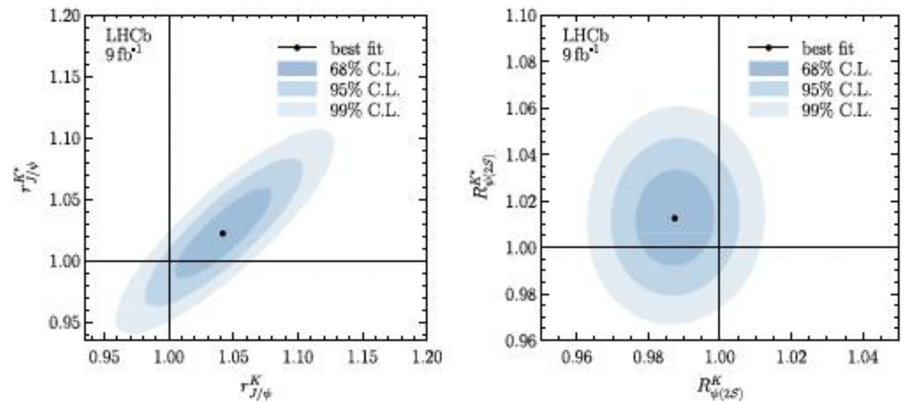

FIG. 22. Two dimensional likelihood scans of (left) $r^K_{J/\psi}$ vs $r^{K^*}_{J/\psi}$ and (right) $R^K_{\psi(2S)}$ vs $R^{K^*}_{\psi(2S)}$. The contours show the 68%, 95% and 99% confidence level regions and the solid markers show the best fit values.

$$\text{low-}q^2 \begin{cases} R_K = 0.994^{+0.090}_{-0.082}(\text{stat})\,^{+0.029}_{-0.027}(\text{syst}), \\ R_{K^*} = 0.927^{+0.093}_{-0.087}(\text{stat})\,^{+0.036}_{-0.035}(\text{syst}), \end{cases}$$

$$\text{central-}q^2 \begin{cases} R_K = 0.949^{+0.042}_{-0.041}(\text{stat})\,^{+0.022}_{-0.022}(\text{syst}), \\ R_{K^*} = 1.027^{+0.072}_{-0.068}(\text{stat})\,^{+0.027}_{-0.026}(\text{syst}), \end{cases}$$

All ratios are consistent with 1.0, the SM expectation so the LFU "tension' is gone!

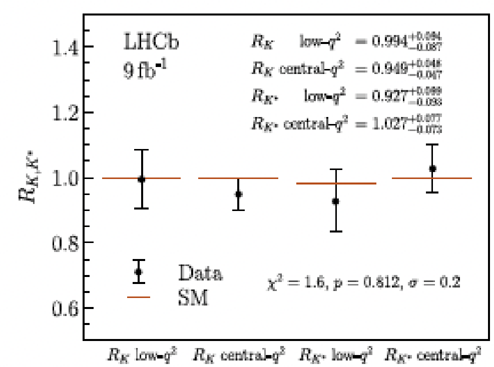

FIG. 28. Measured values of LU observables in $B^+ \to K^+\ell^+\ell^-$ and $B^0 \to K^{*0}\ell^+\ell^-$ decays and their overall compatibility with the SM.

LHCb Assessment of their Recent Results

The results presented here differ from previous LHCb measurements of R_K [24] and R_{K^*} [21], which they supersede. The measured values for R_{K^*} (low- and central-q^2) and R_K (central-q^2) move upwards from the previous results and closer to the SM predictions. Although these shifts can be attributed in part to statistical effects it is understood that the change in R_K is primarily due to systematic effects. In the case of R_K, the data sample is the same as in Ref. [24], but subject to a revised analysis. For R_K (central-q^2) the statistical component of the difference is evaluated using pseudoexperiments and found to follow a Gaussian distribution of width 0.033 in the absolute value of R_K. In the case of R_{K^*}, the data correspond to more than a factor of 5 increase in the number of $b\bar{b}$ pairs produced relative to Ref. [21] and hence there is a much larger statistical component of the difference. For R_K (central-q^2) the expected systematic shifts caused by the improved treatment of misidentified hadronic backgrounds in the electron mode

are also evaluated using pseudoexperiments. The biggest shift (0.064 with respect to Ref. [24]) is found to be due to the more stringent PID criteria applied here, which reduce the contribution from misidentified background processes that had previously not been accounted for appropriately. In addition, the residual misidentified backgrounds are explicitly modeled in the fit, resulting in a further shift (0.038) compared to the previous analysis. These shifts add linearly. The systematic shift due to misidentified backgrounds to electrons, and the uncertainties assigned to the results presented here, are greater than the systematic uncertainties in the earlier publication of R_K. The assigned systematic uncertainties on the new measurements presented in this paper are smaller than in previous papers, except for R_K (central-q^2) where the new result has a smaller overall relative uncertainty despite an increase in the systematic uncertainty from that of Ref. [24]. In all cases, the statistical uncertainties remain significantly larger than the systematic uncertainties and therefore additional data will continue to challenge the Standard Model.

Ratio of tauonic to muonic semileptonic decays at BELLE

- Belle checked the ratio of semi-electron to semi-muon B decays and found no difference as expected:

$$\frac{\mathcal{B}(\mathbf{B^0} \to \mathbf{D}^{*-}\mathbf{e}^-\nu)}{\mathcal{B}(\mathbf{B^0} \to \mathbf{D}^{*-}\mu^-\nu)} = 1.01 \pm 0.01 \pm 0.03 \qquad \frac{\mathcal{B}(\overline{\mathbf{B}}^0 \to \mathbf{D}^*\tau^-\overline{\nu})}{\mathcal{B}(\overline{\mathbf{B}}^0 \to \mathbf{D}^*\mathbf{l}^-\overline{\nu})}$$

- Belle and BaBar both studied the ratio of semitauonic to semimuonic decays using B candidates on the Υ(4S) opposite fully reconstructed B mesons, so that the full momentum vector of the semileptonic candidate was known despite the missing neutrino.
- The method was to fully reconstruct a B^0, referred to as the "tag", and then "close" the kinematics by using:

$$\vec{p}_B = -\vec{p}_{tag}$$

  – A strength of running on the Υ4s)!

BELLE

First Belle II R(D*) measurement

arXiv:2401.02840

Talk by M. Prim

- Hadronic tag then search for $B \to D^* \tau \nu$ in the remaining tracks and clusters
  - **leptonic tau decay**
  - **charged and neutral *B***
- **Additional energy in calorimeter** and missing mass used as signal extraction variables

$$R(D^*) = 0.26 \pm 0.04^{+0.04}_{-0.03}$$

  - Systematic uncertainty related mainly to size of control samples
  - **Comparable precision to equivalent Belle result with ¼ the sample**

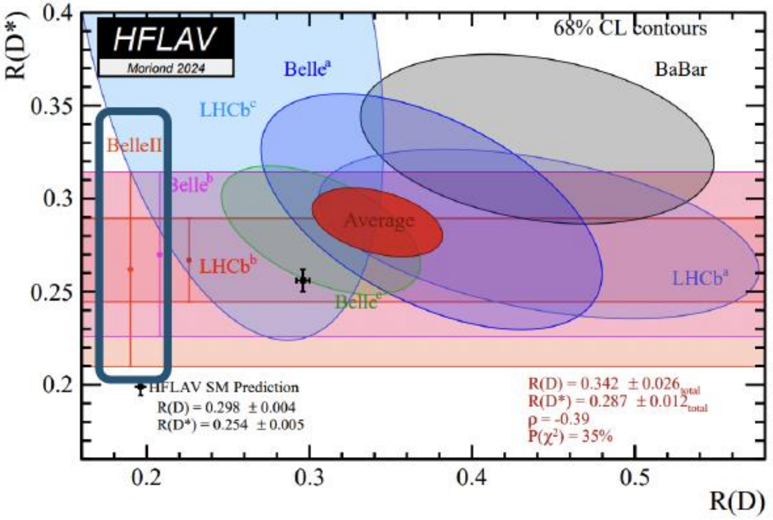

BELLE

$B^+ \to K^+ \nu\bar{\nu}$: a new one

PRD 109, 112006 (2024)

Talk by M. Liu

- Theoretically clean and third generation sensitive *b*→*sll* transition
- Inclusive tag developed that exploits topology
    - 8% efficiency

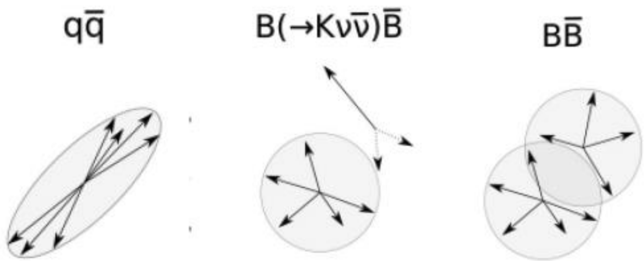

- Fit to invariant mass of neutrinos (q^2) and classifier
    - Checked and combined with lower efficiency hadronic *B* tag

$$\mathrm{B}(B^+ \to K^+ \nu\bar{\nu}) = \left(2.3 \pm 0.5(\mathrm{stat})^{+0.5}_{-0.4}(\mathrm{syst})\right) \times 10^{-5}$$

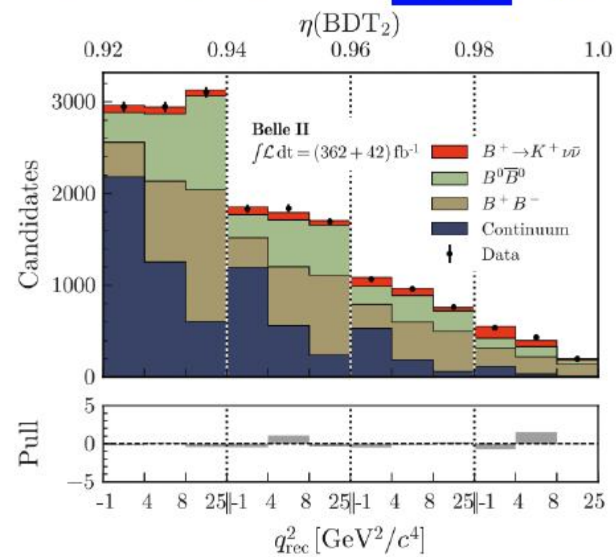

Evidence @ 3.5σ
Tension with SM prediction of 0.6×10^{-5} @ 2.7σ

LFU in B_c

- Reminder
  - Mass: 6274.5 MeV
  - Lifetime: 0.510+/- 0.009 ps
  - Decay modes: **$J/\psi(1S)$** $\mu^+ \nu$; : **$J/\psi(1S)$** $\tau^+ \nu$; $J/\psi(1S)\ \pi^+$, $J/\psi(1S)\ \pi^+\pi^-\pi^+$, several other modes with J/ψ and Ds,Ks and πs.
  - Measurement of

$$R(J/\psi) = \frac{\mathcal{B}(B_c^+ \to J/\psi\, \tau^+ \nu_\tau)}{\mathcal{B}(B_c^+ \to J/\psi\, \mu^+ \nu_\mu)}$$

- SM prediction: ~0.25
- Previously studied by LHCb
- **CMS study** with 60 fb^{-1} taken at 13 TeV in 2018
- Result:

$$R(J/\psi) = 0.17^{+0.18}_{-0.17}\,(\text{stat.})^{+0.21}_{-0.22}\,(\text{syst.})^{+0.19}_{-0.18}\,(\text{theo.})$$

- Consider this as the beginning of the investigation

https://cms-results.web.cern.ch/cms-results/public-results/preliminary-results/BPH-22-012/index.html

An Abundance of Riches

- Flavor physics is much bigger then the sliver of B physics I covered. It includes
  - More B physics
  - Charm Physics
  - Top physics (will it contribute to B physics)
  - Kaon physics
  - QCD and spectroscopy whee there has been great progress
  - Leptons
    - **Charged leptons (μ–>e conversion, g-2, ..)**
    - **Neutrinos**

Concluding Remarks

- Flavor is one of the great mysteries of nature
- It is intimately connected to the Higgs, Z, and W
- Its known properties greatly constrain the building of new models
- It offers a huge space of possibilities for searches for BSM physics
  - A fissure could develop anywhere, and we need to be alert to similar clues elsewhere in particle physics
    - **There are still unresolved anomalies**
  - Areas like LFU (discussed) were not getting attention they deserved but in the case of LFU are now
    - **There are undoubtedly other promising but neglected topics**
- Once something is found, in flavor physics or elsewhere, we have to ask what implications it has for flavor physics and why we see it, or not, at the observed level
  - Why didn't the dog bark → the "Flavor problem"
    - Gregory: "The dog did nothing in the night-time"
    - Holmes: "That was the curious incident

Let's hope for a "big effect smoking gun", but let's strap in for precision physics

Thank you for your attention! I will be glad to try to answer questions and hear your comments.

Backup Slides

Lepton flavor violation [LHCb-PAPER-2024-114]

M. Artuso LHCP 2024

- Lepton flavor is conserved in decays mediated by the Standard Model
- New physics models predict deviations especially involving the 3rd family ⇒ it is important to look!

First limit of this lepton flavor violaDng decay

$$\mathcal{B}(B_s^0 \to \phi\mu^+\tau^-) < 1.0 \times 10^{-5} \text{ at } 90\% \text{ CL},$$
$$\mathcal{B}(B_s^0 \to \phi\mu^+\tau^-) < 1.1 \times 10^{-5} \text{ at } 95\% \text{ CL}.$$

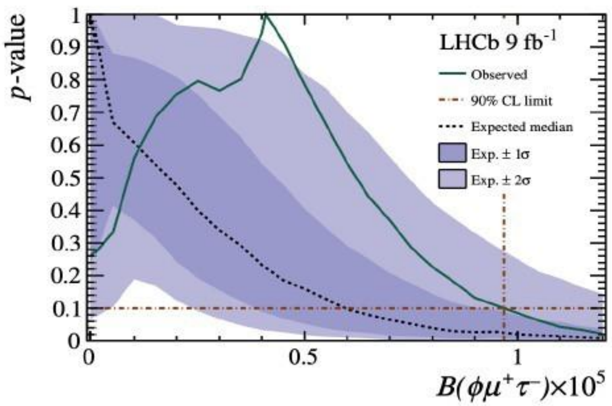

No significant excess is observed

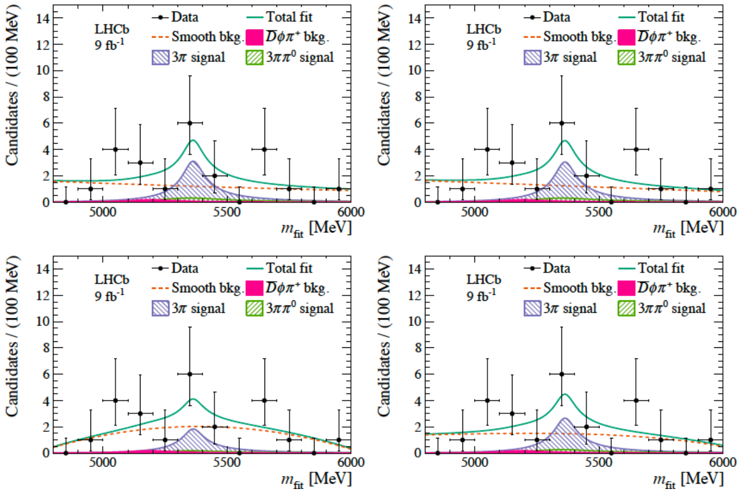

$B_s \rightarrow \phi(k^+k^-)\mu^+\mu^-$ from LHCb

Phys. Rev. Lett. 127 (2021) 151801 , *JHEP* 2111 (2021) 043

$$\frac{1}{\mathrm{d}(\Gamma+\bar{\Gamma})/\mathrm{d}q^2}\frac{\mathrm{d}^3(\Gamma+\bar{\Gamma})}{\mathrm{d}\cos\theta_l\,\mathrm{d}\cos\theta_K\,\mathrm{d}\phi} = \frac{9}{32\pi}\Big[\frac{3}{4}(1-F_\mathrm{L})\sin^2\theta_K(1+\frac{1}{3}\cos 2\theta_l) + F_\mathrm{L}\cos^2\theta_K(1-\cos 2\theta_l) + S_3\sin^2\theta_K\sin^2\theta_l\cos 2\phi + S_4\sin 2\theta_K\sin 2\theta_l\cos\phi + A_5\sin 2\theta_K\sin\theta_l\cos\phi + \frac{4}{3}A_\mathrm{FB}^{CP}\sin^2\theta_K\cos\theta_l + S_7\sin 2\theta_K\sin\theta_l\sin\phi + A_8\sin 2\theta_K\sin 2\theta_l\sin\phi + A_9\sin^2\theta_K\sin^2\theta_l\sin 2\phi\Big],$$

F_L and $S_{3,4,.5}$ are CP averages and A^{CP}_{FB} and $A_{5,8,9}$ are CP asymmetries. A8 and A_9 are T-odd CP asymmetries (near 0 in SM)

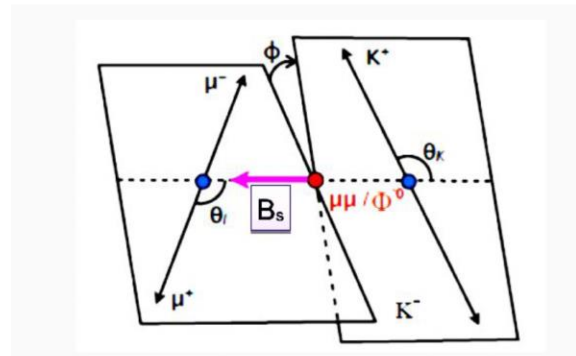

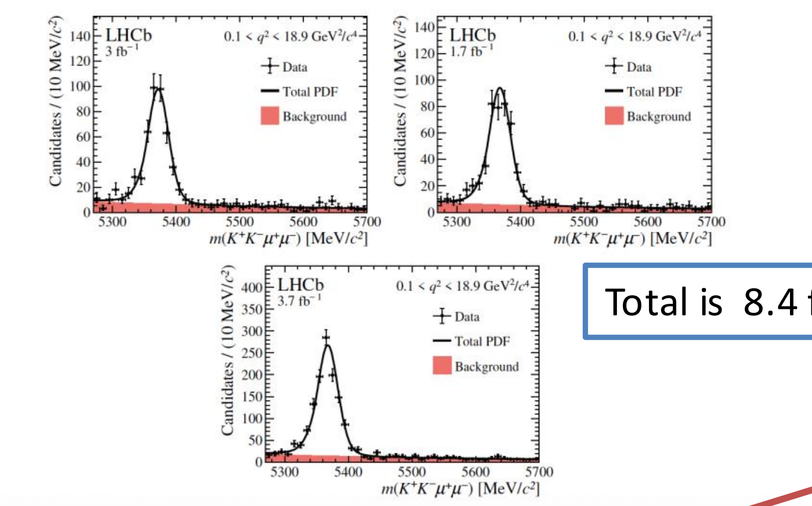

Total is $8.4\ \mathrm{fb}^{-1}$

Phys.Rev. Lett. 127, 151801 (2021)

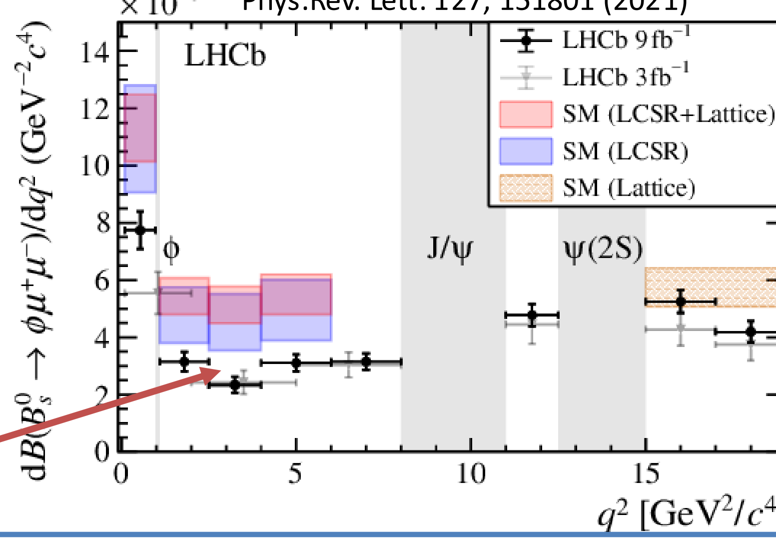

In the q^2 region between 1.1 and 6.0 GeV^2/c^4, the measurement is found to lie 3.6 standard deviations below a standard model prediction based on a combination of light cone sum rule and lattice QCD calculations. $\mathcal{B}(B^0 \rightarrow \phi(\mu^+\mu^-)) \rightarrow (8.14 \pm 0.21 \pm 0.16 \pm 0.03 \pm 0.39) \times 10^{-7}$.

$\Lambda_b \rightarrow \Lambda$ (1520) (pK) $\mu^+\mu^-$ (LHCb)

[arXiv:2302.08262](https://arxiv.org/abs/2302.08262)

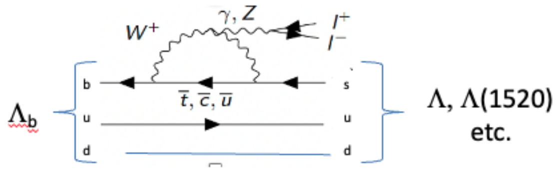

Λ(1520): 0(3/2)$^-$
M = 1519 MeV, Γ = 16 MeV
B(pK) = 22.5%

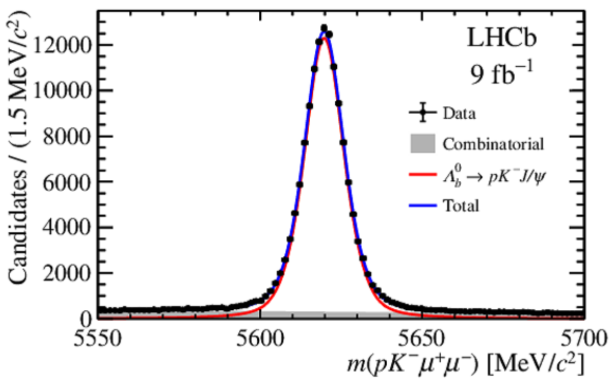

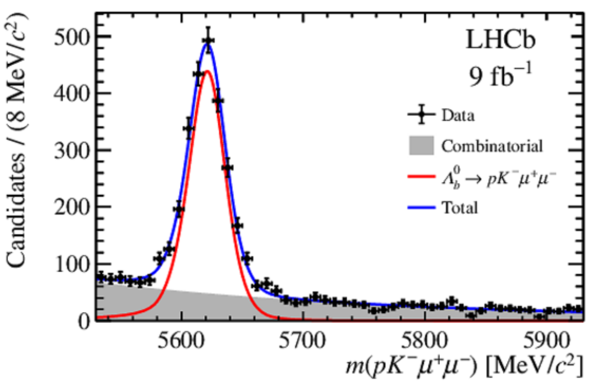

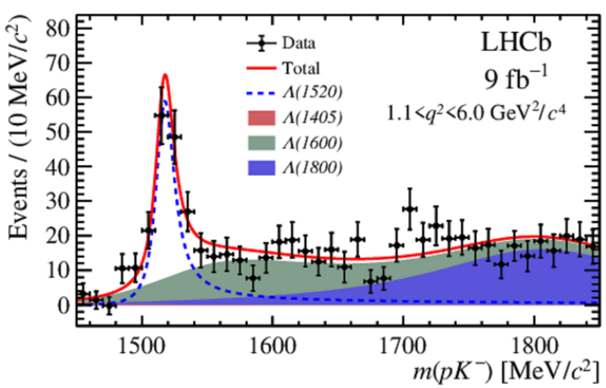

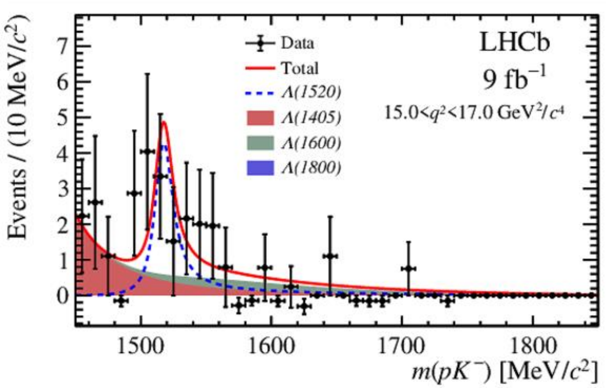

$\Lambda_b \rightarrow \Lambda, \Lambda(1520)\ (pK)\ \mu^+\mu^-$ fromLHCb

arXiv:2302.08262

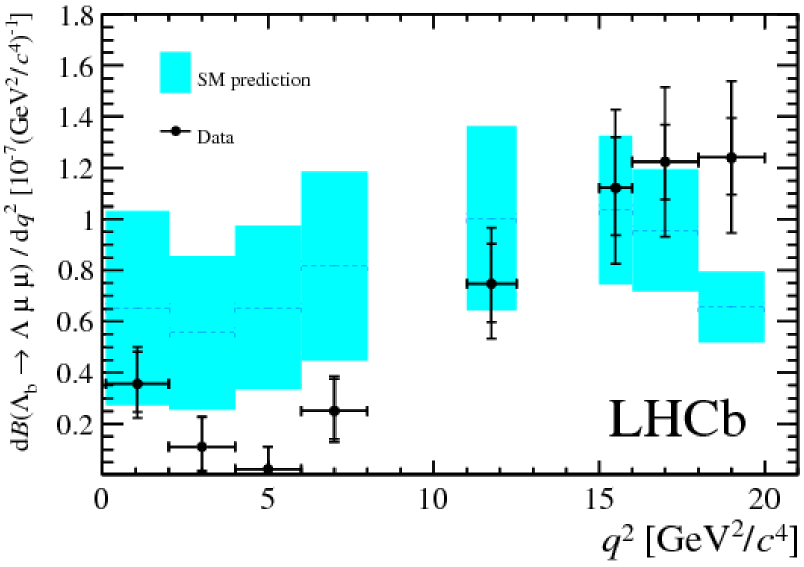

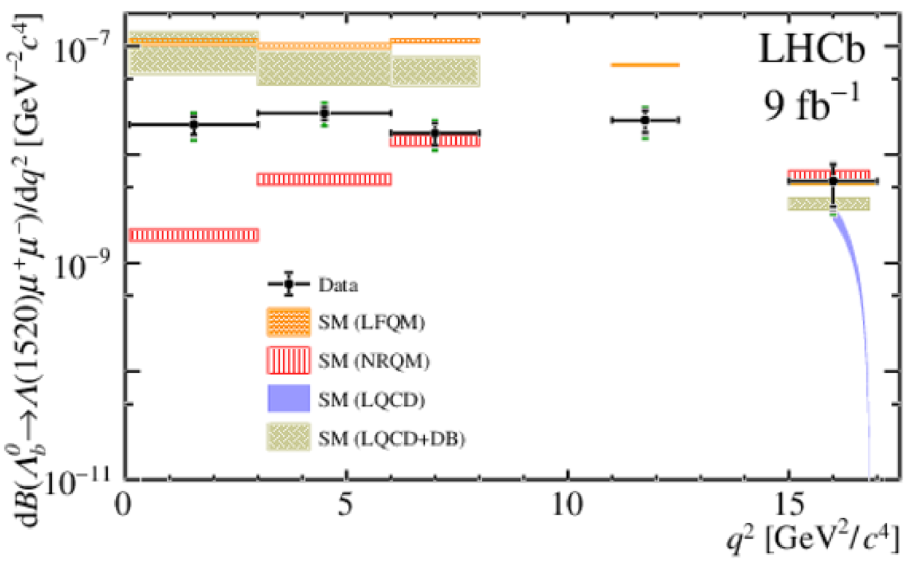

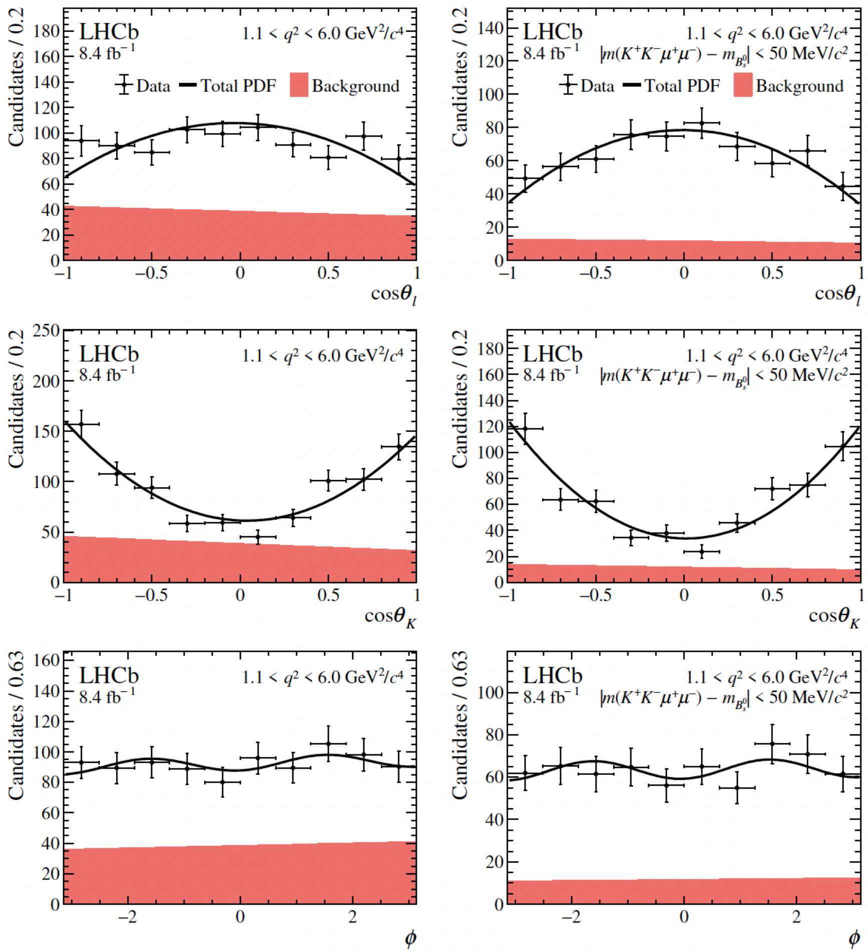

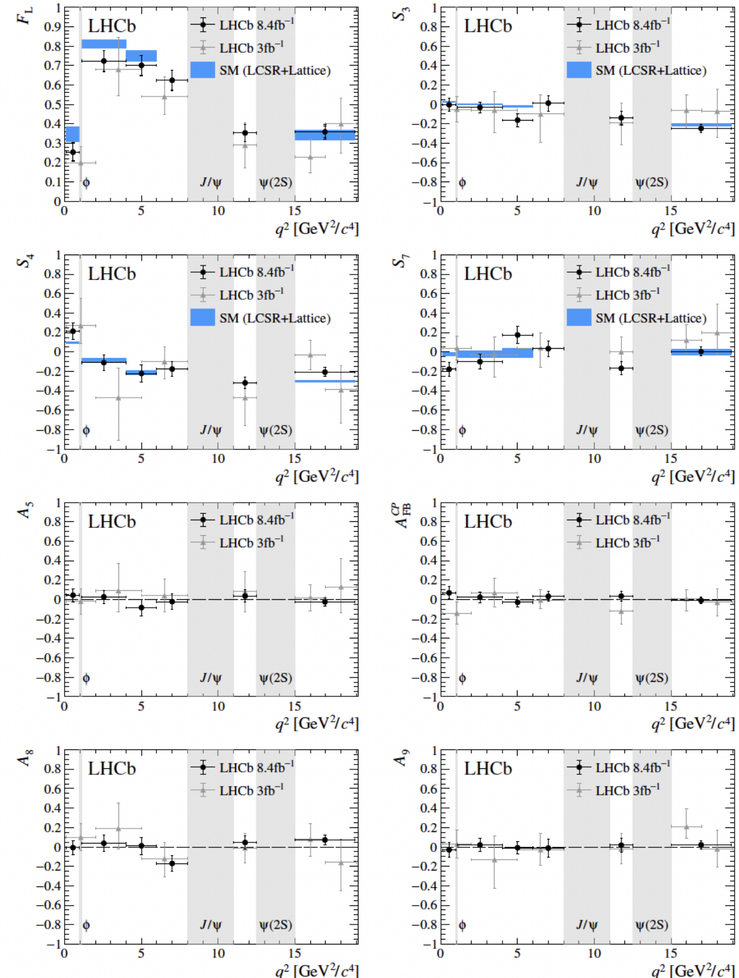

- $B_s \rightarrow f_2'(1525)\,\mu^+\mu^-$ **(f_2' is a spin 2 meson)**

$$\mathcal{B}(B^0_s \rightarrow f'_2\,\mu^+\mu^-) = (1.57 \pm 0.19 \pm 0.06 \pm 0.06 \pm 0.08) \times 10^{-7}$$

Statistical significance of 9 standard deviations and the resulting branching fraction agrees with SM predictions.

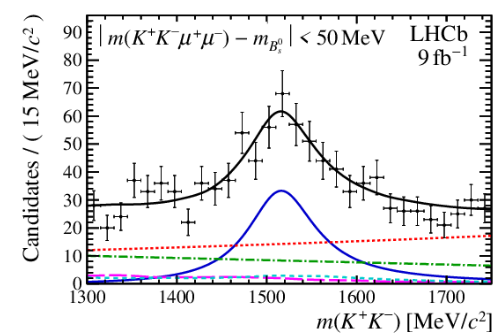

Calibration strategy (and other tricks)

- **A** **multi-pronged strategy** **has been devised to improve the ω_{tag} estimation and suppress systematic effects**
  1. All models are constructed from the start as *probability estimators*, i.e. score~ω_{tag}
     - Loss function: *cross-entropy*, which is the likelihood for the probability P(true class | score)
     - Output layer: *Sigmoid* function, which normalizes the output to a probability distribution
  2. All DNNs are calibrated with the *Platt scaling*, which ensures that the calibrated score is still a probability
     - The Platt scaling is a linear calibration of the score before the last sigmoid layer
  3. In calibrating the charge-based taggers (which provide a probability for B_s vs $\overline{B_s}$):
     - A. The output is *symmetrized* due to the initial LHC charge imbalance

$$s_{DNN}^{sym}(x) = \frac{s_{DNN}(x) + [1 - s_{DNN}(\overline{x})]}{2}$$

     - B. The symmetry is explicitly forced in the calibration function by removing the constant term

This strategy **cancels** **almost all the systematic effects associated with flavor tagging**

OS-Muon calibration (*muon-tagging* trigger 2018)

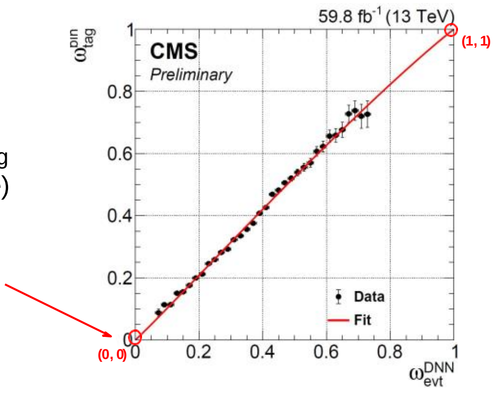

OS-jet calibration (2018)

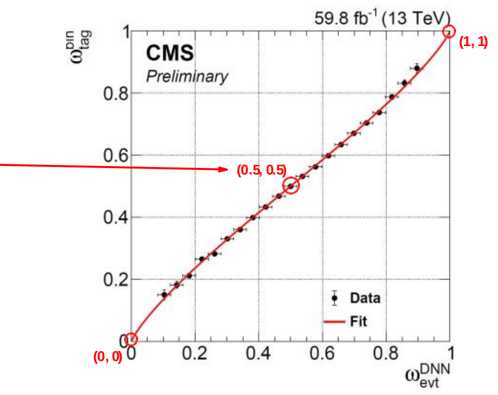

Event selection and efficiency

Event selection and efficiency

- **Trigger**: $J/\psi \rightarrow \mu^+\mu^-$ candidate with p_T > 20 (25) GeV for 2016 (2017-18)
- **Offline $K_S \rightarrow \pi^+\pi^-$ selection**
  - Displaced by >15σ from the beamspot and >5σ from the B_s vertex
  - Invariant mass within 70 MeV from world-average value
- **Background sources**
  - $\Lambda \rightarrow p\pi^-$: suppressed with constraints on the decay kinematics
  - $B^0 \rightarrow J/\psi K_s$: irreducible, treated as a control channel
  - $B^0 \rightarrow J/\psi K^{*0}$: negligible
  - Combinatorial: suppressed with dedicated BDT selection
- **Time efficiency**
  - Measured in simulations for B_s and B^0 (control channel)

$$\epsilon(t) = \frac{t_{reco}}{t_{gen} \otimes \delta(t)}$$

  - Modeled with a combination of polynomials and logistic functions

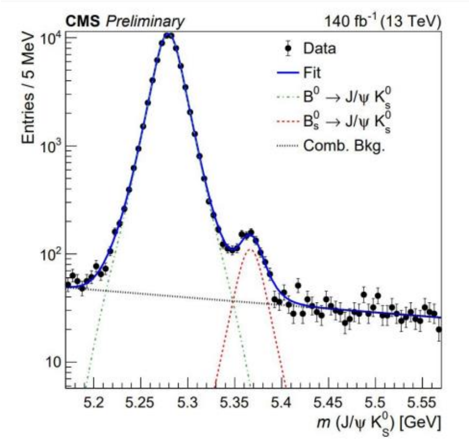

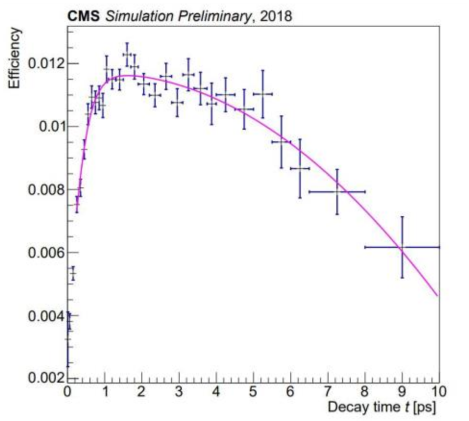

Acceptance and efficiency effects

- **The efficiency in selecting and reconstructing the B_s candidates is not independent of the decay time and angular observables**
  - To properly fit the decay rate model an efficiency parametrization is needed

Time efficiency

- Modeled in the $B^0 \to J/\psi\, K^{*0}$ data control channel with corrections from simulations
- Ultimately parametrized with Bernstein's polynomials

$$\varepsilon_{B^0}^{\text{data}}(ct) = \frac{N_{B^0}(ct)}{e^{-\Gamma_d^{\text{w.a.}}} \otimes P_{B^0}(\sigma_{ct})}$$

$$\varepsilon_{B_s}^{\text{data}}(ct) = \varepsilon_{B^0}^{\text{data}}(ct) \cdot \frac{\varepsilon_{B_s}^{\text{MC}}(ct)}{\varepsilon_{B^0}^{\text{MC}}(ct)}$$

Angular efficiency

- Estimated with KDE distributions in simulated events
- The simulated data samples are corrected to match the data
  - An iterative procedure is used to simultaneously correct the kinematics of the final state particles and the differences in the physics parameters set in the MC with respect to what measured in the data

ct efficiency for the *standard* trigger category (2018)

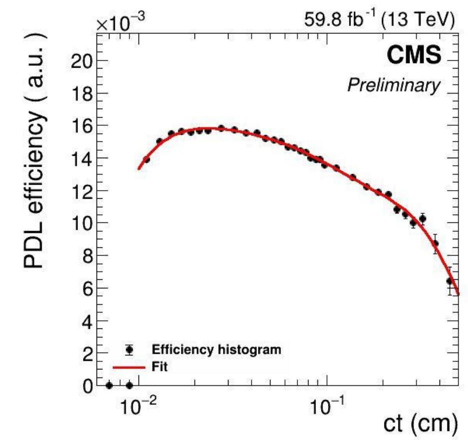

ct efficiency for the *muon-tagging* trigger category (2018)

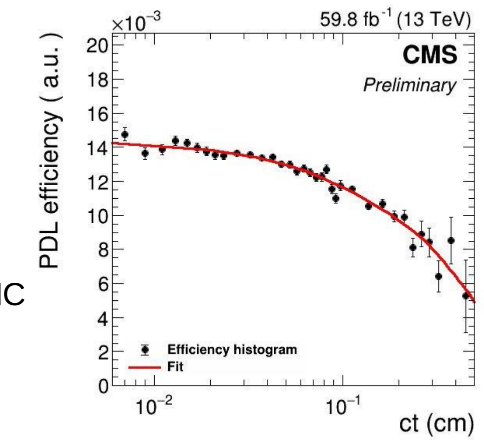

Combination with 8 TeV results

- These results supersede PLB816(2021)136188 and are further combined with those obtained CMS at 8 TeV [PLB757(2016)97], yielding

$$\phi_s = -74 \pm 23 \text{ [mrad]}$$
$$\Delta\Gamma_s = 0.0780 \pm 0.0045 \text{ [ps}^{-1}\text{]}$$

- Due to the high difference in statistical power between the two results the sensitivity gain is small
- **The combined value for the weak phase ϕ_s is consistent with the SM prediction, the latest world average, and with zero (no CPV) at 3.2 s.d.**
  - **This is the first evidence of CPV in $B_s \to J/\psi K^+K^-$ decays**
- These results helps to further constrain possible BSM effects in the B_s system

Comparison with other LHC experiments

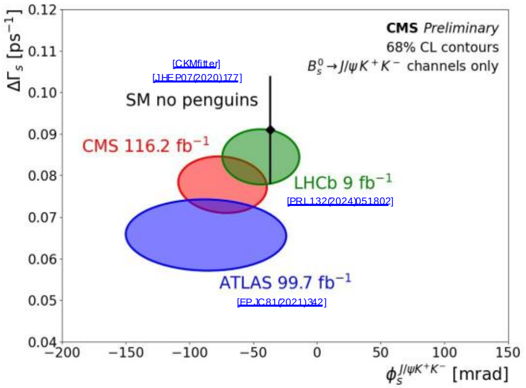

1, 2, 3 standard deviations contours

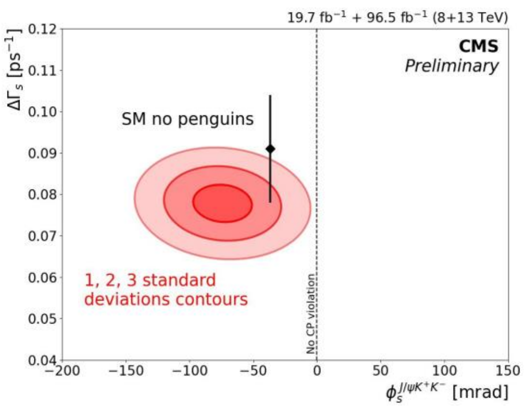

CMS Trigger for B→ $\mu^+\mu^-$ Analysis

"The events used in this analysis were collected with a set of dimuon triggers designed to select events with :

$$B \to \mu^+\mu^-,\ B^+ \to J/\psi K^+,\ and\ B^o_s \to J/\psi\phi(1020)$$

To achieve an acceptable trigger rate, the **first-level trigger** required two high-quality oppositely charged muons restricted to $|\eta| < 1.5$.

At the **high-level trigger**, a high-quality dimuon secondary vertex (SV) was required and the events were restricted to mass ranges of *4.5–6.0 GeV* and *2.9–3.3 GeV* for the *B and J/ψ* mesons, respectively. The J/ψ triggers additionally required the SV to be displaced from the beam spot (defined as the average interaction point in the plane transverse to the beams) and the displacement vector to be aligned with the dimuon momentum."

Example of B+→J/ψ ($\mu^+\mu^-$)K+ in CMS

- Early 8 TeV result

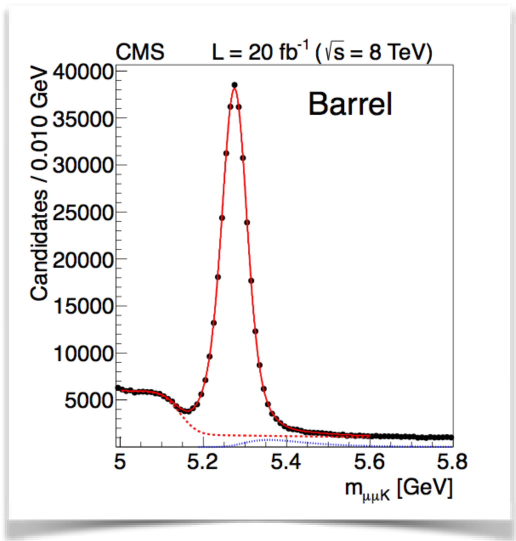

Test of Use of Future Absolute B_s Branching Fraction for Normalization

- "We also estimate the branching fractions using the $B^o{}_s \rightarrow J/\psi\phi(1020)$ decays for the normalization.

- While this result is free from the explicit systematic uncertainty in the fs/ fu ratio, it depends on the $B^o{}_s \rightarrow J/\psi\phi(1020)$ branching fraction.
  - At the moment, this branching fraction measurement uses the fs/ fu ratio measurement as an input, but this dependence may be eliminated when new independent measurements of the $B^o{}_s \rightarrow J/\psi\phi(1020)$ branching fraction become available, such as the measurement planned by the Belle II Collaboration at the KEKB e^+e^- collider [using the $Y(5S)$ data. Experimentally, the measurement based on the $B^o{}_s \rightarrow J/\psi\phi(1020)$ normalization channel has slightly larger systematic uncertainties due to the presence of the second kaon in the final state."
    - Work will need to be done to reduce this this source of uncertainty.

Angular analysis of the decay $B^+ \to K^+\mu^+\mu^-$ in proton-proton collisions at $\sqrt{s} = 8$ TeV

The CMS Collaboration*

Abstract

The angular distribution of the flavor-changing neutral current decay $B^+ \to K^+\mu^+\mu^-$ is studied in proton-proton collisions at a center-of-mass energy of 8 TeV. The analysis is based on data collected with the CMS detector at the LHC, corresponding to an integrated luminosity of 20.5 fb^{-1}. The forward-backward asymmetry A_{FB} of the dimuon system and the contribution F_H from the pseudoscalar, scalar, and tensor amplitudes to the decay width are measured as a function of the dimuon mass squared. The measurements are consistent with the standard model expectations.

Published in Physical Review D as doi:10.1103/PhysRevD.98.112011.

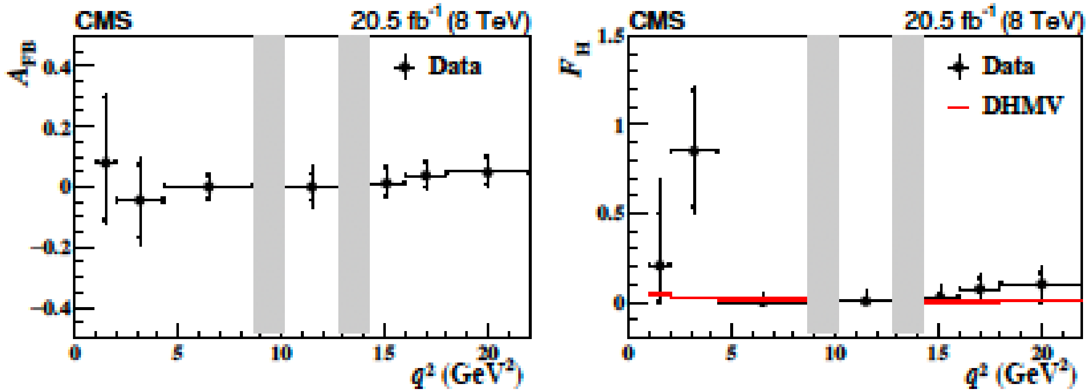

Figure 5: Results of the A_{FB} (left) and F_H (right) measurements in ranges of q^2. The statistical uncertainties are shown by the inner vertical bars, while the outer vertical bars give the total uncertainties. The horizontal bars show the q^2 range widths. The vertical shaded regions are 8.68–10.09 and 12.86–14.18 GeV^2, corresponding to the J/ψ- and $\psi(2S)$-dominated control regions, respectively. The horizontal lines in the right plot show the DHMV SM theoretical predictions [32, 33], whose uncertainties are smaller than the line width.

$\Lambda_b \rightarrow \Lambda, \Lambda$ (1520) (pK) $\mu^+\mu^-$ fromLHCb

[arXiv:2302.08262](https://arxiv.org/abs/2302.08262)

Λ(1520): 0(3/2)[-]
M = 1519 MeV, Γ = 16 MeV
B(pK) = 22.5%

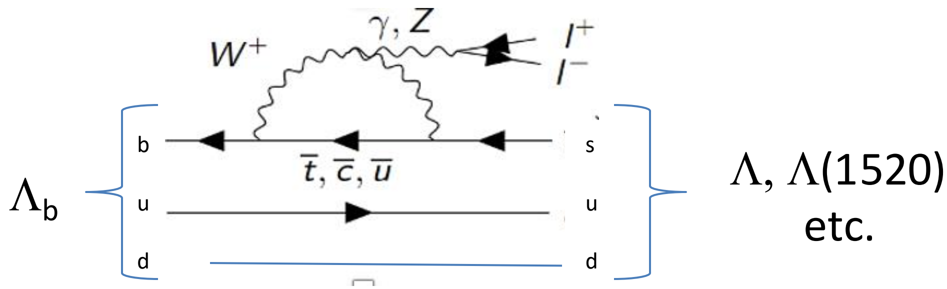

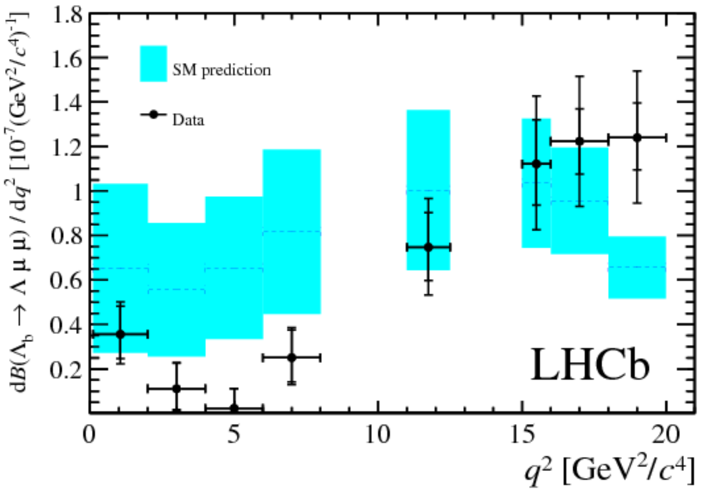

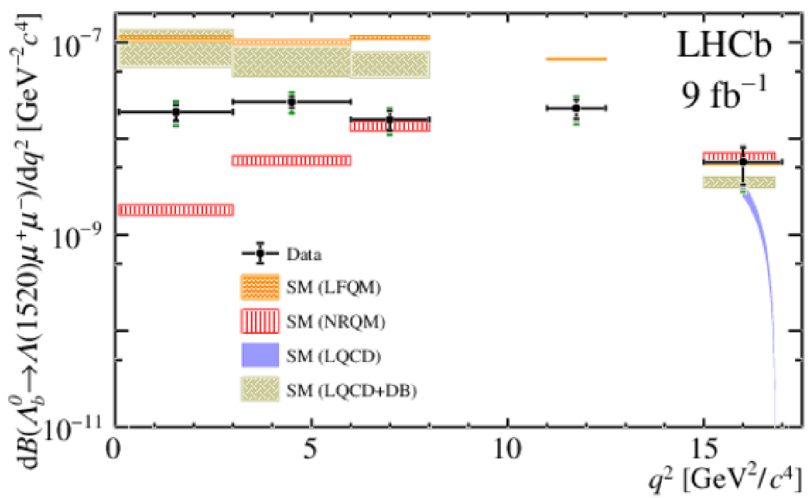

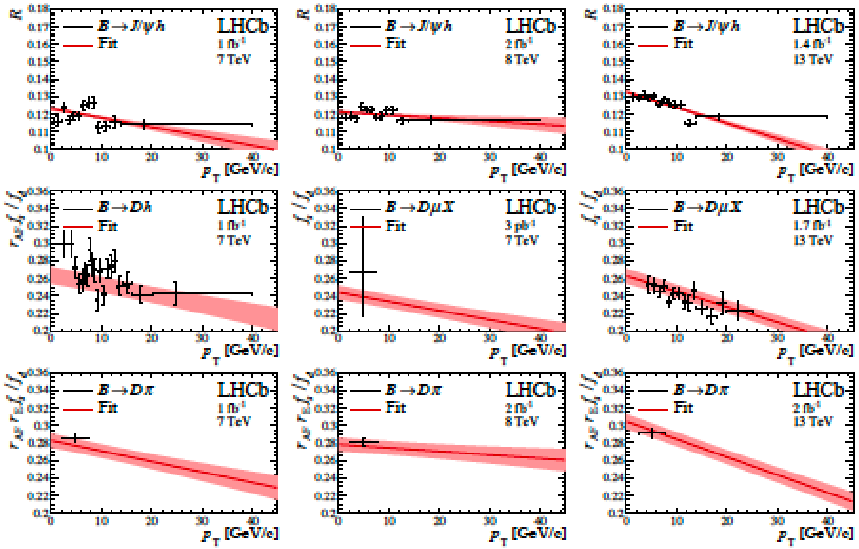

Figure 1: Measurements of f_s/f_d sensitive observables as a function of the B-meson transverse momentum, p_T, overlaid with the fit function. The scaling factors r_{AF} and r_E are defined in the text; the variable $\mathcal{R}$ is defined in Eq. 4. The vertical axes are zero-suppressed. The uncertainties on the data points are fully independent of each other; overall uncertainties for measurements in multiple p_T intervals are propagated via scaling parameters, as described in the text. The band associated with the fit function shows the uncertainty on the post-fit function for each sample.

$$
\begin{aligned}
f_s/f_d \quad (p_T, 7\,\text{TeV}) &= (0.244 \pm 0.008) + ((-10.3 \pm 2.7) \times 10^{-4}) \cdot p_T\,, \\
f_s/f_d \quad (p_T, 8\,\text{TeV}) &= (0.240 \pm 0.008) + ((-\ \ 3.4 \pm 2.3) \times 10^{-4}) \cdot p_T\,, \\
f_s/f_d \quad (p_T, 13\,\text{TeV}) &= (0.263 \pm 0.008) + ((-17.6 \pm 2.1) \times 10^{-4}) \cdot p_T\,,
\end{aligned}
$$

Table 3: Observables and related parameters of the default fit. See text for a detailed explanation.

Observable	Parameters	Fit mode
f_s/f_d	$a(7\,\text{TeV})$, $a(8\,\text{TeV})$, $a(13\,\text{TeV})$	Free
	$b(7\,\text{TeV})$, $b(8\,\text{TeV})$, $b(13\,\text{TeV})$	Free
$\mathcal{B}(B_s^0 \to D_s^- \pi^+)$	r_{AF}	Gaussian constrained
	r_E	Gaussian constrained
$\mathcal{B}(B_s^0 \to J/\psi\phi)$	$\mathcal{F}_R$	Free
	S_1	Gaussian constrained
	S_2, S_3, S_4	Gaussian constrained

S_2, S_3, and S_4, the parameters propagating experimental systematic uncertainties on the input measurements.

$$
\begin{aligned}
f_s/f_d \quad (p_T, 7\,\text{TeV}) &= (0.244 \pm 0.008) + ((-10.3 \pm 2.7) \times 10^{-4}) \cdot p_T\,, \\
f_s/f_d \quad (p_T, 8\,\text{TeV}) &= (0.240 \pm 0.008) + ((-\ \ 3.4 \pm 2.3) \times 10^{-4}) \cdot p_T\,, \\
f_s/f_d \quad (p_T, 13\,\text{TeV}) &= (0.263 \pm 0.008) + ((-17.6 \pm 2.1) \times 10^{-4}) \cdot p_T\,,
\end{aligned}
$$

$$\mathcal{B}(B_s^0 \to J/\psi\phi, \phi \to K^+K^-) = (5.01 \pm 0.16 \pm 0.17) \times 10^{-4}$$

$$\mathcal{B}(B_s^0 \to J/\psi\phi) = (1.018 \pm 0.032 \pm 0.037) \times 10^{-3}\,,$$

Precise measurement of the f_s/f_d ratio of fragmentation fractions and of B_s^0 decay branching fractions

LHCb collaboration†

Abstract

The ratio of the B_s^0 and B^0 fragmentation fractions, f_s/f_d, in proton-proton collisions at the LHC, is obtained as a function of B-meson transverse momentum and collision centre-of-mass energy from the combined analysis of different B-decay channels measured by the LHCb experiment. The results are described by a linear function of the meson transverse momentum, or with a function inspired by Tsallis statistics. Precise measurements of the branching fractions of the $B_s^0 \to J/\psi\phi$ and $B_s^0 \to D_s^-\pi^+$ decays are performed, reducing their uncertainty by about a factor of two with respect to previous world averages. Numerous B_s^0 decay branching fractions, measured at the LHCb experiment, are also updated using the new values of f_s/f_d and branching fractions of normalisation channels. These results reduce a major source of systematic uncertainty in several searches for new physics performed through measurements of B_s^0 branching fractions.

Published in Phys. Rev. D104 (2021) 032005

Forecast

➡ **Next target is $B_d \to \mu^+\mu^-$**

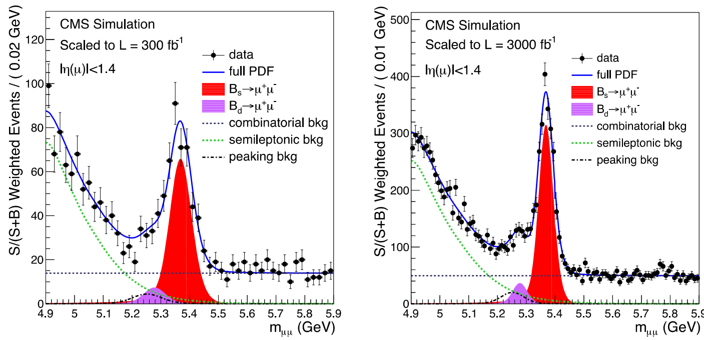

Figure 3: Projections of the mass fits to 300 fb^{-1} (left) and 3000 fb^{-1} (right) of integrated luminosity (L), respectively assuming the expected performances of Phase-I and Phase-II CMS detectors.

Notice better mass resolution in CMS for HL-LHC

Estimate of analysis sensitivity

$\mathcal{L}$ (fb^{-1})	$N(\mathrm{B}_s^0)$	$N(\mathrm{B}^0)$	$\delta\mathcal{B}(\mathrm{B}_s^0 \to \mu^+\mu^-)$	$\delta\mathcal{B}(\mathrm{B}^0 \to \mu^+\mu^-)$	B^0 sign.	$\delta\frac{\mathcal{B}(\mathrm{B}^0\to\mu^+\mu^-)}{\mathcal{B}(\mathrm{B}_s^0\to\mu^+\mu^-)}$
20	18.2	2.2	35%	$>100\%$	$0.0-1.5\,\sigma$	$>100\%$
100	159	19	14%	63%	$0.6-2.5\,\sigma$	66%
300	478	57	12%	41%	$1.5-3.5\,\sigma$	43%
300 (barrel)	346	42	13%	48%	$1.2-3.3\,\sigma$	50%
3000 (barrel)	2250	271	11%	18%	$5.6-8.0\,\sigma$	21%

Observable	Current	LHCb-U1a	LHCb-U2	ATLAS	CMS
$\mathcal{B}(B_s^0 \to \mu^+\mu^-)$ ($\times 10^9$)	±0.46	±0.30	±0.16	$\pm(0.50)$	±0.39
$\frac{\mathcal{B}(B^0\to\mu^+\mu^-)}{\mathcal{B}(B_s^0\to\mu^+\mu^-)}$	$\sim 70\%$	$\sim 34\%$	$\sim 10\%$	–	$\sim 21\%$
$\tau_{\mu\mu}$	$\sim 14\%$	±0.16 ps	±0.04 ps	–	±0.05 ps

Table 3: Summary of the current and expected experimental precision for $B_s^0 \to \mu^+\mu^-$ and $B^0 \to \mu^+\mu^-$ observables. The expected uncertainty are reported for LHCb at 23 fb^{-1} (LHCb-U1a) and 300 fb^{-1} (LHCb-U2) while for ATLAS and CMS are evaluated at 3 ab^{-1}.

BELLE Branching Fraction Measurements on Y(5S)

[17] Belle collaboration, F. Thorne *et al.*, *Measurement of the decays $B_s^0 \to J/\psi\phi(1020)$, $B_s^0 \to J/\psi f_2'(1525)$ and $B_s^0 \to J/\psi K^+K^-$ at Belle*, Phys. Rev. **D88** (2013) 114006, arXiv:1309.0704

We report a measurement of the branching fraction of the decay $B_s^0 \to J/\psi\,\phi(1020)$, evidence and a branching fraction measurement for $B_s^0 \to J/\psi\, f_2'(1525)$, and the determination of the total $B_s^0 \to J/\psi\, K^+K^-$ branching fraction, including the resonant and non-resonant contributions to the K^+K^- channel. We also determine the S-wave contribution within the $\phi(1020)$ mass region. The absolute branching fractions are $\mathcal{B}[B_s^0 \to J/\psi\,\phi(1020)] = (1.25 \pm 0.07\,(\text{stat}) \pm 0.08\,(\text{syst}) \pm 0.22\,(f_s)) \times 10^{-3}$, $\mathcal{B}[B_s^0 \to J/\psi\, f_2'(1525)] = (0.26 \pm 0.06\,(\text{stat}) \pm 0.02\,(\text{syst}) \pm 0.05\,(f_s)) \times 10^{-3}$ and $\mathcal{B}[B_s^0 \to J/\psi\, K^+K^-] = (1.01 \pm 0.09\,(\text{stat}) \pm 0.10\,(\text{syst}) \pm 0.18\,(f_s)) \times 10^{-3}$, where the last systematic error is due to the branching fraction of $b\bar{b} \to B_s^{(*)}B_s^{(*)}$. The branching fraction ratio is found to be $\mathcal{B}[B_s^0 \to J/\psi\, f_2'(1525)]/\mathcal{B}[B_s^0 \to J/\psi\,\phi(1020)] = (21.5 \pm 4.9\,(\text{stat}) \pm 2.6\,(\text{syst}))$. All results are based on a 121.4 fb^{-1} data sample collected at the $\Upsilon(5S)$ resonance by the Belle experiment at the KEKB asymmetric-energy e^+e^- collider.

$$(1.25 \pm 0.07 \pm 0.23) \times 10^{-3}$$

This seems to use f_s to get the BR!

Historical Summary

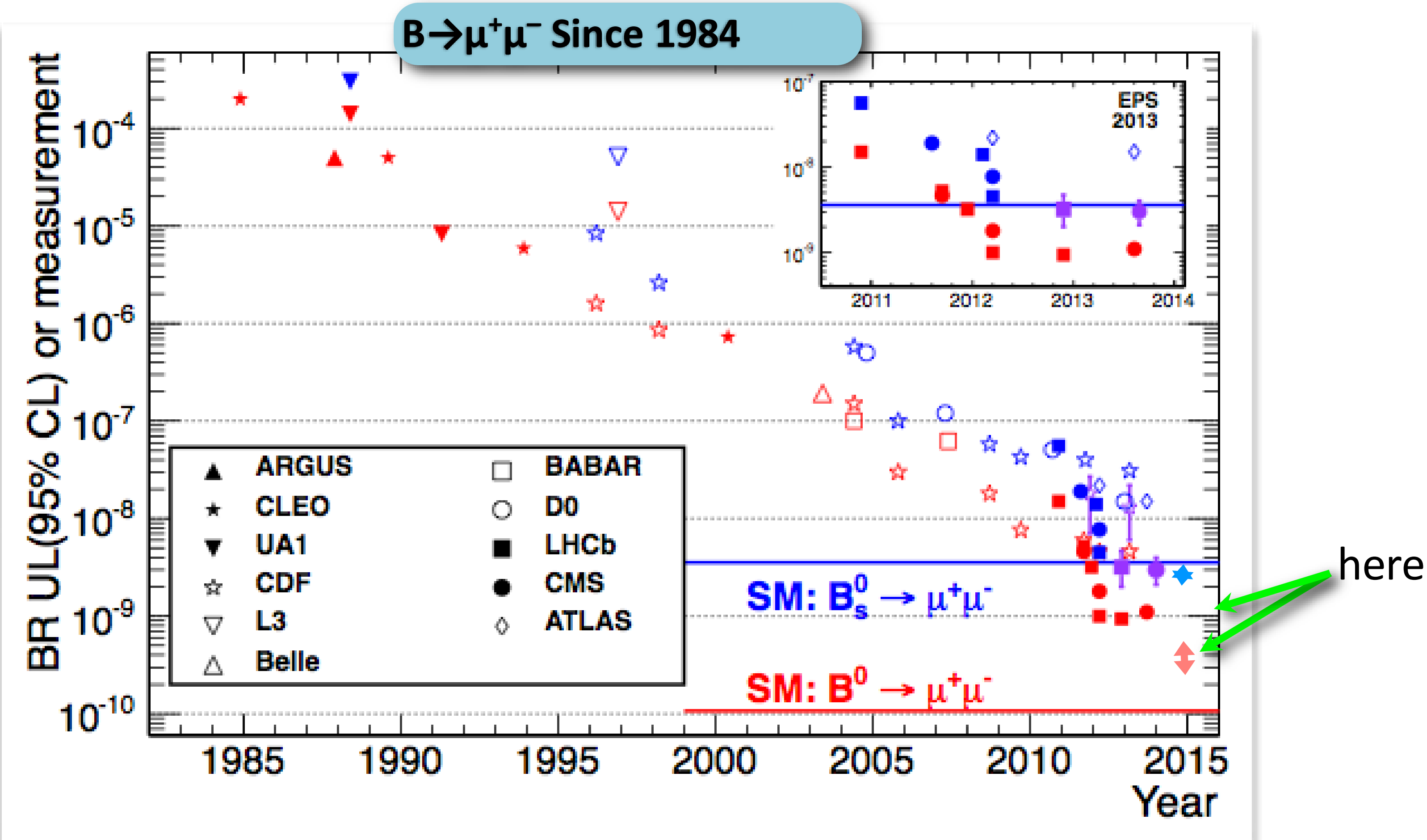

It took 30 years to finally measure the $B_s \to \mu^+\mu^-$ decay; The result turns out to be very close to the prediction and gives a stringent limit on the physics beyond the Standard Model. **There is still a possibility of ~50% deviation from the SM, which will be resolved by more statistics in the next few years.**

LHCb PARTICLE ID

- LHCb has a dedicated (active) particle identification device: RICH (Ring Imaging Cherenkov) detector.
- **A global particle ID likelihood** is constructed based on the information from the **RICH** detectors, calorimeters (**CALO**), and **MUON** system.

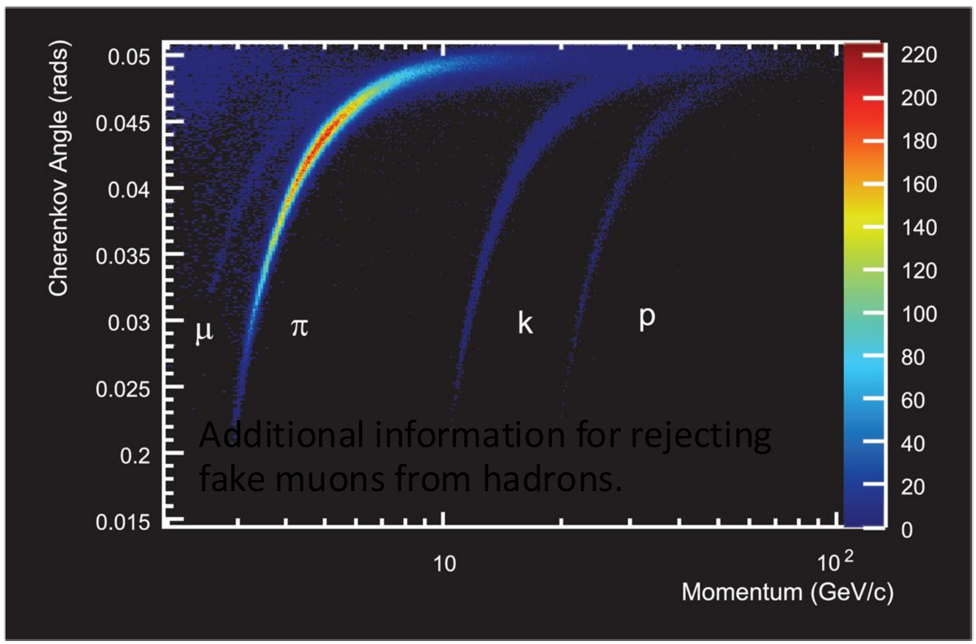

Powerful muon identification with high (~98%) efficiency:
Based on muon chambers information + the global PID likelihood:
$\varepsilon(\pi \rightarrow \mu)$~0.6%
$\varepsilon(K \rightarrow \mu)$~0.4%
$\varepsilon(p \rightarrow \mu)$~0.3%

Note: I will add Γ and τ numbers for completeness

Some B_s, B_d meson properties

- The B_s meson is a $\bar{b}s$ bound state; the B_d meson is a $\bar{b}d$ bound state
- The Mass of the B_s is 5366.7 MeV/c^2 and the B_d is 5279.55 MeV/c^2
  - $M_{B_s} - M_{B_d} = \sim 87$ MeV/c^2
- B_s^0 is a flavor eigenstate, not a mass eigenstate, and oscillates rapidly between B_s and $\overline{B}_s$
- The interactions that produce mixing also can produce a difference in lifetimes between the two mass eigenstates B_{sH} and B_{sL} of about 10%
- The B_d^0 has weaker mixing, oscillates more slowly and there is almost no difference in the lifetimes of its two mass eigenstates
- Both B_d and B_s have mean lifetimes of 1.5ps, corresponding to $c\tau$ of ~450μ m
- The distance from the production (primary) vertex to the B decay (secondary) vertex can be measured and used to eliminate most prompt backgrounds

Review: Properties of B_s and B_d

Property	B_d	B_s	Comment
Mass (MeV)	5279.55	53667.7	M_{Bs} - M_{Bd}=87.34
Δ M B_d(10^{12} h/2π s^{-1})	0.510		Δ [M(B^0_H) - M(B^0_L)]
Δ M B_s (10^{12} h/2π s^{-1})		17.769	Δ [M(B_{sH}) - M(B_{sL})]
Mean Lifetime (ps)	1.519	1.469	
B_{sH} mean life (ps)		1.70	
$\Delta\Gamma$ (B_d) (ps^{-1})	(42+/-10)x10^{-4} Γ		$\Delta\Gamma(B_d)=\Gamma(B_{dL}) - \Gamma(B_{dH})$
$\Delta\Gamma$ (B_s) (ps^{-1})		0.091+/- 0.016	$\Delta\Gamma(B_s)=\Gamma(B_{sL}) - \Gamma(B_{sH})$
Δ M/Γ (B_d)	0.774		
Δ M/Γ (B_s)		26.85	

B Production at the LHC is large

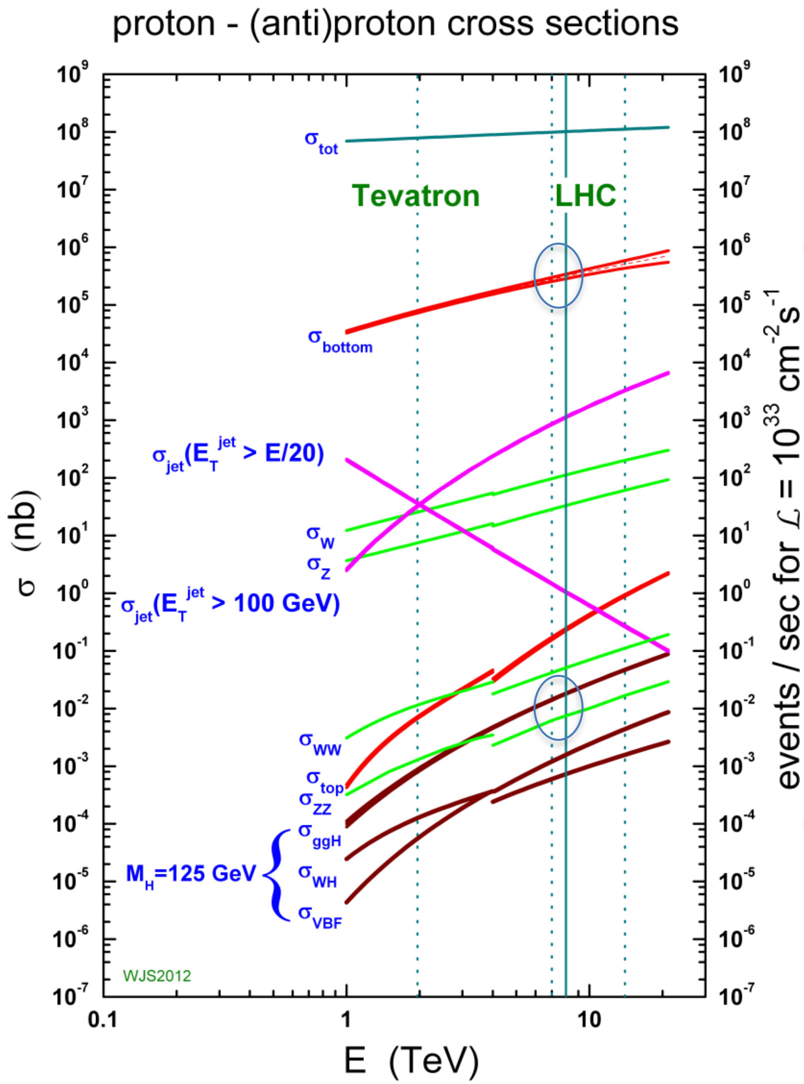

LO – Pair creation

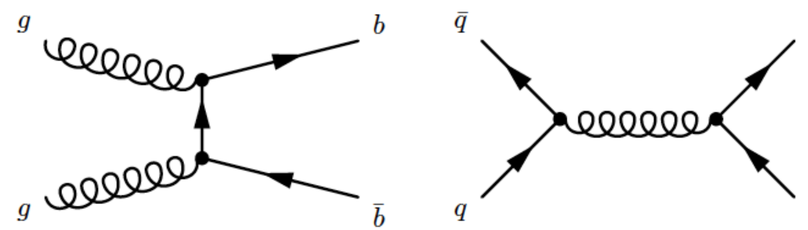

NLO –
pair creation, Flavor Excitation, Gluon splitting

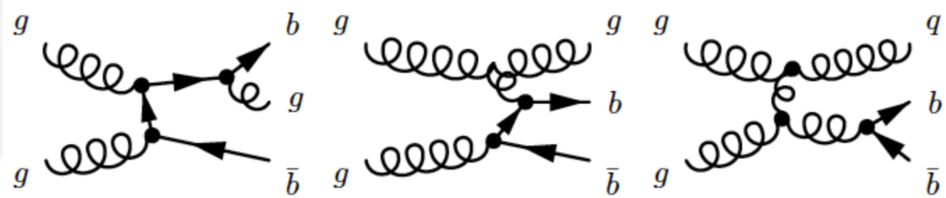

Observable	Current	LHCb-U1a	LHCb-U2	ATLAS	CMS
$\mathcal{B}(B_s^0 \to \mu^+\mu^-)$ $(\times 10^9)$	± 0.46	± 0.30	± 0.16	$\pm(0.50)$	± 0.39
$\frac{\mathcal{B}(B^0 \to \mu^+\mu^-)}{\mathcal{B}(B_s^0 \to \mu^+\mu^-)}$	$\sim 70\%$	$\sim 34\%$	$\sim 10\%$	–	$\sim 21\%$
$\tau_{\mu\mu}$	$\sim 14\%$	± 0.16 ps	± 0.04 ps	–	± 0.05 ps

Table 3: Summary of the current and expected experimental precision for $B_s^0 \to \mu^+\mu^-$ and $B^0 \to \mu^+\mu^-$ observables. The expected uncertainty are reported for LHCb at $23\,\mathrm{fb}^{-1}$ (LHCb-U1a) and $300\,\mathrm{fb}^{-1}$ (LHCb-U2) while for ATLAS and CMS are evaluated at $3\,\mathrm{ab}^{-1}$.

This is after Moriond 2021 so does not contain all recent results, view as illustrative only

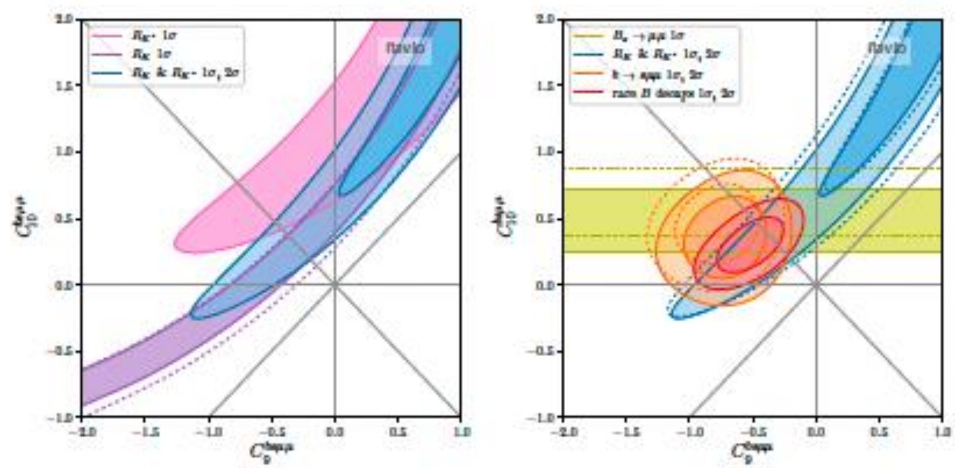

Figure 4: Constraints in the Wilson coefficient plane $C_9^{bs\mu\mu}$ vs. $C_{10}^{bs\mu\mu}$. Left: LFU ratios only. Right: Combination of LFU ratios, combination of $b \to s\mu\mu$ observables, $\mathrm{BR}(B_s \to \mu^+\mu^-)$, and the global fit. The dashed lines show the constraints before the recent updates [11, 13, 14, 41].

https://arxiv.org/abs/2103.13370v3

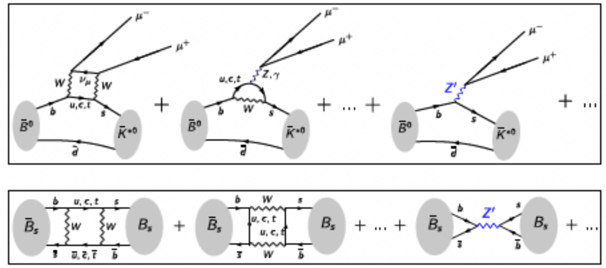

Figure 3: Schematic representation of the (top) $\overline{B}^0 \to \overline{K}^{*0}\mu^+\mu^-$ decay and (bottom) B_s^0-$\overline{B}_s^0$ mixing amplitudes as sums over all possible Feynman diagrams. The diagrams on the left are examples of SM contributions, while the diagram on the right is an example of an NP contribution in theories with a flavor-changing neutral gauge boson Z'.

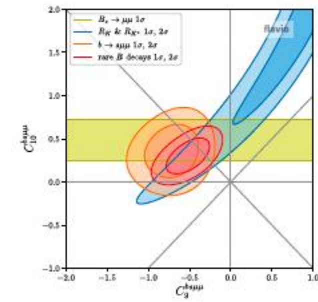

Figure 1: Constraints at 1σ (darker) and 2σ (lighter) in the plane $C_9^{bs\mu\mu}$ *vs.* $C_{10}^{bs\mu\mu}$ resulting from $B(B_s^0 \to \mu^+\mu^-)$ (yellow-green), combination of the lepton-flavor-universality ratios R_K and $R_{K^{*0}}$ (blue), combination of $b \to s\mu^+\mu^-$ observables (orange), and global fit of rare b decays (red) [9]. The Wilson coefficients $C_9^{bs\mu\mu}$ and $C_{10}^{bs\mu\mu}$ are the NP contributions to the couplings of the operators $O_9 = (\bar{s}\gamma_\mu b_L)(\bar{\mu}\gamma^\mu\mu)$ and $O_{10} = (\bar{s}\gamma_\mu b_L)(\bar{\mu}\gamma^\mu\gamma_5\mu)$, respectively. The global fit result is inconsistent with the SM point (the origin) by $\sim 5\sigma$.

This is after Moriond Snowmass 2021 so does not contain all recent results, view as illustrative only

https://arxiv.org/abs/2208.05403v2

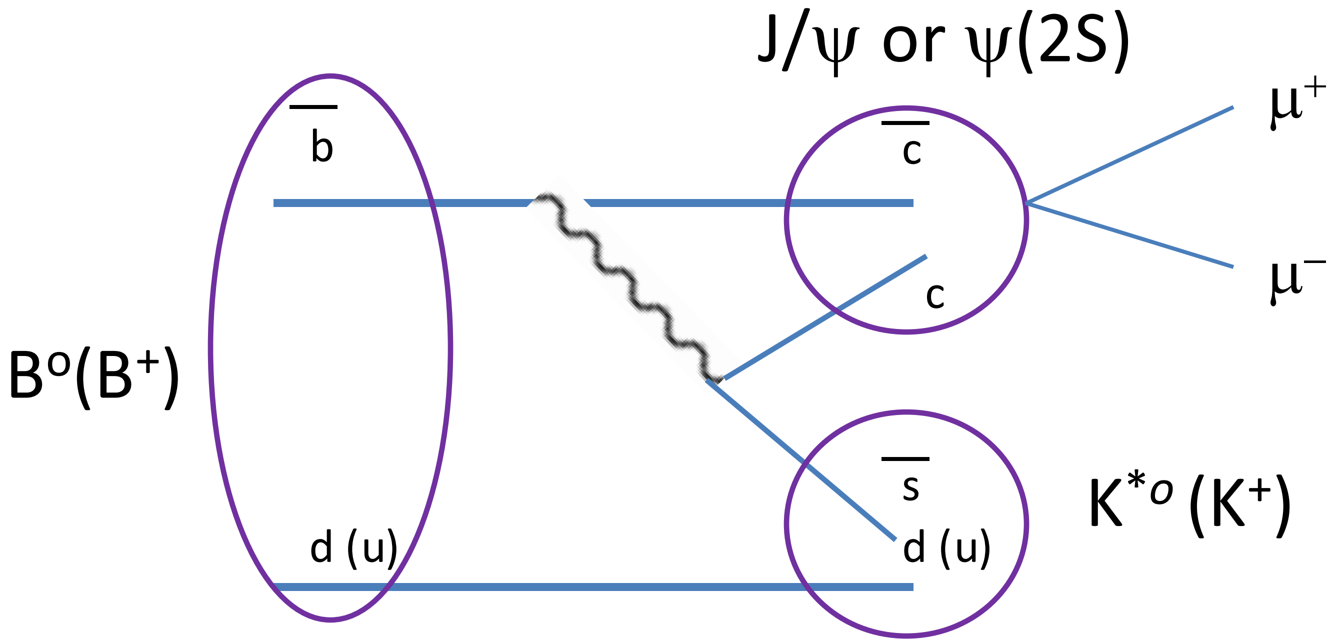

The anti-b quark does not decay through a loop diagram. These are CKM and Cabibbo favored decays that, far from being suppressed, have high branching fractions. The J/ψ or $\psi(2S)$ decay into a $\mu^+\mu^-$ creates the resonant contribution that is excluded by the q^2 cuts in the $B^o \rightarrow K^{*o}\,\mu^+\mu^-$ analysis. The B^+ is used as a normalization channel in the $B_{s,d} \rightarrow \mu^+\mu^-$ for its similarity to the signal decay (one extra particle, same muon content).